Computational Studies of Substituted Zirconocenium Catalysts for Olefin Coordination Polymerization

Svetlana Popenova

A Thesis

in

The Department

of

Chemistry and Biochemistry

Presented in Partial Fulfillment of the Requirements
For the Degree of Master of Science (Chemistry) at
Concordia University
Montreal, Quebec, Canada

April 2009

Your file Votre référence
ISBN: 978-0-494-63254-3
Our file Notre référence
ISBN: 978-0-494-63254-3

ABSTRACT

Computational Studies of Substituted Zirconocenium Catalysts for Olefin Coordination Polymerization

Svetlana Popenova

Olefin coordination polymerization catalysts consisting of Group 4 metallocene dichloride have received considerable industrial interest, as they constitute a highly active and selective class of catalysts for α-olefin polymerization. For zirconocene dichlorides of general formula $[Zr\{\eta^5\text{-}C_5H_{5\text{-}n}R_n\}_2Cl_2]$, the Zr atom is η^5-coordinated to cyclopentadienyl rings that may be substituted or not (R = H, alkyl, aryl…).

When reacted with an excess of co-catalyst, the zirconocenium complexes $[Zr\{\eta^5\text{-}C_5H_{5\text{-}n}R_n\}_2Me]^+$ responsible for the polymerization activity are formed. The catalytic performance of these catalysts is greatly influenced by electronic and steric factors due to the R substituents on the cyclopentadienyl rings.

The aim of this work is to understand how the introduction of various length alkyl chains modified with Si and F atoms alters the coordination environment and the electronic properties of the active metal center, and how these changes may affect the olefin polymerization process. A combination of theoretical methods, such as density-functional theory with natural bond orbital analysis and the quantum theory of atoms in molecules, is used to explore these issues. The results of calculations for zirconocenium complexes with various substituents are reported, and the structure, energy, electron density distribution for the different species are examined, focusing on the factors that might control catalytic activity in order to identify optimal substituents. The nature of possible intramolecular interactions between substituents and the metal, as well as the influence of such interactions on catalytic performance, are also investigated.

Acknowledgements

I would like to thank my supervisor Dr. Gilles H. Peslherbe for his help, support and guidance in the course of scientific research presented here. He led me into the wonderful world of computational chemistry and trained me to become a confident researcher in this field. This widened my horizons in overall chemistry and eventually made me a better specialist in application and research chemical areas.

I wish to thank Dr. Heidi M. Muchall and Dr. Peter H. Bird for serving in my advisory committee and for their helpful suggestions. I am thankful to my former supervisors Dr. Georg H. Schreckenbach and Dr. Philppe G. Merle, who also contributed during my studies at Concordia University to my development as a researcher and a person.

I am grateful to all former and current members of the CERMM research group, especially to Robert Mawhinney, Qadir Timerghazin, Denise Koch and Grygoryi Dolgonos.

Finally, I am indebted to my family, especially my husband Oleg Popenov, for their love, patience and encouragement, as well as to all my friends and colleagues at Canadian Technical Tape Ltd. for their support.

Table of Contents

List of Figures

List of Tables

List of Abbreviations and Symbols

LDPE	Low-density polyethylene
HDPE	High -density polyethylene
Z-N	Ziegler – Natta
M	Central metal atom
MAO	Methyl aluminum oxide
Cp	Cyclopentadienyl
R	Alkyl group
TS	Transition state
P	Growing polymer chain
DFT	Density-functional theory
B3LYP	Becke's three parameter exchange functional with the Lee-Yang-Parr correlation functional
LANL2DZ	Los Alamos National Laboratory 2-double-zeta basis set
3D	Three-dimensional
GOP	Gross orbital population
GAP	Gross atom population
NBO	Natural bond orbital analysis
NAO	Natural atomic orbital
NHO	Natural hybrid orbital
AO	Atomic orbital
MO	Molecular orbital
AIM	Atoms-in-molecules quantum theory
CP	Critical point

BCP	Bond critical point
VDW	Van der Waals

CHAPTER 1

General introduction

1.1 Olefin polymerization

Polyolefins are a class of polymers that includes mostly polyethylene, polypropylene and their copolymers with a wide range of monomers. Nowadays, polyolefins with a broad variation of chemical and mechanical properties are produced in bulk amounts. These polyolefins are used on a large scale for packaging, car bumpers and dashboards, fibres and films. Polymerization of α-polyolefins comprises 2/3 of the overall production and is the fastest growing segment of the polymer industry. The estimated worldwide production of polyolefins in 2010 will reach 140 million tons.[1-6] This increase is caused largely by the use of new catalysts which make possible the synthesis of a polymer with a predictable, controlled structure and, thus, desirable physical properties. Such compounds can be designed, if the molecular aspects of the catalytic process are all well understood. Some of the key questions are: What happens exactly at the metal center? Precisely which factors determine selectivity, polymer chain growth and chain transfer? What causes catalyst deactivation?

1.1.1 Historical background of olefin polymerization

The first polyolefin of industrial interest was polyethylene. Its synthesis was achieved in 1933 by E. Fawcett and R. Gibson at the ICI works in Northwick, England. The reaction proceeds only under high pressure (several hundred atmospheres) and became the basis for industrial Low Density Polyethylene (LDPE) production beginning in 1939. The reaction mechanism is radical.

Subsequent landmarks in polyethylene synthesis have revolved around the development of the catalyst that promotes ethylene polymerization under milder temperature and pressure conditions. In 1953, the German chemist K. Ziegler developed a highly active heterogeneous catalytic system based on titanium halides and organoaluminum compounds that worked at relatively mild conditions and resulted in high molecular weight polyethylene.[7] At the same time G. Natta, using a similar catalytic system, obtained polypropylene (Figure 1.1).[8] This reaction, called Ziegler-Natta (Z-N) polymerization, has been used for high density polyethylene (HDPE) and polypropylene production ever since.[9] The main advantage of the method is the easy recovery of the catalyst, but the stereospecificity is relatively low.

A homogeneous type of catalytic system, based on metallocenes of group 4 transition metals and soluble in organic solvents, was discovered in Germany by W. Kaminsky and H. Sinn.[10] In Kaminsky-type catalysts, the metallocene dichloride M $\{\eta^5\text{-}C_5H_5\}_2Cl_2$, where M is a group 4 transition metal, reacts with an excess of a co-catalyst, to produce active species responsible for the polymerization activity. The cyclopentadienyl (Cp) rings can bear various substituents. Specifically engineered Kaminsky catalysts are among the most highly active and selective catalysts for α-olefin polymerization. The catalyst yields around 100 tons of polymer per gram of catalyst per hour. They also offer unique possibilities for controlling the polymer structure and its properties, and the proper choice of catalyst can produce isotactic, syndiotactic or atactic polypropylene, or a combination of these. They also allow a better quantitative control, with a much greater ratio of desired tacticity or narrower molecular weight distribution than previous heterogeneous Z-N techniques.

K. Ziegler, 1955

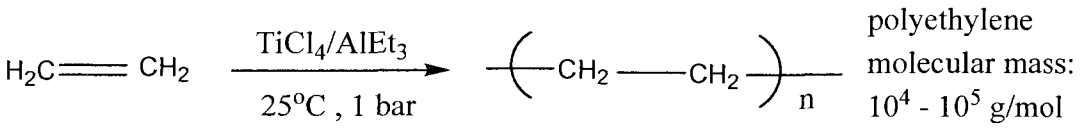

G. Natta, 1955

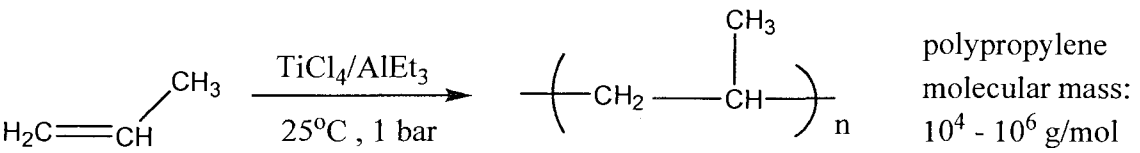

Figure 1.1. Ziegler-Natta polymerization schemes.

During recent decades, olefin polymerization by metallocene catalysis has drawn a lot of attention. Zirconoceniums are the most studied active species for α-olefin coordination polymerization, both experimentally and theoretically. The performances of new catalysts are typically compared to that of zirconocene dichloride.[11]

1.1.2 Reaction mechanism of Z-N olefin polymerization

The reaction mechanism of coordination polymerization for "single-site" catalysts is rather complex and not fully understood. However, it is now widely agreed that it follows the Cossee-Arlman mechanism.[12, 13] The zirconocene dichloride pre-catalysts are species of general formula $[Zr\{\eta^5\text{-}C_5H_4R\}_2Cl_2]$, where the zirconium atom is η^5-coordinated to cyclopentadienyl rings, and R may be H, an alkyl or aryl substituent. Organometallic co-

catalysts, usually methylalumoxide $[MeAlO]_n$ (MAO) or borate anion $[B(C_6F_5)_4]^-$, cause the alkylation of the transition metal, the creation of a vacant coordination site, and assist scavenging of moisture from the reaction environment.[14]

When the pre-catalyst is reacted with an excess of a co-catalyst, the active species responsible for the polymerization activity are formed; it is now agreed that these species are the 14-electron cationic zirconocenium complexes $[Zr\{\eta^5\text{-}C_5H_4\text{ -R}\}_2Me]^+[MAO]^-$ (Figure 1.2), where the zirconium center acts as a Lewis acidic coordination site *cis*- to another methyl ligand. These are also often called "single-site" catalysts.[15, 16]

For the reaction to proceed two coordination sites are required, one for binding the unsaturated substrate, and one for the alkyl group R. The polymerization process starts by coordination of an alkene at the vacant site of the cationic group 4 metal-alkyl complex (π-complex formation), followed by insertion of the alkene into the metal-alkyl bond.

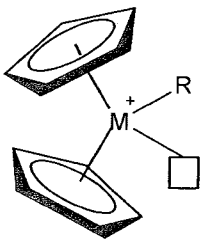

$[M(Cp)_2R]^+$ M = Group 4-10 transition metal

Figure 1.2. Catalytic active species made of cationic and coordinatively unsaturated metal-alkyl complexes.

Subsequent alkene coordination and insertion leads to chain growth. The Cossee-Arlman mechanism, depicted in Figure 1.3, provides a framework for all studies of catalysis these days.

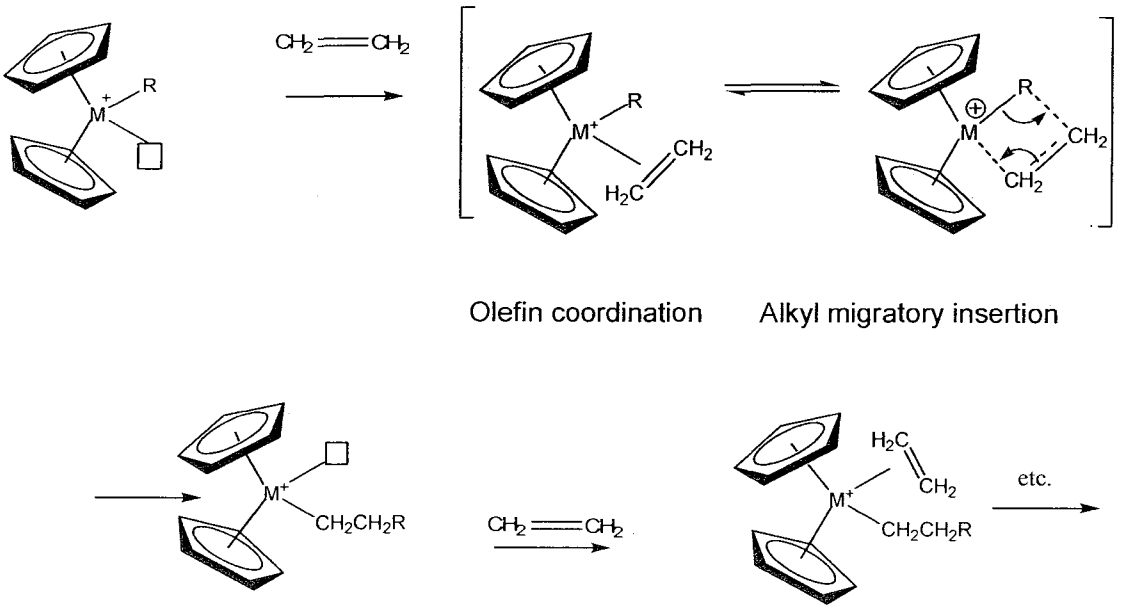

Figure 1.3. Cossee-Arlman mechanism of α - olefin coordination polymerization.

The Dewar-Chatt-Duncanson diagram of orbital interactions for coordination polymerization is also often used to explain why these catalysts are so highly active (Figure 1.4).[17-19]

In general, the olefin binds to the metal center by donation of electron density from the π-orbitals of the olefin double bond. This bond is relatively weak and can be stabilized by π back donation of electron density from the occupied metal d-orbitals to the empty anti-bonding olefin π-orbitals. In the case of group 4 transition metals, the metallocene catalyst metal is in a +4 oxidation state (d^0), the electron density from the olefin π bond is donated to the empty metal d-orbitals, but the stabilization of the intermediate olefin adduct by back-bonding is not possible.

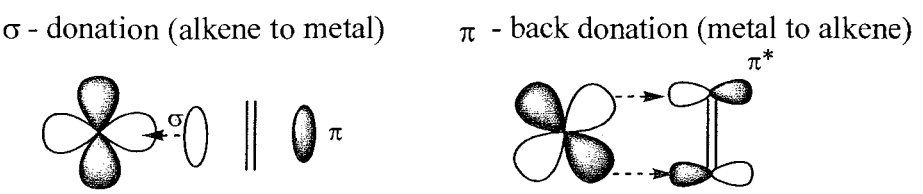

(a)

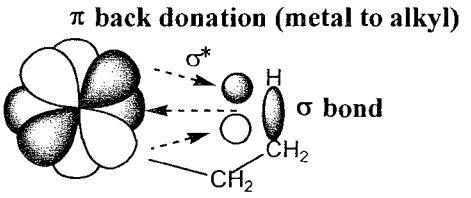

(b)

Figure 1. 4. Dewar-Chatt-Duncanson diagram of orbital interactions for alkyl coordination (a) and alkyl migratory insertion (b) steps.

The olefins are very weak Lewis bases and the bonding without that stabilization is very weak. The d-orbitals of early transition metals are high in energy and, if occupied, would greatly increase the activation barrier of the alkyl migration step. In this case, migratory insertion does not require much energy to overcome the activation barrier and polymer chain grows easily. The chain termination may occur via a variety of pathways, but the most common pathways are: β-hydrogen transfer to metal, β-hydrogen transfer to monomer, and chain transfer to activator) (Figure1.5). The relative rates of chain propagation to chain termination determine the chain length and molecular weight of polymer. The activity of a catalyst is usually expressed as:

Activity = weight of polymer / [mole or weight of catalyst x time x moles of monomer] or

Activity = weight of polymer / [mole or weight of catalyst x time]

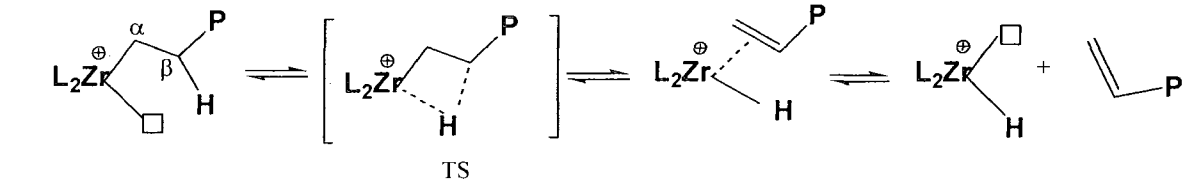

(a)

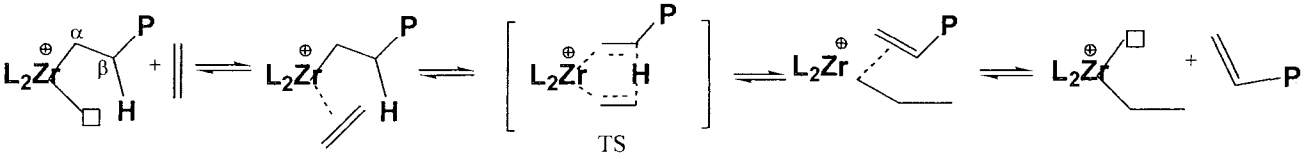

(b)

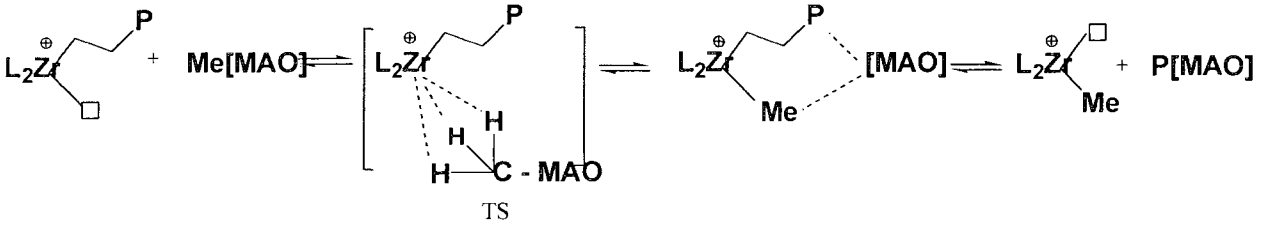

(c)

Figure1.5. Three reaction mechanisms for Z-N polymerization chain termination pathways. β-hydrogen transfer to metal (a); β-hydrogen transfer to monomer (b); transfer to activator (c).

In the case, for example, of the termination pathway by β-hydrogen elimination from back-bonding stabilization by electron density, donation from the metal to the empty anti-bonding σ^*-orbital of the CH_2-H bond is not possible (Figure 1.4 b), and the polymer chain coordination to the metal is weak. Moreover, the C-H bond is not weakened by receiving electron density in its anti-bonding orbital. Hence, for group 4 metal catalysts, the activation barrier for hydrogen elimination is higher than for any other metal system with occupied d-orbitals.

Since the overall reaction rate is determined by the ratio of chain propagation and chain termination rates, Z-N polymerization results in relatively high molecular weight polyolefins. Tailoring the Cp-ring with electron-donating or electron-withdrawing substituents allows "tuning" the electron density on the metal center. The balanced amount of electron density on the metal center is believed to be very important for determining the structure of polymers and the activity of catalysts.

1.2 Substituent effects on olefin coordination polymerization

Catalytic performance is sensitive to both the electronic and steric surroundings of the active site. These factors can be regulated by careful manipulation of the ligands, and several reports show that the choice of ligands and catalysts' performance is related. In the case of metallocenes, it can be achieved by tailoring the Cp ring with various substituents. Systematic modification of the ring allows enhancement of catalyst activity and control over polymer properties. Therefore ligand design is very important for obtaining stereospecific catalysts for olefin polymerization. A rich and varied class of catalysts has been obtained by variation of the Cp substituents and bridging group. Substituent effects in metallocene complexes of group 4 metals on their performance in catalytic olefin polymerization have been reported in the literature.[16, 20-31]

1.2.1 Steric effect of rigid (aromatic) substituents on polymerization activity

The steric effect of bulky substituents manifests itself by decreasing the overall accessibility of the metal, thus preventing monomers from reacting and decreasing the catalyst activity. In fact, the catalytic activity has been claimed to reach a maximum for the most accessible zirconium center.[32] The reduced accessibility can be achieved, for

example, if the ligand is a bulky indenyl, which also can be viewed as a Cp ring with substituent(s) (Figure 1.6). As observed experimentally, this ligand considerably reduces the catalyst activity from 1490 (Figure 1.6 a) to 580 kg (PE)(g Zr h)$^{-1}$ (Figure 1.6 b).

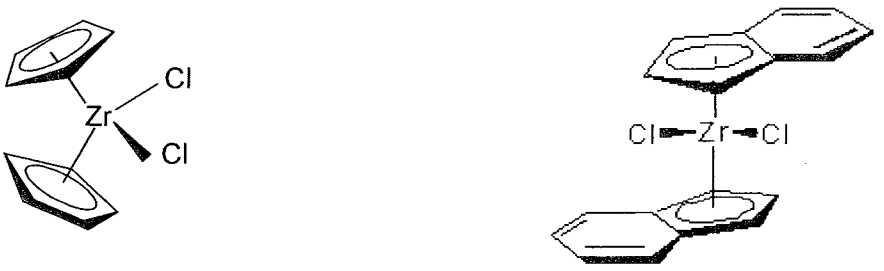

(a) (b)

Figure 1.6. Complexes used for illustration of steric effect of bulky substituents on polymerization activity, unsubstituted (a) and substituted (b).

1.2.2 *Ansa*-effect on polymerization activity

Increased accessibility can be illustrated by the *ansa*-effect. If the Cp ligands are connected with a bridge to prevent their rotation, the catalyst is called an *ansa*-catalyst.[33] It is now generally recognized that metallocenes with a short, single-atom, rigid bridge structure exhibit high activity and stereoselectivity in olefin polymerization. Therefore, many single-atom bridged metallocenes, especially single-carbon, silicon or germanium bridged metallocenes, have been synthesized and studied for olefin polymerization.[6, 34-36]

The amount of distortion from the normal metallocene geometry caused by the bridge is reflected in the geometrical parameters shown in Figure 1.7. The degree of ring tilt is usually represented by the dihedral angle (α) between the ring planes. The angle γ is between vectors originating in the ring centroids and ending on the metal, β is the

angle between vectors normal to the ring centroids. The difference between the angles γ and (180° - β) reflects the amount of slippage of the metal from an ideal η^5 coordination to each ring. A single-atom bridge can cause substantial slippage by as much as 20°, which might be considered as significant structural distortion. A single carbon atom bridge, usually, changes the angle α by 10-13°.[37]

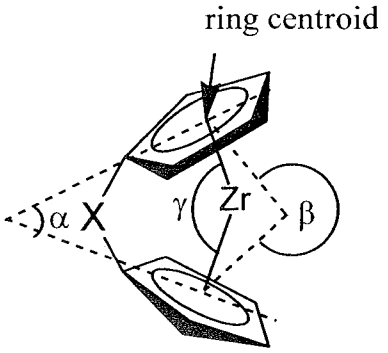

Figure 1.7. Angular parameters used for the geometry characterisation of bridged metallocenes.

A consequence of the bridging unit is the change in the position of the metal relative to an imaginary line connecting the Cp rings (Figure 1.8). The larger the distance D between the rings, the more accessible the metal and the higher the activity of the catalyst.[38]

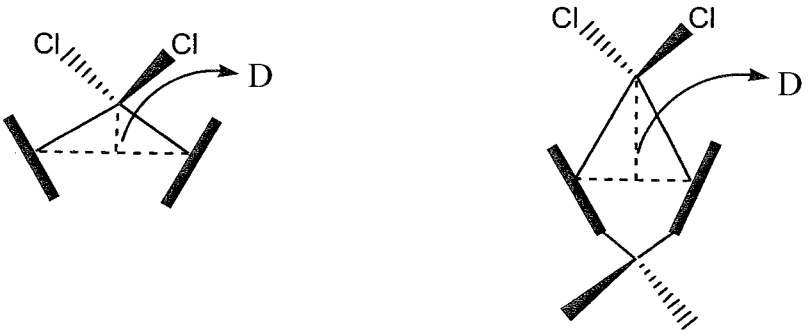

Figure1.8. Position of the metal in metallocene and *ansa*-metallocene dichlorides.

1.2.3 Orientation effect of bulky substituents

Polymerization with catalysts such as those depicted in Figure 1.9 results in atactic, isotactic or syndiotactic polymers. Depending on the geometry, bulky substituents, by limiting accessibility from one side, orient the methyl group of polypropylene away from themselves, and give stereospecific polymers.

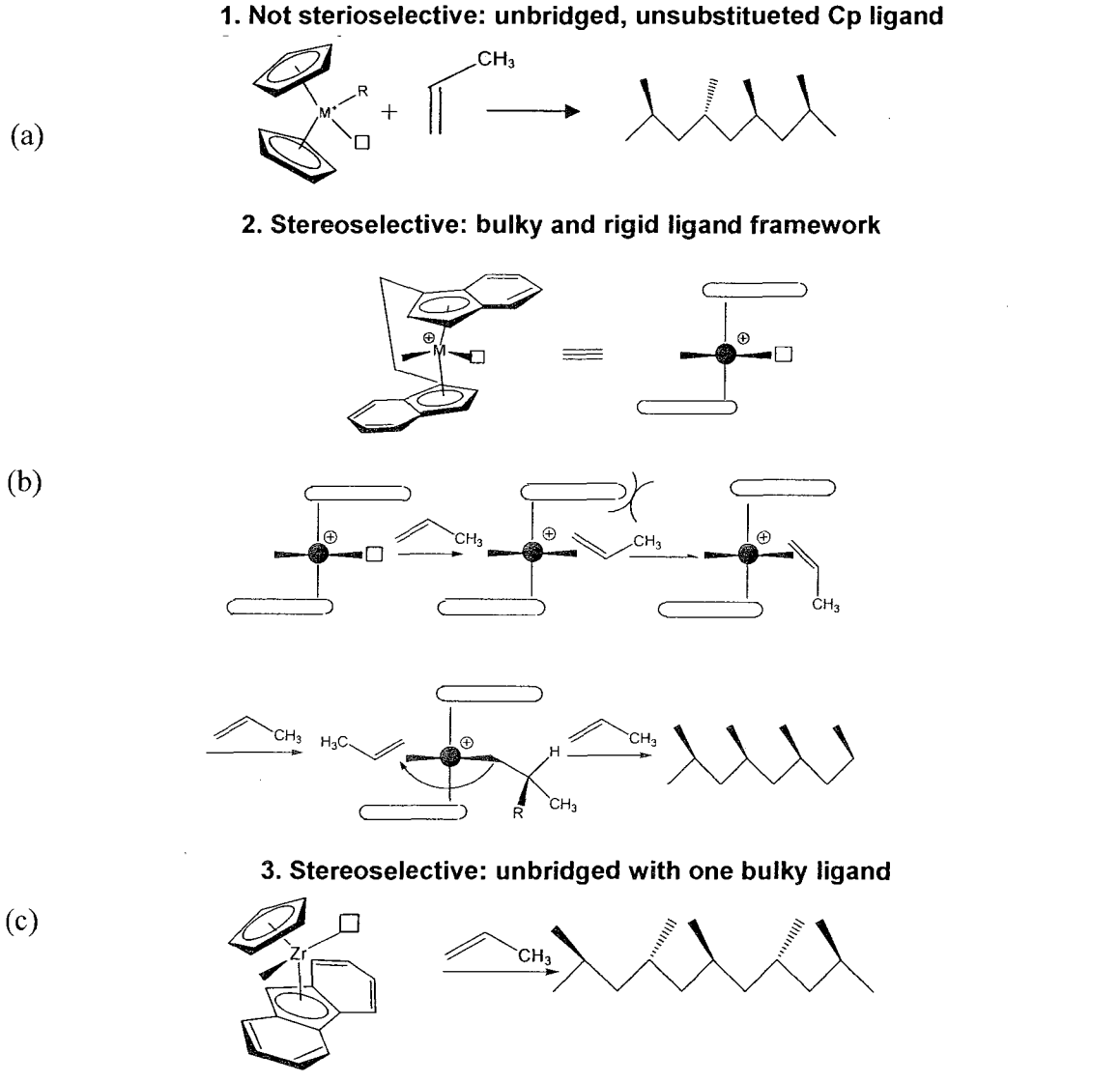

Figure 1.9. Orientation effect of bulky substituents, resulting in atactic polypropene for unsubstitued circonocenium catalyst (a) and isotactic polypropene (b) or syndiotactic polypropene (c) for rigid and bulky substituent framework.

1.2.4 Effect of solvent or activator on coordination polymerization

There is growing experimental evidence that the co-catalyst counterion and solvation play a significant role in the structure and energies of ion pairing, and hence, in catalytic activity and selectivity. Bulky ligands can prevent competitive solvent (Sol) coordination (Figure 1. 10), which without that may result in an inactive catalyst (Path II), rather than in an out- of-sphere bonding of A to the catalyst, which must be displaced by weakly coordinated alkenes prior to migratory insertion (Path I). Also, depending on the substituent nature, the ligand can increase the solubility of the catalyst in different solvents.[39-41]

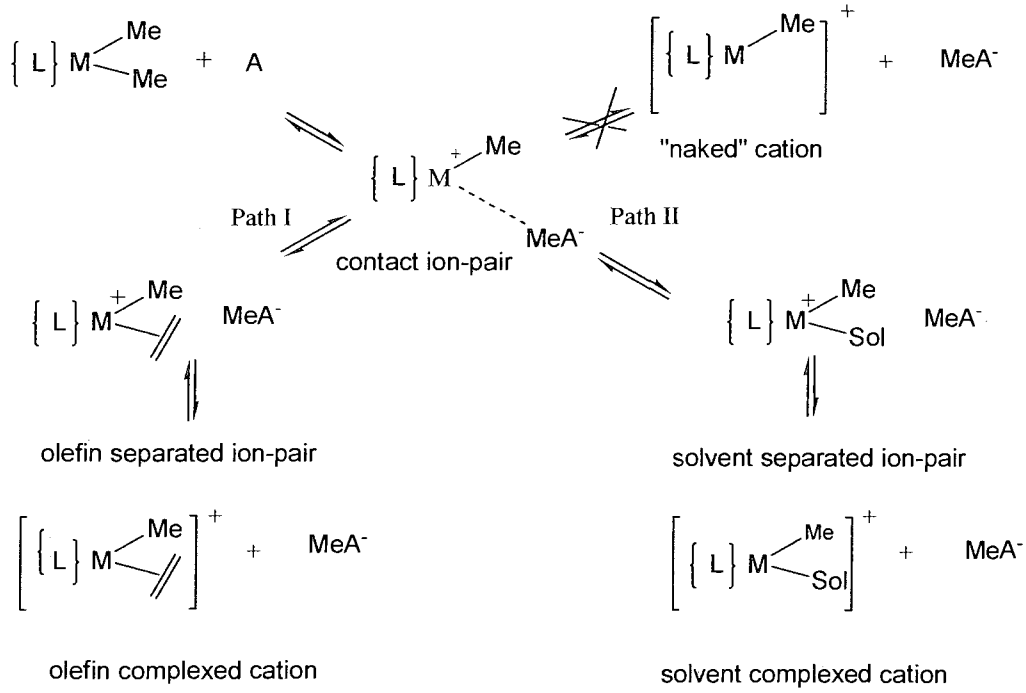

Figure 1.10. Possible reactions of contact ion-pair under typical polymerization conditions.

1.2.5 Electronic effects on polymerization activity

Electronic properties of the aromatic ligands are mainly associated with the electron-withdrawing or electron-donating ability of their substituents. One can presume that placing electron withdrawing substituents on the Cp ligand would make the metal center more electrophilic, thus affording a potentially more active catalyst by favouring the coordination step of Z-N polymerization. But it was found, for example, that electron-withdrawing groups placed on the Cp ring lower both the propagation rate and the molecular weight of polymer.

The effect of electron withdrawing substituents on the polymerization activity can be illustrated by the data in Figure 1.11 and Table 1.1,[42] where it is seen that electron withdrawing substituents as the F and Cl atoms lead to a decrease in catalytic activity. In the studies cited above, significantly lower activities for the complexes with strong π donor such as a methoxy-substituents explained by the coordination of these groups to MAO leading to inductive electron withdrawal from the indenyl ligand.

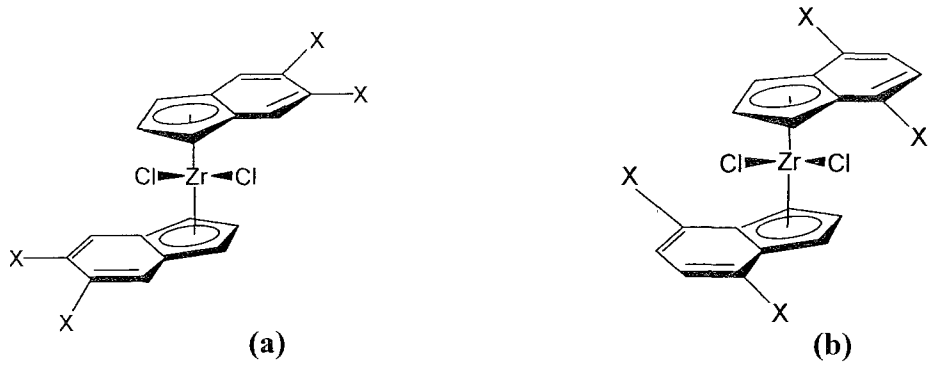

Figure 1.11. Complexes used to illustrate catalytic activity of electron-withdrawing substituents on indenyl ligands. Atoms X for (a) and (b) are given in Table 1.1.

Table 1.1. Catalyst activity of metallocene catalysts depicted in Figure 1.11.

Complex (a)		Complex (b)	
Atom X	**Activity, kg PE (mol Zr h)$^{-1}$**	**Atom X**	**Activity, g PE (g Zr bar h)$^{-1}$**
H	14000	**H**	43000
-Cl	1900	**-F**	18000
-OCH_3	122	**-OCH_3**	2300
-Me	2500	**-Me**	40000

Electron-donating substituents increase the electron density on the central atom and should, therefore, reduce activity. As shown in Figure 1.12 and Table 1.2, this is true for methyl and short hydrocarbon chains. Si-containing substituents on the Cp ring also have a negative influence on the activity for short chains, compared to Cp_2ZrCl_2, the activity is highest for intermediate-length chains (n=4) before it decreases again for longer alkyl chains.[43] Results are obviously very difficult to interpret in terms of the electron-donating or withdrawing ability of the substituents.

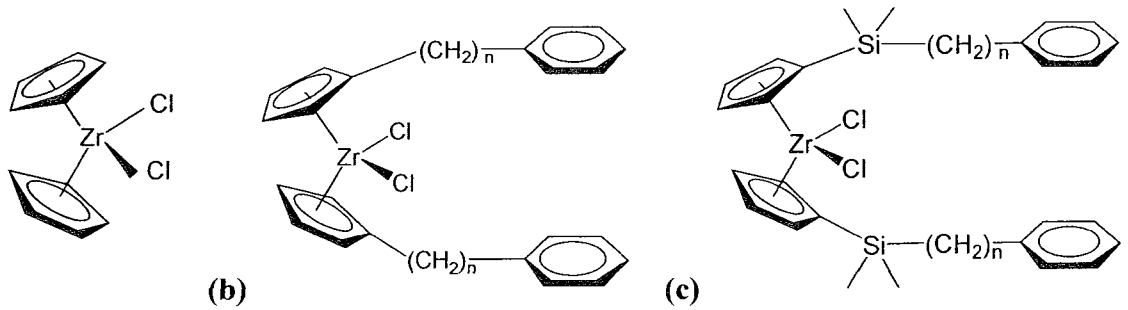

(a) **(b)** **(c)**

Figure 1.12. Complexes used to illustrate catalytic activity for catalysts with unsubstituted Cp rings(a), electron-donating hydrocarbon substituents on Cp rings (b), and Si-containing substituents on Cp rings (c).

Table 1.2. Catalyst activity of metallocene catalysts depicted in Figure 1.12.

Activity, kg PE (g Zr h)$^{-1}$		
Complex (a)	**Complex (b)**	**Complex (c)**
1490	(n = 0) 129 (n = 1) 529	(n = 1) 140 (n = 2) 350 (n = 4) 4970 n>4 decreases

1.3 Intramolecular interactions effect on polymerization activity

In general, early attempts to divide substituents effects into steric (bulky groups attached to the Cp ring) and electronic (substituents with electron withdrawing and electron donating groups) showed that in the case of steric effects, the more accessible the metal center the more active the catalyst, and in case of electronic effects, contrary to common belief: the less electron-deficient the metal the more active the catalyst. These electronic effects are more difficult to explain. In addition, for molecules where the substituent on the Cp ring is a long and flexible chain, no consistent trend is observed at all, although using such relatively long chains of alkyl-like substituents (R) for tailoring the Cp ring is common practice in olefin polymerization.[27, 44]

1.3.1 Long-chain fluorous substituents

Among long-chain flexible electron-withdrawing substituents, fluorous substituents are of particular interest, due to the introduction of the electronegative fluorine atom. The application of fluorous catalysts in chemistry and industry relies on ligand modification

by attaching fluorous substituents or tails, such as $(CH_2)_x(CH_2)CF_3$ or $(CH_2)_x(C_6F_5)$ to the ancillary ligand backbone, such as phosphines, phosphates, porphyrins and cyclopentadienes.[45-47]

Varying the number of fluorine atoms in the alkyl chain makes complexes soluble at ambient temperature in hydrocarbon and/or fluorous solvents. Moreover, solubility can change with temperature. Those transition metal complexes bearing ancillary ligation containing fluorous appendages have been, to date, mainly utilized to render catalysis possible in biphasic fluorous/organic or super critical CO_2 media. Coordination polymerization in fluorous media using fluorous ligands in pre-catalysts has been reported.[48] The polymerization using catalyst with fluorous substituents could possibly lead to improved physical properties of the polymer produced and could affect the reaction mechanism. Several fluorous cyclopentadienyl ligands have been reported.[49-53]

Since zirconocenes are extremely air- and moisture-sensitive, they are used strictly under anhydrous conditions and require special manipulation techniques and equipment. The hydrophobic properties of fluoroalkanes are well known. That is why fluoruos substituents are of particular interest as they might help prevent hydrolysis of Lewis acid-type catalysts and improve the stability and storage properties of catalysts. In some cases, Lewis acid- type catalysts with fluorinated ligands can be used even in water emulsions.[54]

Theoretically, fluorous substituents can increase the catalytic activity of the zirconocenes by increasing the positive charge on the metal center, because of the highly electron-withdrawing ability of the fluorine atoms. But, like for other electron-withdrawing atoms in substituents, is was found that ligands with C-F bonds are not innocent bystanders; it was in fact proven by X-ray crystal structure analysis, that

intramolecular C-F....Metal interaction often takes place in Z-N catalysts. The energy of this interaction is reported to lie around 10± 0.5 kcal/mol, and therefore C-F coordinating ligands have typical features of hemilabile ligands.[55] They can even permanently block available sites for olefin binding if the F atoms strongly coordinate to the metal.[42] Or they can decompose at room temperature because of defluorination.[56]

To prevent this interaction, ethylene or dimethylsilyl spacers are usually introduced between the cyclopentadienyl and the perfluoroalkyl chain.[57-59] The spacer group is found necessary to effectively insulate the cyclopentadienyl ring from the electron- withdrawing effect and prevent defluorination (F coordination to the metal) of the perfluoroalkyl chain.

1.3.2 Flexible long chain (agostic) interactions with metal, its characteristics and effect on polymerization

Electron-donating, alkyl and silicon containing alkyl-like substituents, depending on the chain length and the nature of alkyl substituents can interact directly with the Cp ring to which they are attached and, as a result, they can increase or decrease the electron density on the ring itself, and through inductive-like effects, also change the electron density around the metal center. Furthermore, if atoms from the chain are in close proximity to the metal center, they can also interact with it. In the case of fluorous substituents, the fluorine electron lone pair coordinates to the positively charged metal empty orbitals. When the alkyl-like group does not contain electron-withdrawing atoms or groups, the only possible interaction is that between C or H atoms and the positively charged, coordinatively unsaturated metal center. This type of interactions is called agostic (Figure1.13)

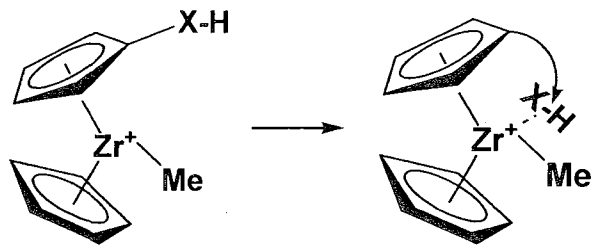

Figure 1.13. Intramolecular interactions between the positively charged metal and the flexible ligand framework.

The word agostic is the Greek word for "to hold on to oneself" and refers to the bonding interaction between a H-X polar bond (X = C, Si, Ge) and a metal, and it is characterized by distortion of the organometallic moiety which brings an appended X - H bond into close proximity with the metal center.[60] Agostic interactions belong to the so-called secondary bonding interactions, and can be recognized geometrically, when the distance between atoms falls bellow the simple sum of their van der Waals radii, and the distance is too long to be a single bond. Also it is somewhat directional. The bond energy is weak compared to covalent bonds. The most common interactions of this class and their energy are shown in Table 1.3.

Agostic interactions can be determined and characterized in many alkyl systems using a number of techniques, described, for example, in Schere's review.[61] Since agostic interactions exhibit severe bond distortion in the alkyl moieties, they can be characterized structurally by neutron diffraction, which can provide more precise hydrogen positions than X-ray diffraction. The redistribution of bonding electron density can be revealed by using spectroscopic techniques. For example, NMR analysis has been used to determine

Table 1.3. Energy of secondary bonding interactions.

Interaction	Energy, kcal/mol
Hydrogen bonds	2 - 20
Ion- dipole interactions	10 – 50
Dipole-dipole interactions	1 – 10
Agostic interactions	**1 - 10**
π- π stacking	< 10
van der Waals interactions	< 1
Cation - π interactions	1-20

^{1}H shifts to high field (δ = -5 to -15 ppm), and reduced coupling constants [^{1}J(C, H) = 75-100 Hz]. Vibrational spectroscopy also gives low vibrational frequencies for the M-H-C moiety ν(CH) (2100-2300 cm^{-1}) for the stretching mode. Topological analysis of the known molecular charge density, which can be experimentally or computationally determined, is also one of the powerful tools used recently to detect and study agostic interactions in organometallic compounds. The earlier concept invoked metal coordination to the methyl fragment, C-H, in a M - - η^2-HC manner, where the two, C and H, dangling atoms coordinate to the metal or metal ion with available coordination sites. The bonding was attributed to donation of electron density from one of the C-H σ orbitals to the metal orbitals.[62, 63] This mode of coordination is referred to as a classical agostic interaction. More recently, neutron diffraction structural characterization showed the C-H bond does not necessarily point towards the metal atom (Figure1.14). A survey of the structures showed in a number of complexes,[64] complex geometry consistent with a non-classical M - - η^3 –H_2C mode of binding. It was also pointed out that the non-

classical mode of binding is more common for longer alkyl chains (n >2) than the classical one.[65]

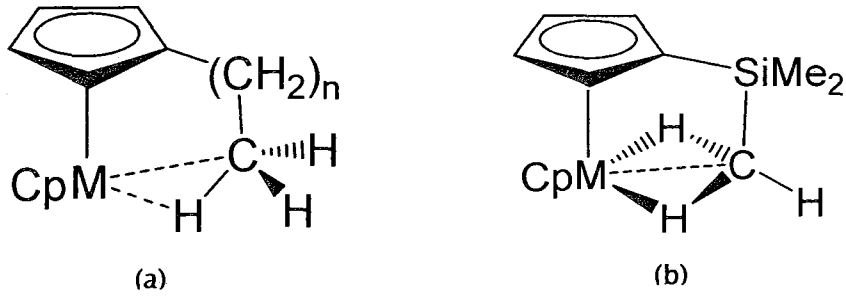

Figure 1.14 Types of M...H_3C agostic interactions, classical M - - η^2–HC (a) and non-classical M - - η^3–H_2C (b).

Negative hyperconjugation also can be used to explain the bonding mechanism of agostic interactions. This is similar to the hyperconjugation concept for carbocations in organic chemistry, but $C\text{-}C^{+\delta}$ should simply be changed for $C\text{-}M^{+\delta}$.

Generally, hyperconjugation, i.e. the interaction of σ bonds with a π network in molecules, provides electron density to electron deficient centers or withdraws electron density from electron-rich centers, and influences the conformational equilibrium. Three types of hyperconjugative interactions are presented in Figure 1.15 as double-bond/no-bond resonance structures. There is no evidence for sacrificial hyperconjugation in neutral hydrocarbons, where the interaction is between a filled σ-bond and a π-framework, as for example in toluene (Figure 1.15a). This is called sacrificial hyperconjugation because the contributing structure contains one two-electron bond less than the normal Lewis formula. The concept of hyperconjugation also applies to carbenium ions and radicals, where the interaction is now between σ-bonds and an

unfilled or partially filled π- or p-orbital; referred to as positive hyperconjugation (Figure 1.15b). The interaction between filled π- or p-orbitals and adjacent antibonding σ*-orbitals is referred to as negative hyperconjugation, as for example in the fluoroethyl anion (Figure 1.15c). These two latter cases are examples of isovalent hyperconjugation (the contributing structure containing the same number of two-electron bonds as the normal Lewis formula). Hyperconjugation is widely used in organic chemistry to explain the anomeric effect, the conformational behaviour of backbones in nucleic acids, torsional barriers and etc.

Agostic interactions play an important role in the chemical behaviour of saturated organic ligands, especially σ-bond (C-H, C-X, H-X) activation processes.[66-68] In 1983, Brookhart, Green and Rooney proposed a complementary mechanism to the Cossee-Arlman chain growth scheme, which involves electronic stabilization of the ground state

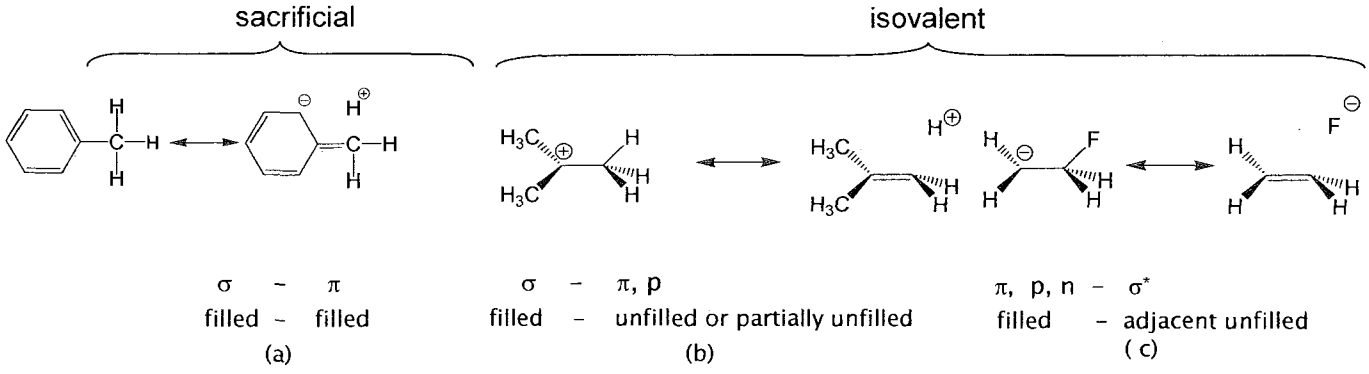

Figure 1.15. Double-bond/no-bond resonance hyperconjugation representations: sacrificial hyperconjugation (a), positive (b) and negative (c).

and the transition state by interaction of the metal with one of the α-hydrogen atoms from the polymer chain, a so-called α-agostic interaction. This is known as the modified

density distribution for the different species are examined. The nature of possible intramolecular interactions between substituents and the metal will be examined and discussed.

In Chapter 3, the calculations are repeated for modified alkyl substituents adding into their chains the silicone and fluorine atoms. How the substituent modifications changed the nature of possible intramolecular interactions between substituents and the zirconium is presented.

Finally, Chapter 4 focuses on the factors calculated in Chapter 2 and 3 that might control catalytic activity. Concluding remarks and outlook are given in Chapter 5.

There is a large body of literature on computational studies of Z-N catalyzed olefin polymerization with *ab initio* quantum chemistry and especially density-functional theory (DFT) methods. Today DFT is an important tool for computational investigations on group 4 complexes.[73]

1.5 Outline of the thesis

Our aim is to understand how the introduction of alkyl flexible chains, silicon-containing, and fluorous substituents, alters the coordination environment and the electronic properties of the active metal center.

On the basis of the literature survey just discussed, model zirconocenium complexes of general formula $[Zr(\eta^5\text{-}C_5H_5)(\eta^5\text{-}C_5H_4R)Me]^+$, are investigated, where R = H, ^{t}Bu, $(CH_2)_nCH_3$, CF_3, SiF_3, $SiMe_2Y$, Y = Me, F, $(CH_2)_nCH_mF_{3-m}$, the number of fluorine atoms (m) and the length of the hydrocarbon chain (n) varies from 0 to 3. This choice of unbridged model complexes does not impose structural constraints and allows free ring rotation. Flexible alkyl chains, with or without silicon, and fluorine-containing alkyls represent electron-donating and electron withdrawing ligands respectively. The hydrocarbon chain between the Cp rings and the fluorous part of the ligand, when present, can serve as a model of spacer effects. It is also of interest to understand how substituents affect the olefin binding energy and the Zr-Me bonding, factors that are deemed crucial for the catalytic activity of the complexes in the polymerization process. Olefin-catalyst complexes will be studied, for the same model systems.

Further in Chapter 2, results of calculations for zirconocenium complexes with alkyl substituents with different chain lengths are reported. The structure, energies, electron

Green-Rooney Z-N polymerization mechanism with agostic assistance (Figure 1.16).[60, 63, 69, 70] In Z-N polymerization, the α-agostic transition state (TS) assists the alkene insertion, and controls tacticity of the growing polymer chain (P); β- and γ-agostic interactions stabilize the growing polymer chain between periods of chain growth.

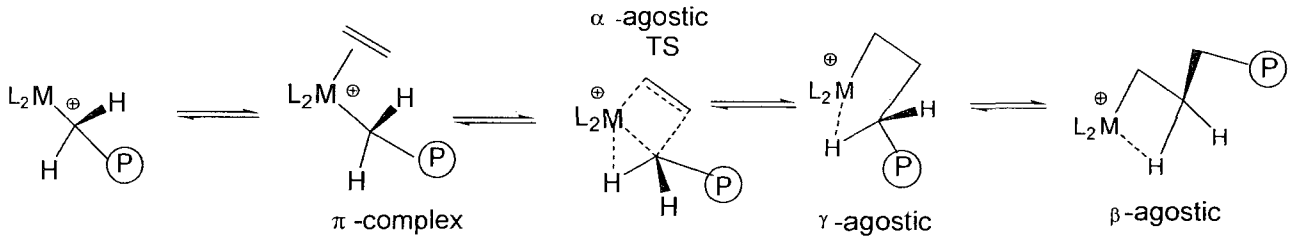

Figure 1.16. Modified Green-Rooney polymerization mechanism with agostic assistance.

1.4 Computational studies of metallocene catalysts for olefin polymerization

Catalytic processes, including olefin coordination polymerization, are by nature very fast reactions. Very often it is impossible to isolate reaction intermediates experimentally and therefore to determine reaction mechanisms and substituent effects on polymerization. Computational methods based on quantum chemistry[71] have become reliable tools to study mechanisms of catalytic reactions. Quantum chemical characterization provides information in terms of molecular geometry, interaction energies, vibrational spectra and electron density.

Morokuma used the Hartree-Fock method to characterize saddle points for the reaction of ethylene with $[TiCl_2CH_3]^+$.[72] A number of olefin complexation and insertion activation energies using various catalysts have been calculated with different quantum chemistry *ab initio* levels and basis sets.[30]

CHAPTER 2

Classical *vs.* non-classical agostic interactions in zirconocenium polymerization catalyst

2.1 Introduction

Olefin coordination polymerization catalysts consisting of group 4 metallocene dichloride pre-catalysts and co-cocatalyst methylaluminoxane (MAO) have received considerable industrial interest. They belong to one of the most highly active and selective classes of catalysts for α-olefin polymerization, and offer unique possibilities for controlling polymer structure and properties.[6, 14] In the zirconocene dichlorides of general formula $[Zr\{\eta^5\text{-}C_5H_{5\text{-}n}R_n\}_2Cl_2]$, the zirconium atom is η^5-coordinated to cyclopentadienyl rings (Cp). Often one or more hydrogens of the Cp rings are substituted (R≠H) with alkyl, aryl or other groups and elements. According to the Cossee-Arlman mechanism,[17-19] when such pre-catalysts are reacted with an excess of a co-catalyst, the active species responsible for the polymerization activity are formed; it is now agreed that such species are the 14-electron cationic zirconocenium complexes $[Zr\{\eta^5\text{-}C_5H_{5\text{-}n}R_n\}_2Me]^+MAO^-$, where the zirconium center has Lewis acidic coordination sites. Several reports show that the choice of ligands, and catalyst performance, is related and sensitive to both the electronic and steric surroundings of the active site. These factors can be regulated by tailoring the Cp rings with various substituents. Such systematic modification of the ring allows enhancement of the catalyst activity and control of polymer properties. Therefore, understanding how ligand modification affects olefin polymerization is very important. Experimental investigations of the substituent

effect on the catalytic olefin polymerization performance of metallocene complexes of group 4 metals have been widely reported.[16, 20-31]

To increase the solubility of the pre-catalyst complex and to tune the catalytic activity, zirconocenium catalysts substituted with a longer alkyl [R = - $(CH_2)_n$ -CH_3 (usually n = 1 to 8)] chain are often used.[26] If the substituent is a long and flexible chain, then its terminal group of atoms can come close to the metal center. Since the metal is positively charged and coordinatively unsaturated, various interactions are possible between the relatively electron-rich alkyl and the zirconium (Figure 1.13). This type of interaction is known as an agostic interaction.[60, 61] Usually agostic interactions are viewed as an interaction between the metal and a ligand terminal hydrogen, i.e. classical M - - η^2 –HC coordination (Figure 1.14 a). However, a survey of experimental structures showed that, in a number of complexes, the geometry is more consistent with a non-classical M - - η^3 –H_2C mode of binding (Figure 1.14 b).[64] It was also pointed out that the non-classical mode of binding is more common than the classical one for longer alkyl chains ($n \geq 2$).[65] So far there is no explanation for these findings.

The aim of this work is to characterize computationally the possible interactions, if any, between the metal center and the alkyl flexible chains in tailored Cp rings, to investigate their nature, and to understand how they alter the coordination environment and the electronic properties of the active metal center.

Good candidates as model zirconocenium complexes for investigation of agostic interactions, are complexes with the general formula $[Zr(\eta^5\text{-}C_5H_5)(\eta^5\text{-}C_5H_4R)Me]^+$, R = H, ^{t}Bu, $(CH_2)_nCH_3$, where the length of the alkyl chain on the Cp ring is defined by n that varies from 0 to 3. Thus, unbridged zirconocenium catalysts with a monosubstituted

cyclopentadienyl, are chosen as a model complex for further investigation. The structures calculated in this work are depicted in Figure 2.1. This choice of model complex does not impose structural constraints, allows free ring rotation and flexible alkyl chain coordination to the central atom, if present.

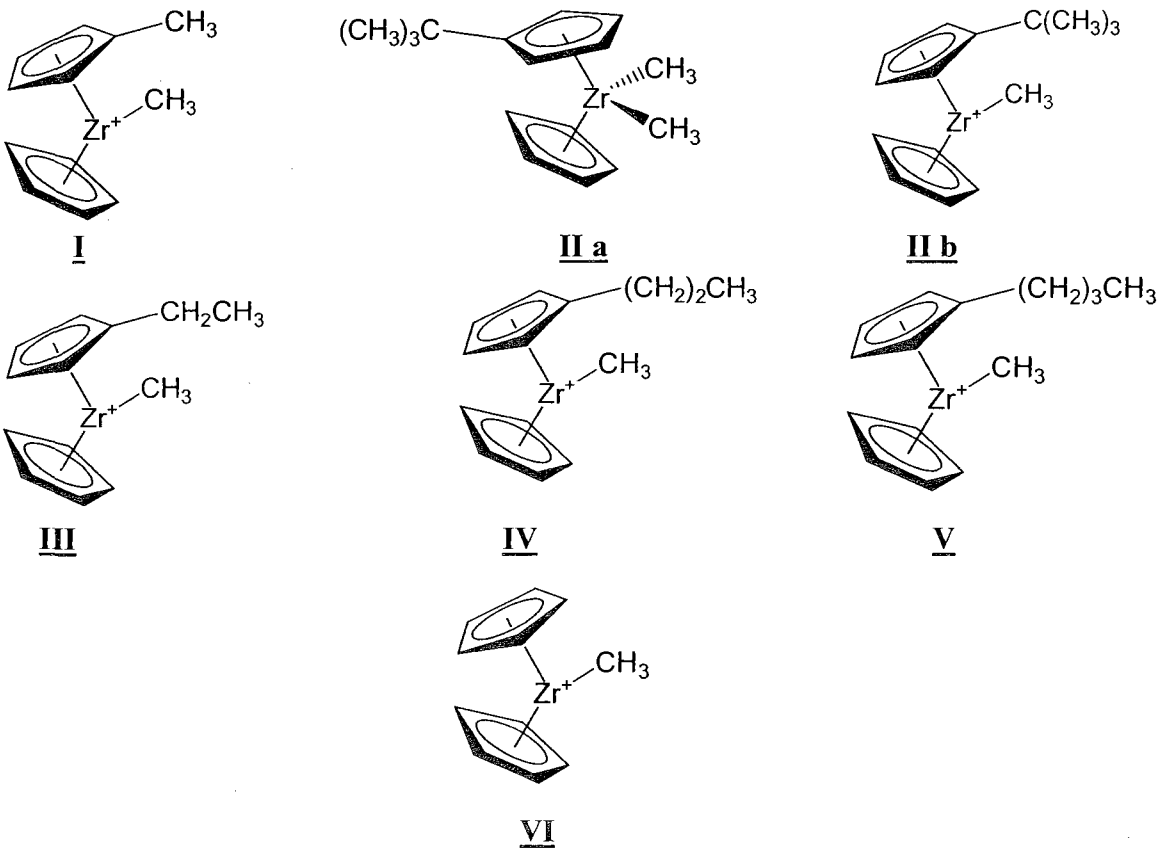

Figure 2.1. Model complexes.

A diagram illustrating the labeling of carbon atoms in the substituents is shown in Figure 2.2. A Greek letter designates the carbon position in hydrocarbon ligand(s). The first carbon attached to Zr is labelled as C_α the next in the chain as C_β the third as C_γ etc.

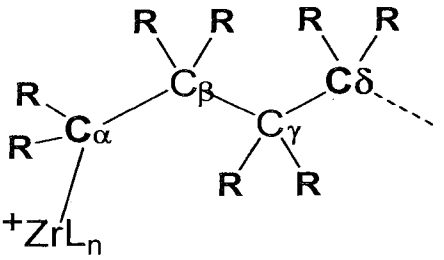

Figure 2.2. Labelling diagram for carbon atoms in alkyl ligands.

2.2 Computational Methodology

To investigate how many and what kinds of interactions are possible in the model complexes investigated, calculations based on density-functional theory (DFT) were performed. In an attempt to gain deeper insight into the nature of the interactions, the Natural Bond Orbital (NBO) analysis and the quantum theory of atoms in molecules (AIM) were used.

DFT has already been successfully used for olefin polymerization studies.[73] Becke's three parameter exchange functional with the Lee-Yang-Parr correlation functional (B3LYP)[82-85] is one of the popular DFT methods which has been proven useful for the description of polymerization using metallocene catalysts. For quantum chemistry calculations of metallocene coordination polymerization, this method is very often combined with the LANL2DZ basis set for the metal and a standard all-electron a double-ζ quality basis set such as 6-31G (d,p)[86,87] for all other atoms. For the calculations performed on complexes similar to those under investigation in this thesis, $[Zr\{(\eta^5\text{-}C_5H_4)_2\ SiH_2\}R]+$ (R - ethyl, - *n*-butyl) + C_2H_4, DFT (B3LYP/LANL2DZ) results are comparable to results of higher-level calculations: geometries are within experimental errors, and energies deviate by ~ 1 kcal/mol.[74]

In this work, all structures were fully optimized using the Gaussian 98 software package.[75] No local symmetry and no geometrical constraints were imposed in the optimizations. Vibrational frequencies were calculated for all stationary points to characterize them as minima (no imaginary frequencies) or transition states (one imaginary frequency). Relative energies reported include zero-point corrections. To evaluate the effect of hyperconjugative interactions and atomic charges, NBO second-order perturbation analysis has been used, as provided within Gaussian 98.

AIM2000 was used to analyze the topology of the electron denisty.[76] In order to include core electrons on the Zr atom, the DZVP (DeMon DFT orbitals) basis set was used to obtain wavefunctions for AIM calculations.[77] The structures were fully reoptimized using this larger basis set before AIM calculations were performed.

2.3. Results

2.3.1 Geometry analysis

The molecular geometry is analyzed by comparing the calculated distance between two atoms with the sum of their Van der Waals (VDW) and their covalent radii values (Table 2.1).[78] In addition, bend angles were compared to the corresponding angles anticipated from the hybridization type of the central atom, e.g. sp^n, or sp^3d^m (n = 1-3, m = 1, 2). An intramolecular interaction is suspected when the distance between two atoms is less than the sum of their VDW radii for the elements in question, and if angles are significantly distorted from the values expected on the basis of hybridization.

Table 2.1. Van der Waals and covalent radii of selected atoms.

Element	Van der Waals radius, (Å)	Covalent radius, (Å)
Hydrogen, H	1.20	0.28
Carbon, C	1.70	0.68
Zirconium, Zr	2.01	1.56

2 3.1.1. Uncomplexed ligand Cp^- - ^tBu

It is of interest to compare the geometry of the uncomplexed ligands with those in zirconium complexes. As an example of uncomplexed ligand for geometry comparison, the ligand with the tertiary butyl substituent was chosen, because it represents a medium-size alkyl chain with two carbon atoms and the experimental structural data for the corresponding catalyst are available.[26]

The optimized molecular geometry of the ligand, selected angles and bond lengths are shown in Figure 2.3. As expected, a methyl group of the tertiary butyl substituent is in the plane with the Cp ring for the minimum energy structure (Figure 2.4 a). This calculated conformational geometry is referred to as planar hereafter and is in a good agreement with reported conformations for similar compounds.[79]

Calculations indicate that the conformation where one of the methyl groups is perpendicular to the Cp plane (Figure 2.4 b) is a transition state lying 1.25 kcal/mol higher in energy than the minimum energy planar conformer; connecting ^tBu ligand rotational isomers. This conformation is referred to as perpendicular hereafter.

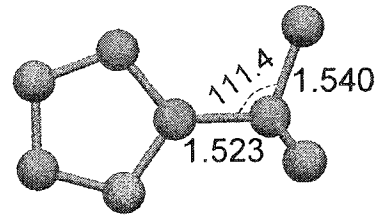

Figure 2.3. Molecular geometry (H – omitted) for the uncomplexed Cp– ^{t}Bu ligand with selected bond lengths (Å) and angles (°).

NBO analysis can be used to explain why the planar conformation is more stable than the perpendicular one. The Cp ligand is aromatic in nature, with the negative charge -1 shared by all five ring carbons. The NBO routine replaces the delocalized MO of the Cp aromatic π-framework with localized Natural Bond Orbitals corresponding to the conventional Lewis σ- or π-bonds and lone pairs (see also Appendix A). The NBO Lewis ^{t}Bu substituted Cp ligand structures correspond to the structures shown in Figure 2.4.

In this case, the Cp ring has five σ-bonds, two π-bonds and a lone pair of electrons (p-orbital in nature), perpendicular to the Cp plane and located on the ring's carbon atom attached to the substituent. Since two lone-pair electrons are also located on this carbon, the negative charge for the Lewis structure has to be localized on the same carbon.

NBO analysis also allows the evaluation of delocalization of localized electron orbitals using a second-order perturbation approach. The NBO predominant hyperconjugative interaction for the perpendicular conformation is the interaction

between the ring p-electrons and one of the substituent adjacent unoccupied σ^*-orbitals (Figure 2.4 b). For the planar conformation similar interaction with the ring p-electrons exists for two substituent carbons σ^*-orbitals (Figure 2.4 a). Overall these two interactions in the planar conformer (13.1 kcal/mol combined) are stronger than that in the perpendicular conformation (8.8 kcal/mol).

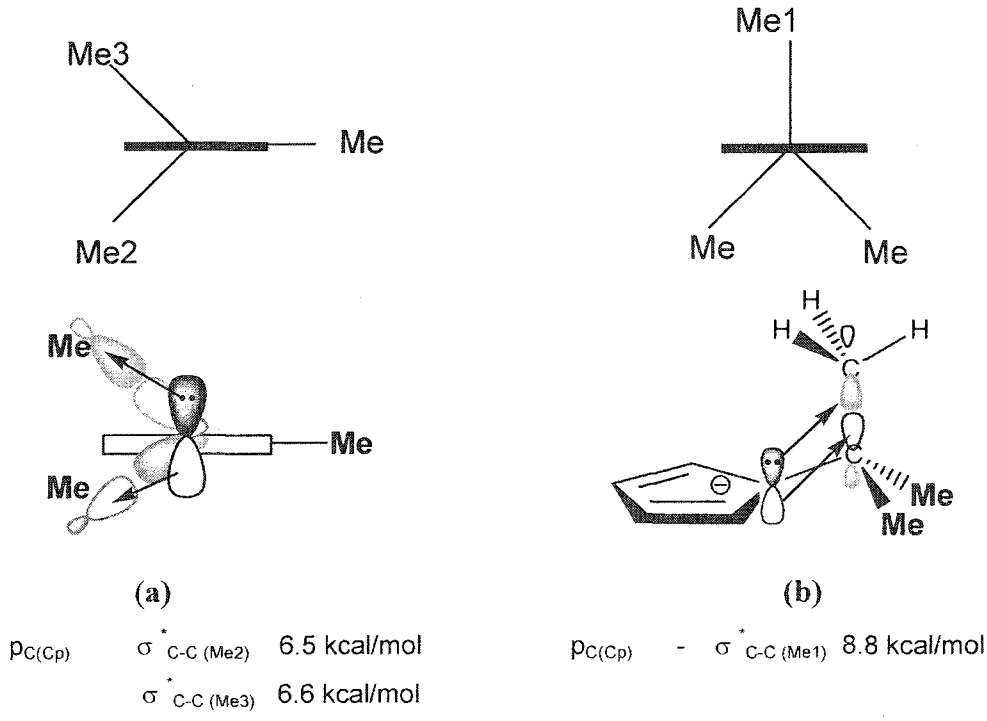

Figure 2.4. NBO Lewis structures and predominant hyperconjugative interaction for the uncomplexed Cp ligand with a ^{t}Bu substituent; perpendicular conformation (a), planar conformation (b).

2.3.1.2 Neutral pre-catalyst

The optimized molecular geometry of the model complex **IIa** is shown in Figure 2.5, along with selected bond lengths and angles. The Cp ring substituent orientations with respect to the other methyl ligands attached to the zirconium center are shown in Figure 2.6.

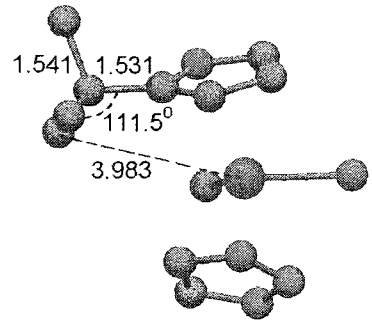

Figure 2.5. Molecular structure of the neutral pre-catalyst, **IIa**, with selected bond lengths (Å) and angles shown (°). (H – omitted, C in green, Zr in purple)

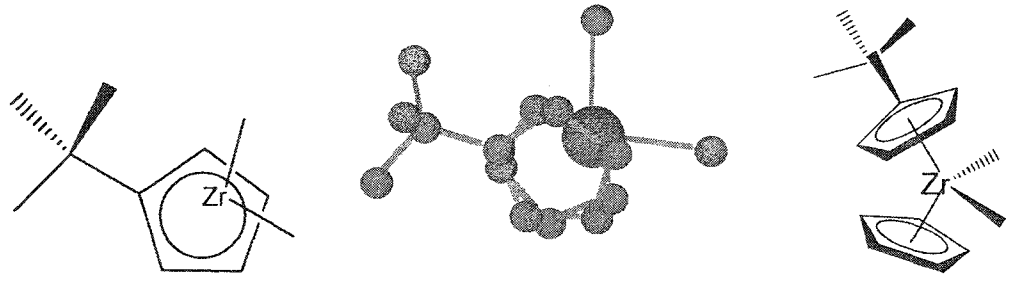

(a) **(b)** **(c)**

Figure 2.6. Cp substituent orientation with respect to the two other methyl ligands in **IIa**; view from above, two Cp rings almost eclipsed (a), 3D view from above (b) and side view (c).

The Cp rings are almost in an eclipsed conformation with respect to each other. The tertiary butyl substituent is in a planar conformation with respect to the Cp plane, and the calculated ligand angles and bond lengths are similar for both the neutral pre-catalyst and the uncomplexed ligand.

Analysis of the geometry of the neutral pre-catalyst does not reveal structural evidence of intramolecular interactions between the substituent of the Cp ring and the metal center. For instance, the distance between the closest carbon atom and the zirconium atom (3.98 Å) is longer than the sum of the VDW radii (3.71 Å) and far longer than covalent radii (2.24 Å) for the corresponding atoms. The same holds for all the hydrogen atoms closest to the metal (the closest hydrogen to the Zirconium is 3.55 Å away from it). Therefore, no weak interactions between the carbon/hydrogen atoms and the metal center can be inferred from the geometry of the neutral pre-catalyst complex.

2.3.1.3 Positively-charged catalysts

In order to transform a neutral pre-catalyst into the catalytically active positively charged species, one methyl ligand attached to the Zr atom has to be removed. The optimized zirconocenium catalyst geometry of **IIb** is depicted in Figure 2.7. In the positively charged zirconocenium catalyst, the Cp ligand bearing a substituent changes position, rotating from the common eclipsed conformation of the neutral pre-catalyst to an almost staggered conformation (Figure 2.8). One of the ligand atoms ($C\gamma$) is now very close to the position of the carbon atom of the methyl ligand that has been removed from **IIa**, suggesting possible interaction between the $C\gamma$ atom and the metal center.

Further analysis of the distances and angles reveals additional structural evidence for an intramolecular interaction between the terminal CH_3 group and the coordinatively unsaturated, positively charged metal center. The Zr - C_γ, Zr – $H_1$and Zr – H_2 distances are 2.85 Å, 2.52 Å and 2.81 Å, respectively, and these distances are shorter than the sums of the van der Waals radii for the Zr/C and Zr/H atom combinations (3.71Å and 3.21 Å,

respectively). However, these interactions can not be classified as typical ionic bonds in Zr hydrides or carbides, since typical Zr-C bond lengths are 2.2–2.3 Å in carbides and typical Zr-H bond lengths are 1.3-1.5 Å in hydrides. This is also consistent with the fact that the interatomic distances are also larger than the sum of the covalent radii for Zr-C (2.24 Å) and Zr-H (1.84 Å). The fragment C_β-C_γ pointing towards Zr also has the longer bond length (1.55 Å), compared to other similar bonds (1.53 -1.54 Å) in methyl groups pointing away from the Zr atom, and analogous bonds in molecules without interactions with the metal, such as the neutral pre-catalyst or the uncomplexed ligand (Figure 2.3 and 2.5).

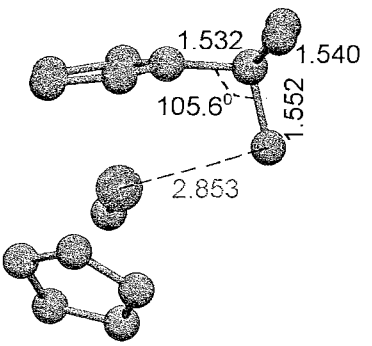

Figure 2.7. Molecular structure of the catalyst, **IIb**, with selected bond lengths (Å) and angles shown (°). (H – omitted, C in green, Zr in purple).

Finally, the distorted tetrahedral C_α - C_β- C_γ angle (105.6°) is smaller than the corresponding angles in the unconmplexed ligand (111.4°) or in the neutral pre-catalyst substituent (111.5°). All of these features point to a weak interaction with the metal center of an agostic type.

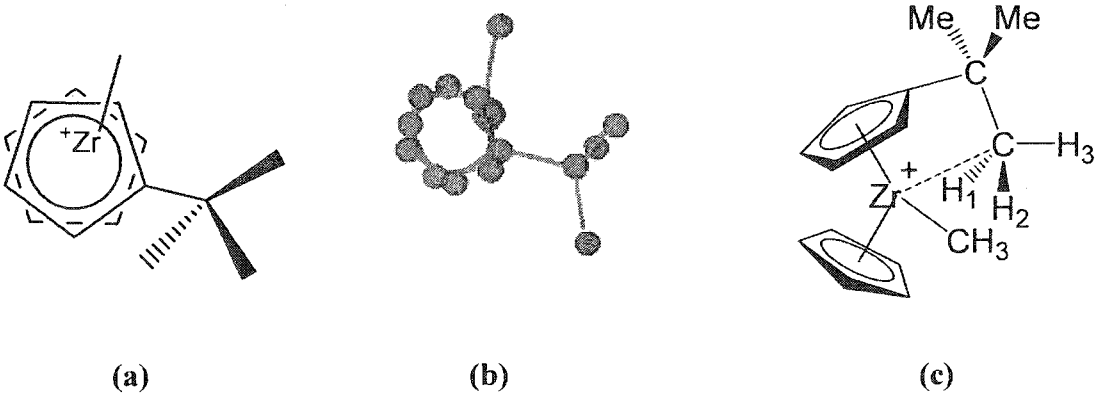

(a) (b) (c)

Figure 2.8. Cp ligand orientation with respect to the methyl ligand position in structure **IIb**; view from above (a), 3D view (b), side view (c).

Optimized molecular geometries of the zirconocenium complexes with longer alkyl chains, structures **III**, **IV** and **V**, are shown in Figure 2.9 along with selected distances between the metal center and the closest carbon/hydrogen atoms of the substituents. To avoid a crowded picture, the Zr-C_δ and Zr-C_ε distances are not shown for complex **V**, but they are 2.95 Å and 2.94 Å, respectively. Based on the analysis of the geometry, intramolecular interactions between the Zr and the alkyl chain atoms could be suspected for all complexes.

The complex **III** with an ethyl substituent is similar to the complex **IIb** with the ^{t}Bu substituent, which also contains two carbon atoms in the chain and was described above. In both complexes the C_γ atom and the two hydrogens attached to it are close to the metal center and agostic interactions can be inferred. In **IV**, with three carbon atoms in the chain, based on the distance analysis, there are most likely no intramolecular interactions between the zirconium and $C_\gamma H_2$ group like those found in **III** or **IIb**. On the other hand,

in **IV**, C_δ and one of the hydrogen atoms attached to it are close to the metal center. This atomic arrangement also meets the criteria for agostic interactions. In **V**, intramolecular interactions with the metal most likely exist for both the C_δ and C_ε atoms, as well as with one of the two hydrogens attached to each of these carbon atoms.

In the case of ^{t}Bu and ethyl substituents, complexes **IIb** and **III** respectively, although two hydrogens (H_1 and H_2 in $C_\gamma H_3$ fragment) are the closest atoms to the metal center, none of them are directly pointing towards Zr; they are almost equally remote from the

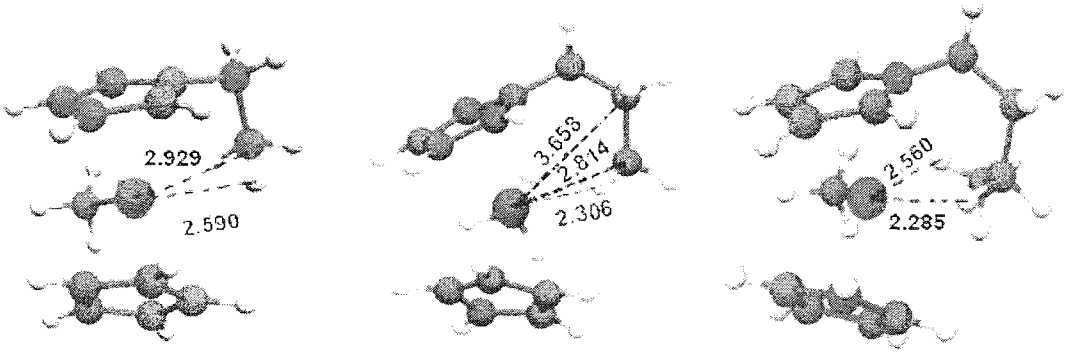

III **IV** **V**

Figure 2.9. Molecular structure of the catalysts, **III**, **IV** and **V** with selected bond lengths (Å) and angles (°) shown. (H in white, C in green, Zr in purple)

metal and lie below and above the C_α-C_γ-Zr plane. The C_γ-H_1 and C_γ-H_2 distances are longer than C_γ-H_3, angles C_α-C_γ-H_1 and C_α-C_γ-H_2 have greater values for two H atoms closest to Zr, and while the angle C_α-C_γ-H_3 is smaller. The geometry of the CH_3....Zr moiety is thus more consistent with a non-classical M - - η^3-H_2C rather than a classical M - - η^2–HC mode of coordination, where only one hydrogen atom (H_1) is relatively close

to the metal. A classical agostic interaction can be inferred for longer chain alkyl substituents as in **IV** and **V.**

2.3.2 NBO analysis of agostic interactions

NBO analysis provides an alternative to the classical bond concept which has proven very useful to characterize weak bonding interactions. A formal electron count would predict the Zr atom to be d^0 in nature. However, NBO analysis allows for departure from this formal Lewis model, and partial occupancy of each of the metal 4d orbitals hybridized with the 5s orbital. In the complexes investigated, five Zr lone-pair-type orbitals were found in the NBO analysis with low electron occupancies, but no two-center bonding or anti-bonding orbitals were found between the Zr and Cp ligands. The remaining orbitals are either core orbitals or Rydberg orbitals. One of the lone-pair-type orbital is mostly 5s in nature, whereas the rest are mostly 4d in nature, slightly hybridized with 5s; they will be referred as Zr d-orbitals in the following. Because the Zr d-orbitals are partially filled, they are capable of both donating and accepting electron density. Due to the flexibility of the alkyl chain, the substituent may locate in close proximity to the Zr atom; therefore, interactions between a relatively electron-rich alkyl frame and the positively-charged, coordinatively-unsaturated central atom become possible. Interactions between filled and anti-bonding NBOs orbitals cause a deviation from Lewis structures and can be used as a measure of delocalization, allowing to evaluate the effect of hyperconjugation. The magnitude of the interaction between each donor and acceptor NBO is estimated by second-order perturbation theory. The stabilization energy of

delocalization is a quantitative measure that allows comparisons of the interactions in various ligand-metal complexes.

In the complex **I** with the methyl-substituted Cp ring, the highest NBO stabilization energy of the substituent C-H σ bond interactions with the metal orbitals is less than 5 kcal/mol. Since there is no noticeable angle and bond distortion for this ligand, it is assumed that there are no intramolecular interactions between the H atoms of the Cp ring substituent and Zr, and all interactions weaker than 5 kcal/mol will not be considered hereafter.

The Lewis structure, the natural charge distribution and hyperconjugative interactions for structure **IIb**, are shown in Figure 2.10.

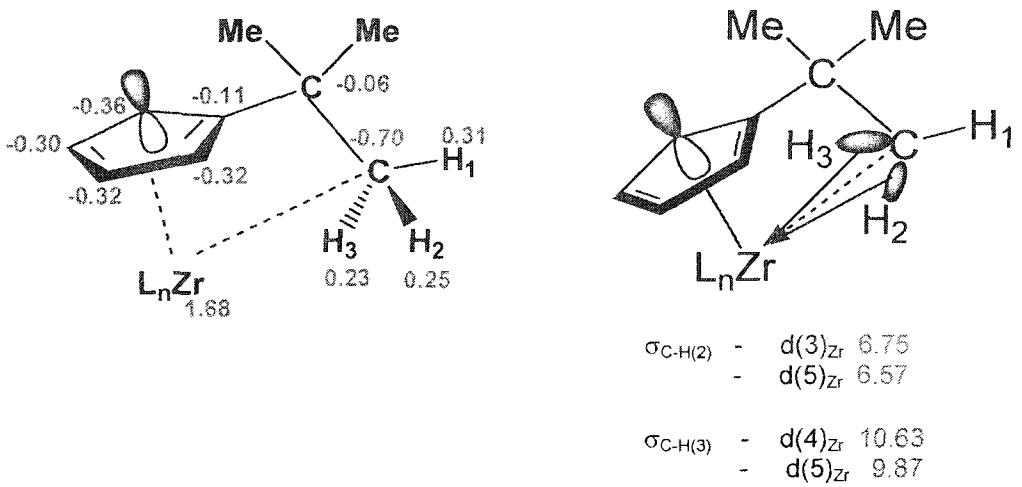

Figure 2.10. NBO Lewis structure, charge distribution (blue) and predominant hyperconjugative interactions for **IIb** substituent in kcal/mol (red).

Unlike the uncomplexed ligand, the ring p-electrons do not interact with the ^{t}Bu substituent; rather, the Cp ligand acts as an electron-density donor to the highly positive Zr atom (the formal oxidation state is +4).

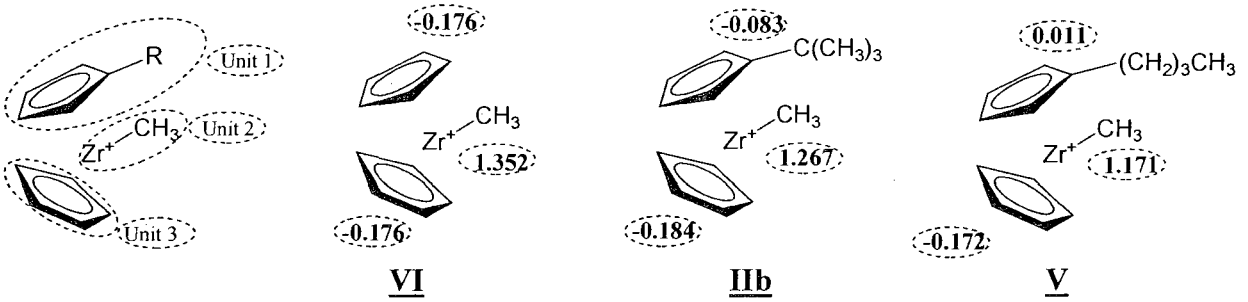

Figure 2.11. NBO charges for molecular units of different zircnocenium complexes.

This results in a reduction of the negative unsubstitued Cp ligand natural charge which is only -0.176 in complex **VI**, whereas the formal uncomplexed Cp ligand charge should be -1.00 (Figure 2.11). The ^{t}Bu-substituted Cp ligand natural charge is even less negative than the charge for the unsubstituted Cp ring and it is equal to -0.083, while the positive charge of the Zr-CH_3 unit decreases for substitueted complexes compared to **VI**. Since the second Cp ligands have almost equal negative charges (-0.17 and -0.18) in all complexes investigated, the ^{t}Bu-substitueted Cp ligand is a better electron donor to Zr than the unsubstituted ligand.

The flexible substituent attached to the ring redistributes electron density to the metal center not only through electron-density donation or electron-density withdrawing with respect to the ring, but also by directly interacting with the metal. The key interactions are a transfer of electrondensity from the C_γ-H_1 and C_γ-H_2 σ orbitals to the zirconium practically vacant d-orbitals. Four $C_\gamma(H_1/H_2)$-Zr orbital interactions larger than 5 kcal/mol

were found for structure **IIb**, with stabilization energies ranging from 6.6 to 10.6 kcal/mol, and the molecular geometry is consistent with the M - - η^3-H_2C mode of agostic coordination. The NBO charge analysis reveals that the C_γ atom is significantly more negative than the adjacent C_β, and the C_α atom carrying the smallest charge.

For structure **V**, with a longer substituent on the Cp ring with R = $(CH_2)_3$-CH_3, the NBO Lewis structure, charge distribution and predominant hyperconjugative interactions are shown in Figure 2.12.

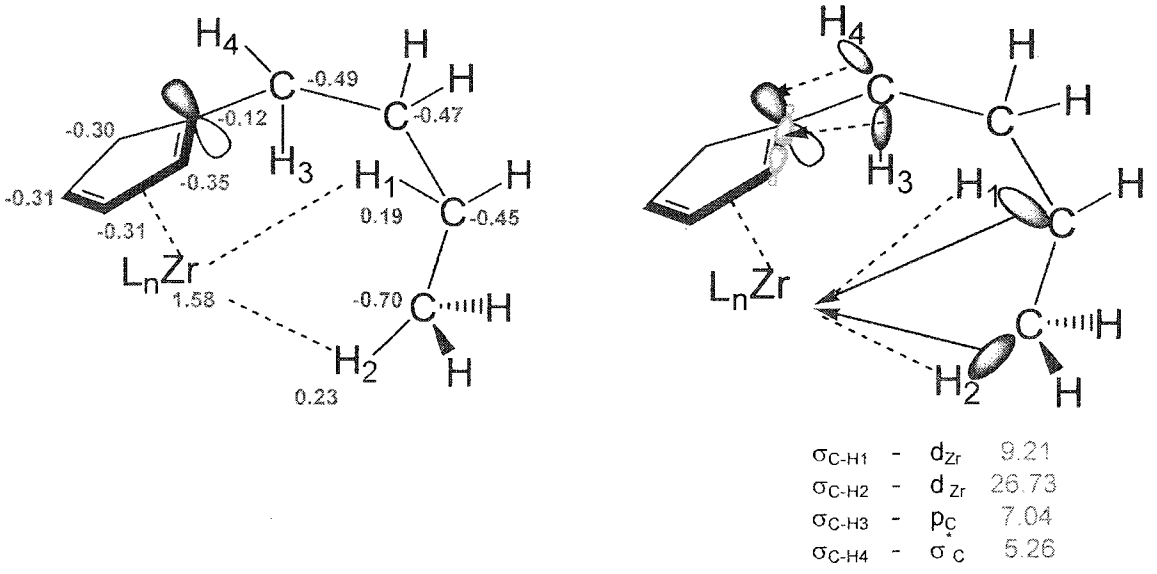

Figure 2.12. NBO Lewis structure, charge distribution (in blue) and predominant hyperconjugative interactions (in kcal/mol, in red) for **V**.

The alkyl group might act as an electron-density donor to the Cp ring, although the stabilization caused is weak. The stabilization energy due to electron-density transfer from the C_β-H_4 σ orbital to the C_α p-orbital is 7.0 kcal/mol. It might appear like an unfavourable 2e-2e orbital interaction, but it can be justified, as NBO only assigns partial occupancy, less than 2 electrons, to the carbon p-orbital. Since NBO only provides an

approximate representation of the Cp aromatic π framework and, based on charge analysis, the charge for C_α is the lowest. It means that electron density is redistributed towards the other carbons, leading to a lower NBO electron occupancy for C_α, possibly making this interaction stabilizing. The stabilization energy for the interaction of the C_β-H_3 σ orbital in plane of the Cp ring with the C_α-$C_{(Cp\ ring)}$ σ^* orbital is 5.3 kcal/mol. The latter interaction is just slightly larger than 5 kcal/mol and might not be significant. The strongest hyperconjugative interactions (up to 26.7 kcal/mol) in this complex involve donation of electron density to the zirconium d-orbitals from the $C_\delta H_1$ and $C_\varepsilon H_2$ σ orbitals. Unlike the shorter substituent in **IIb**, only one of the hygrogens (H_1 or H_2) from each methyl group participates in these interactions. The stabilization energy for the $C_\delta H_1$...Zr interaction is larger than that for the $C_\varepsilon H_2$...Zr interaction. The molecular geometry is more consistent with the classical M - - η^2–HC rather than the non-classical mode of binding.

NBO charge analysis shows that the charge on the Cp ligand with longer n-propyl and n-butyl substituents is not negative as it used to be for the shorter ^{t}Bu-substituted Cp or the unsubstituted Cp ligand. For example, for complex **V**, the charge is +0.011 (Figure 2.11). Therefore, longer alkyls are stronger electron-donating substituents than shorter ones.

Thus, for alkyl substituents, relatively short substituents like ethyl and ^{t}Bu do not donate electron density to the Cp ring, which could be further redistributed to Zr. As a result, the substituent acts only as a direct electron donor to the metal through the agostic interaction of the terminal CH_3 group in a non-classical manner. Angle distortion and bond elongation are more severe than for the longer chains. In the case of longer alkyls,

which are possibly electron-donating groups to the Cp ring, Zr positive charge compensation might occur due to both electron donation to the Cp ring and one or more direct classical-type agostic interactions. Due to the complexity of the interactions of the Cp ligand orbitals with those of the metal, which are not directly comparable for various complexes, further comparative investigation of alkyl electron donation to the Zr through the Cp ring can not be performed using NBO analysis.

2.3.3 Atoms-in-molecules analysis of intramolecular interactions

Figure 2.13 displays the molecular graph for the metal-ligand complexes, while Table 2.2 collects data for the electron density (ρ) and the Laplacian ($\nabla^2\rho$) at bond critical points (BCP). The bond paths connecting carbons and hydrogens with Zr clearly confirm the existence of intramolecular interactions between these atoms. Depending on the substituent chain length attached to the Cp ring, two kinds of intramolecular interactions are found: a non-classical agostic interaction between the Zr and C_γ atoms in shorter substituents (two-carbon chain), and a classical agostic interaction between the Zr and the terminal H atoms in longer alkyl substituents.

The BCP electron densities for the Zr-H1/H2 and Zr-C interactions in the various complexes are 0.11-0.15 e/Å^3 and 0.11 e/Å^3, respectively (Table 2.2). Taking into consideration the magnitude of the electron density and the sign of the Laplacians at the BCPs, the agostic interactions between the ligands and the central metal can be classified as closed-shell, therefore, mostly electrostatic in nature. A closed-shell interaction can be characterized by charge concentrations within the basin of each atom. Selected AIM charges are shown in Figure 2.14 for the two different modes of alkyl ligand agostic

interaction: non-classical for a shorter alkyl and classical for longer alkyl substitents. The C_γ atom in shorter substituents is negatively charged, and so are both hydrogen atoms.

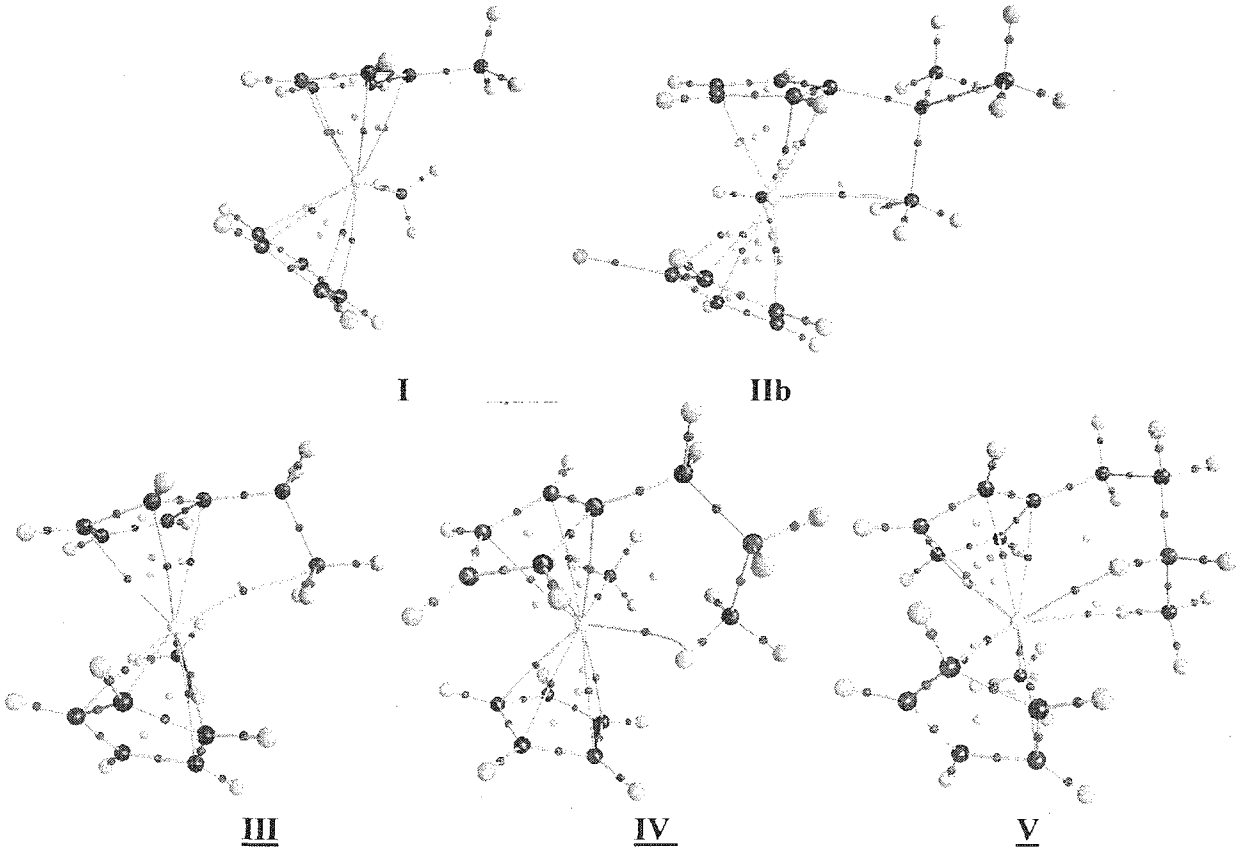

Figure 2.13. AIM molecular graph, for metal-ligand complexes.

Table 2.2. Electron-density (ρ) and Laplacian ($\nabla^2\rho$) at the BCP for model complexes.

Properties	Interactions				
	$C(CH_3)$-Zr	C(Cp) – Zr	C_{ag} – Zr in **IIb, III**	H_{ag} – Zr in **IV**	H_{1ag} – Zr H_{2ag} – Zr in **V**
ρ(BCP), e/Å^3	0.655	0.310- 0.340	0.105	0.158	0.150 0.109
$\nabla^2\rho$(BCP), e/Å^5	1.259	3.181	1.459	2.476	2.354 1.779

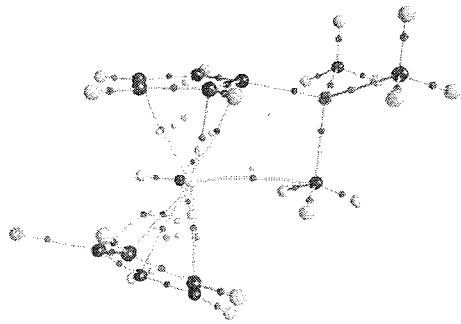

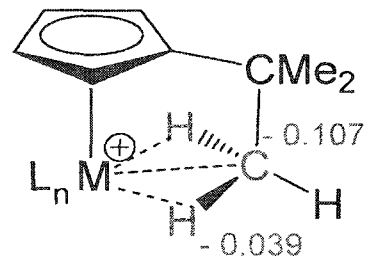

IIb

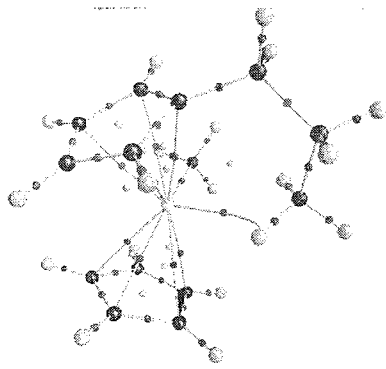

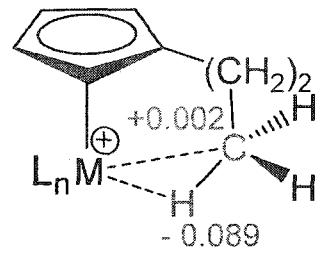

IV

Figure 2.14. AIM molecular graphs and selected charges for M - - η^3 –H_2C and M - - η^2 –HC modes of agostic interactions. (H charge is shown for the closest atom to Zr).

The AIM results concerning the hydrogen charges and the terminal carbon charge in **IV**. are opposite to what was found with NBO analysis. The negatively-charged CH_2-fragment in **IIb** adopt an orientation that maximizes the electrostatic attraction to the positive metal center, resulting in a $Zr^{\delta+}$ –$H_2^{\delta-}C^{\delta-}$ interaction, and M - - η3 – H_2C binding. On the other hand, for longer substituenst, the carbon atom of the methyl group is slightly positively charged, while the hydrogen atom closest to the zirconium is negatively charged, and its interaction with the metal center is more favourable. This results in a classical M - - η_2 –HC, agostic interaction between the $Zr^{\delta+}$ and the $H^{\delta-}$ atoms.

2.4 Conclusions

The analysis of metal-ligand complexes shows geometric evidence of the presence of agostic interactions in terms of substituent orientation, angle distortion, short Zr…C or Zr….H distances. Although failing to detect two different modes of agostic interaction, NBO analysis for hyperconjugation established the existence of these interactions in principle. Shorter substituents do not donate electron density to the Cp ring, resulting in an electron-rich terminal $C_\gamma H_3$ group, whereas longer alkyls might act as electron-density donors to the Cp ring, causing a small electron density deficiency on the substituent terminal carbon atoms. On the other hand, AIM analysis provides not only evidence for the existence of intramolecular interactions, but also clearly distinguishes between classical and non-classical agostic interactions. The classical agostic interaction is an interaction of the negatively-charged hydrogen with the metal center, while the carbon to which the hydrogen are attached is slightly positively charged. The non-classical agostic

interaction is in fact the interaction of the metal center and the carbon; which in this case is negatively charged. The non-classical interaction is weaker compared to the classical one. Both NBO and AIM analyses help explain why the alkyl substituent arranges itself around the metal center in two binding modes, depending on chain length and the charge distribution on the terminal atoms in the chain.

CHAPTER 3

Computational chemistry studies of intramolecular interactions in zirconocenium catalysts with modified alkyl substituents

3.1 Introduction

The Cp ring substituent properties which affect the polymerization activity of the group 4 metallocene catalysts, are mainly associated with their electron-withdrawing or electron-donating ability with respect to the Cp ring, resulting, via a sequence of inductive-like effects, in variation of the metal center electronegativity. It is believed, that Cp ring electron-donating substituents, for example alkyls, decrease the activity of the catalysts by making the metal center less electrophilic and therefore making coordination of olefin more difficult. However, the experimental data do not endorse this straightforward statement.[43] In Chapter 2, the electron-density donating or withdrawing ability of alkyls with respect to the Cp ring was investigated in zirconocenium catalysts. It was shown that, based on the alkyl chain length, alkyls can act both as an electron-donating and as an electron-withdrawing groups. In addition, due to the chain flexibility, some alkyl groups can move towards the metal center and interact with it directly. Electron-withdrawing substituents on the Cp ligand would make the metal center more electropositive, thus it may facilitate an olefin coordination step, resulting in higher polymerization activity. Nevertheless, it was found that electron-withdrawing groups placed on the Cp ring lower both the polymerization activity and molecular weight of the polymer .[42]

Theoretically, because of the high electron-withdrawing ability of the fluorine atom, fluorous substituents can increase the catalytic activity of the zirconocenium catalysts by

increasing the positive charge on the metal center. It was confirmed by X-ray crystal structure analysis that, very often, intramolecular coordination of a C-F fragment to the metal takes place.[55] In some cases, it can even permanently block available sites for olefin binding if the F atoms coordinate to the metal too strongly,[42] or lead to decomposition at room temperature because of defluorination.[56] To prevent this ethylene or dimethylsilyl spacers are usually introduced between the cyclopentadienyl and the perfluoroalkyl chain.[57-59]

Therefore, in spite of the obvious electron-donating or electron-withdrawing properties of the substituents, the effects on polymerization are very difficult to interpret or predict based on experimental data. Computational chemistry can provide valuable insight into the metal center electronic properties, which are important for understanding the polymerization mechanism. It also allows modeling possible intramolecular interactions of the alkyl substituents with the Zr atom. Theoretical methods have already proved to be very useful for investigation of similar complexes.[74]

The electron-withdrawing and electron-donating ability of the alkyl substituents can be modified by including into the hydrocarbon chain more electropositive atoms, for example Si, and/or more electronegative atoms, for example F. This chapter focuses on computational chemistry studies of the possible intramolecular interactions of the flexible, modified, alkyl substituents with the central metal. Good candidates to model active catalytic species with modified alkyl substituents are zirconocenium complexes of general formula $[Zr(\eta^5\text{-}C_5H_5)(\eta^5\text{-}C_5H_4R)Me]^+$, R = H, $SiMe_3$, CF_3, SiF_3, $SiMe_2(CH_2)_nF$, where the length of the hydrocarbon chain (n) varies from 0 to 3. The $SiMe_2(CH_2)_n$ group between the Cp ring and the fluorine atom can also serve to model spacer-effects

modeling. These unbridged zirconocenium catalysts with monosubstituted cyclopentadienyl do not impose structural constraints and allow free Cp rings rotation. The selected model complexes for this study are shown in Figure 3.1.

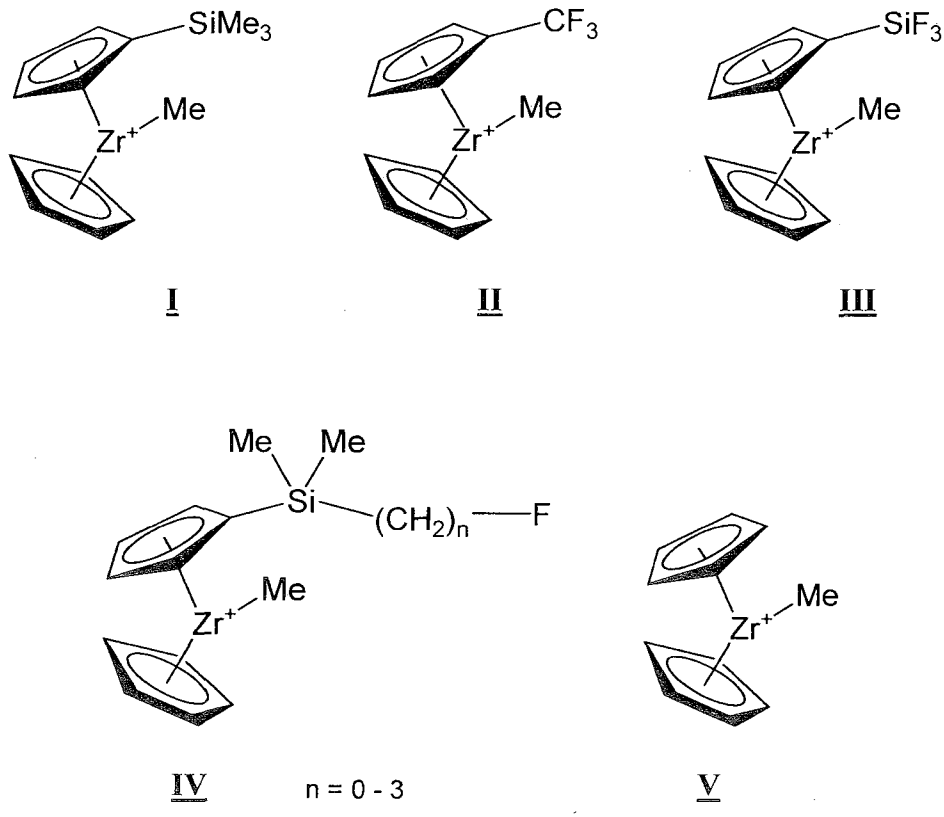

Figure 3.1. Model complexes.

The molecular structures, energies, electron density distribution and the nature of possible intramolecular interactions for the modified alkyls will be compared to those for the unmodified ones described in Chapter 2.

3.2 Computational methodology

In this work, all structures were fully optimized using the Gaussian 98 software package[75] at the Becke three-parameter Lee-Yang-Parr (B3LYP)[82-85] level of theory utilizing LANL2DZ pseudopotentials for the Zr, atom and the standard all electron double-ζ quality basis set 6-31G (d,p) for all other atoms. No local symmetry and no geometrical constraints were imposed in the optimizations. Vibrational frequencies were calculated for all stationary points to characterize them as minima (no imaginary frequencies) or transition state (one imaginary frequency). Relative energies (ΔE) reported include zero-point corrections. For selected cases, enthalpies ($\Delta H°_{298}$), entropies (ΔS) and free energy changes ($\Delta G°_{298}$) were also calculated at 298 K.

To evaluate the effect of hyperconjugative interactions and atomic charges, a Natural Bond Orbital (NBO) second-order perturbation analysis was used, as provided within the Gaussian 98 package. AIM2000 was used to analyze the topology of the electron density with the quantum theory of atoms in molecules (AIM).[76] In order to include the core electrons of the Zr atom, a DZVP basis set (DeMon DFT orbitals for charges and electron delocalization) was used in calculations.[77] The structures were fully reoptimized using this larger basis set before the AIM analysis was performed. The optimized molecular structures were drawn using the MOLEKEL 4.1 molecular visualization program.[80]

3.3 Results

3.3.1 Geometry analysis

Quantum chemistry calculations were performed for the three negatively charged Cp-substituted ligands, namely Cp-$Si(Me)_3$, Cp-SiF_3 and Cp-CF_3. All of three substituents adopt perpendicular conformations in contrast to the Cp-^{t}Bu ligand in Chapter 2.

The substituent perpendicular conformations are determined by the hyperconjugative interactions of the substituents with the Cp ring π network. According to the NBO analysis, the predominant hyperconjugative interaction for the Cp–$Si(Me)_3$ ligand is between the C_α p-orbital and a Si -C_γ low energy σ^* orbital (Figure 3.2 a). The stabilization energy calculated from second-order perturbation theory for this interaction is 13.2 kcal/mol.

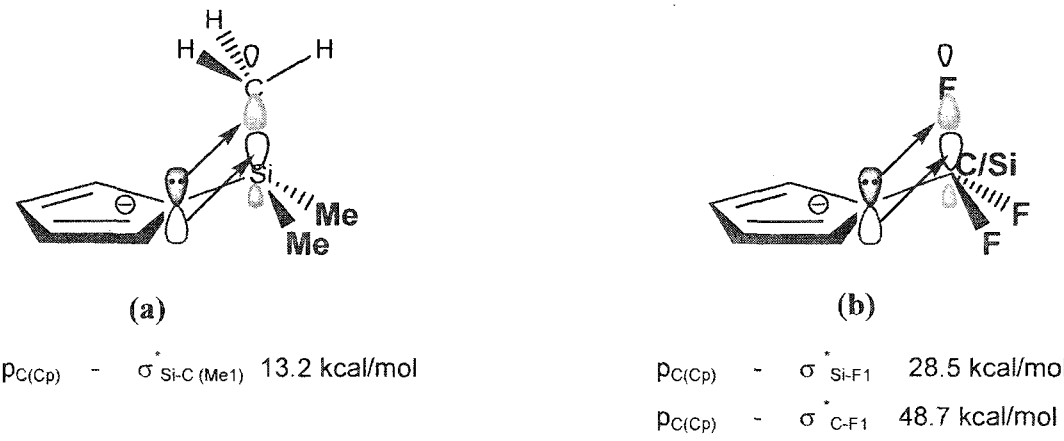

Figure 3.2. NBO Lewis structures and predominant hyperconjugative interactions for uncomplexed $Si(Me)_3$ (a), and SiF_3 or CF_3 (b).

For the Cp–CF_3 ligand, the interaction is between the C_α p-orbital and a C_β -F σ^* orbital, with a relatively high stabilization energy of 48.7 kcal/mol (Figure 3.2 b). The interactions and molecular geometry for the Cp ligand with SiF_3 substituent are similar to those for the Cp–CF_3 ligand and they are also shown in Figure 3.2 b. In spite of the significant difference in electronegativity, introduction of F or Si atoms in the alkyl chain

results in similar orbital interactions and similar conformational geometries, since all three substituents act as electron-withdrawing groups with respect to the Cp ring. As was shown earlier (Chapter 2), in the analogous uncomplexed ligand, the tertiary butyl substituent is in a planar conformation and it withdraws electron density from the Cp ring, with a major hyperconjugative interaction between two of the C_β-C_γ substituent σ^* orbitals and the Cp C_α lone pair. Compared to the modified alkyl substituents described above, the stabilization effect from withdrawing electron density from the Cp ring by the ^{t}Bu is weaker.

The molecular structures for the calculated modified alkyl substituents are shown in Figure 3.3 along with selected bonds and angles.

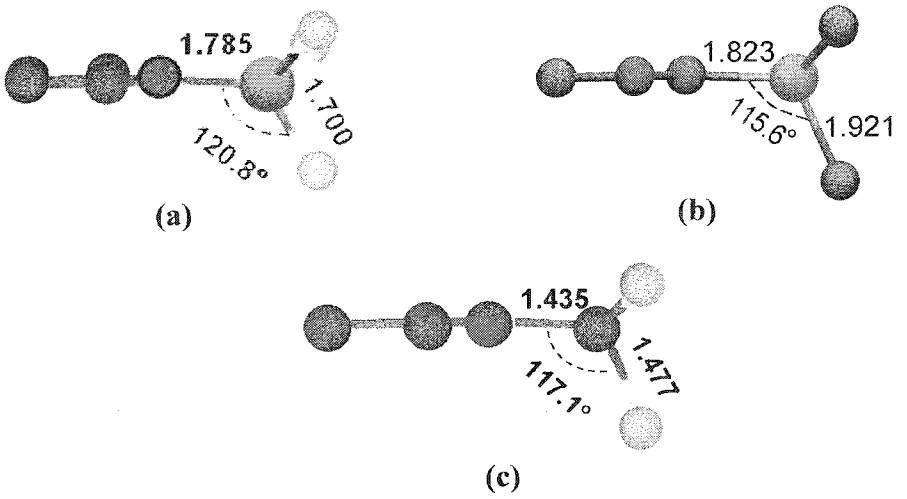

Figure 3.3. Molecular geometry (H – omitted, C in green, Si in blue, F – in yellow) of the uncomplexed Cp substituted ligands along with selected bond lengths (Å) and angles (°) shown.

The dihedral angles between the Cp ring and the C_α-Si/C_α-C/C_α-F bonds vary from 175.3° to 177.2° (Table 3. 1). Compared to the analogous angle in the ligand with ^{t}Bu substituents (180°, Chapter 2), these angles are smaller and more distorted due to stronger interactions of the modified substituent and the Cp ring electron density π network.

Table 3.1. Selected bond lengths and angles for the tertiary butyl, trimethylsilyl, $Si(Me)_3$, and fluorous, SiF_3/CF_3 substituents for the uncomplexed Cp^- ligand.

Substituent	**SiF_3**	**$Si(Me)_3$**	**CF_3**
Bond	**Bond Distance (Å)**		
C_{Cp}–C_α	-	-	1.435
C_{Cp}–Si_α	1.785	1.823	-
Si_α–C_1, C_2, C_3	-	1.921, 1.915, 1.915	-
Si_α–F_1, F_2, F_3	1.699, 1.699,1.700	-	-
C_α–F_1, F_2, F_3	-	-	1.477, 1.418,1.418
Bond Angle Atoms	**Bond Angles (°)**		
C_{Cp}-Si_α-F_1, F_2, F_3		-	-
C_{cp}-Si_α–C_1, C_2, C_3	113.4,116.5,120.1	115.6, 112.1, 112.1	-
C_{Cp}-C_α– F_1, F_2, F_3		-	114.25, 114.26, 117.08
Dihedral Angle Atoms	**Dihedral Angle (°)**		
Cp(plane) – (C_α-A / Si_α-A), A = C or F	175.9	177.2	175.3

The molecular geometries optimized in this study for two neutral pre-catalyst compounds are shown in Figure 3.4. Unlike the ^{t}Bu substituent described in Chapter 2, these substituents in the neutral pre-catalysts adopt planar conformations, while the uncomplexed ligands have perpendicular conformations. It is worth mentioning that, for

these neutral pre-catalysts, there are no significant bond or angle distortions, compared to the uncomplexed ligands.

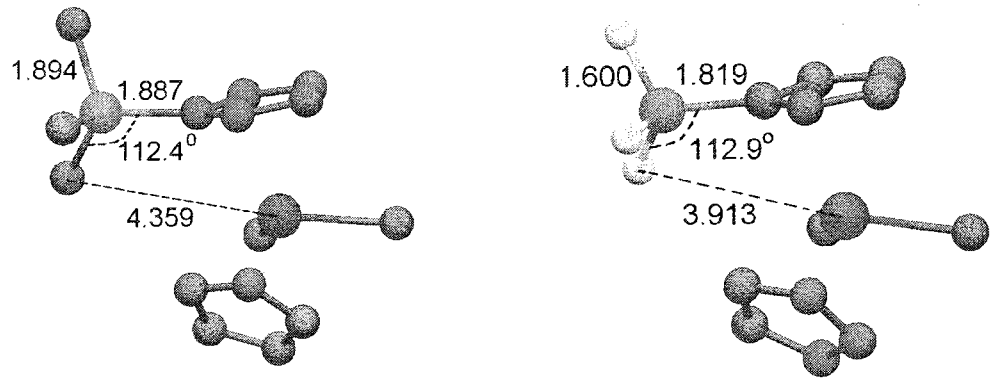

(a) (b)

Figure 3.4. Molecular geometry of the neutral pre-catalysts for corresponding catalysts **I (a) and III (b).** (H – omitted, C in green, Si in blue, F – in yellow, Zr in purple), along with selected bond lengths (Å) and angles (°) shown.

The C or F atoms closest to the metal center are 4.359 Å and 3.913 Å away from the zirconium, respectively. These interatomic distances are longer than the sum of the VDW radii of the corresponding elements and far longer than the sum of their covalent radii given in Table 3.2.[78] Thus, geometry analysis of the neutral pre-catalysts does not reveal structural evidence of intramolecular interactions between the modified Cp substituents and the metal center. The Cp ring substituent orientations with respect to the other two methyl ligands attached to the zirconium center are shown in Figure 3.5. It is also shown

that in these complexes the Cp rings are almost in an eclipsed conformation with respect to each other.

Table 3.2. Van der Waals and covalent radii for selected elements.

Element	Van der Waals radius, Å	Covalent radius , Å
Hydrogen, H	1.20	0.28
Carbon, C	1.70	0.68
Fluorine, F	1.47	0.64
Silicon, Si	2.1	1.2
Zirconium, Zr	2.01	1.56

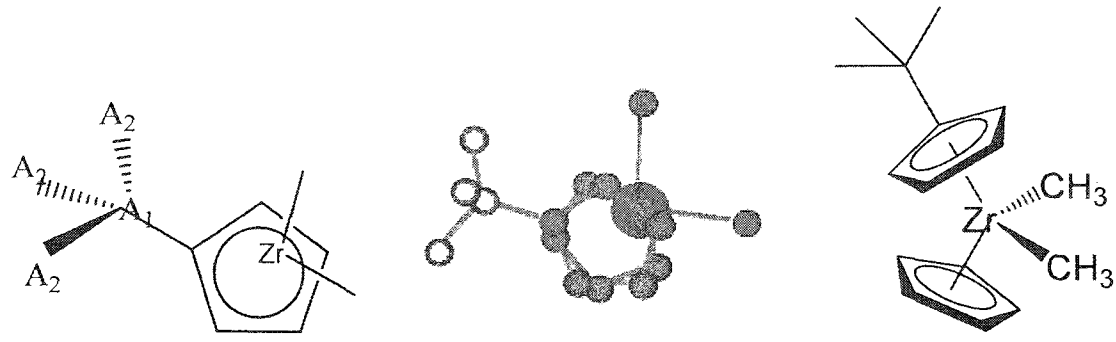

(a) **(b)** **(c)**

A_1- Si or C, A_2 – Me or F

Figure 3.5. Cp ligand substituent position for the neutral pre-catalysts, with respect to other two methyl ligands; view from above (a) two Cp rings are almost eclipsed, 3D view from above (b), side view (c).

According to the Z-N polymerization mechanism, the catalytically-active positively-charged species are formed when one of the methyl ligands attached to the zirconium is removed. Molecular geometries of the zirconocenium catalysts **I, II** and **III** are shown in Figure 3.6. In these complexes, the Cp ligand bearing a substituent changes position, rotating the Cp ring from an eclipsed conformation common for the neutral pre-catalyst into a staggered conformation (Figure 3.7), moving one of the substituent's atoms, A_2 (F or C_γ) into the position where the carbon atom of the removed methyl ligand was located. Moreover, geometry analysis of **I**, **II** and **III** reveals relatively short Zr-A_2 distances (Figure 3.6). In addition, two hydrogens attached to the C_γ are also very close to the metal: they are only 2.58 Å and 2.68 Å away from Zr. These distances are shorter than the sums of the van der Waals radii for the corresponding elements. Besides, pointing towards the Zr atom, the Si-C_γ, Si-F and C_β-F bonds are lengthened, compared to other similar bonds pointing away from the Zr atom and the analogous bonds in the molecules without interactions such as neutral pre-catalysts or uncomplexed ligands. Finally, C_α-Si-C_γ, C_α-Si -F and C_α-C_β-F angles are smaller than those in corresponding neutral pre-catalyst substituents and significantly deviate from the expected tetrahedral values. The calculated dihedral angles for the Cp plane–A_β, the angle is 165.6° in complex **I**, compared to 177.2° in the uncomplexed ligand, it also becomes smaller in **II** and **III** (168.1° and 157.4° respectively). Thus, based on geometry analysis, intramolecular interactions of the terminal CH_3 and F groups with the coordinatively unsaturated, positively charged zirconium can be implied. Nevertheless, the interactions can not be classified as typical ionic bonds, since typical bond lengths in Zr compounds are 2.2–2.3 Å in carbides, 1.8-1.9 Å in fluorides and 1.3-1.5 Å in hydrides. Taking into account the results for the

tertiary butyl substituent from Chapter 2, one can see that the angular distortion increases in the order: ^{t}Bu, $SiMe_3$, CF_3, SiF_3.

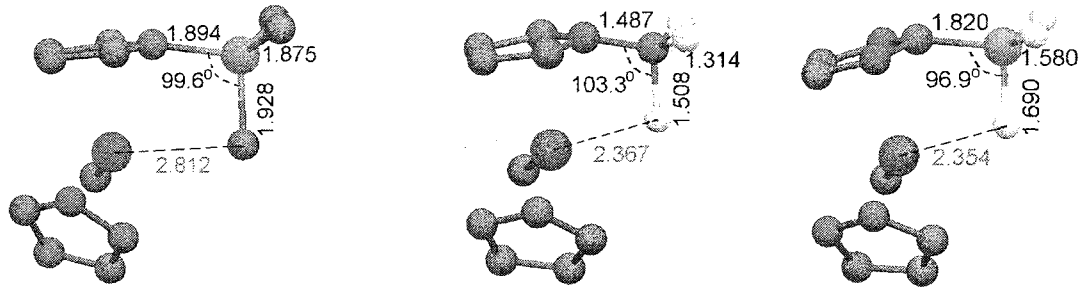

I II III

Figure 3.6. Molecular geometry of the zirconocenium catalysts **I, II and III.** (H – omitted, C in green, Si in blue, F – in yellow, Zr in purple), along with selected bond lengths (Å) and angles (°) shown.

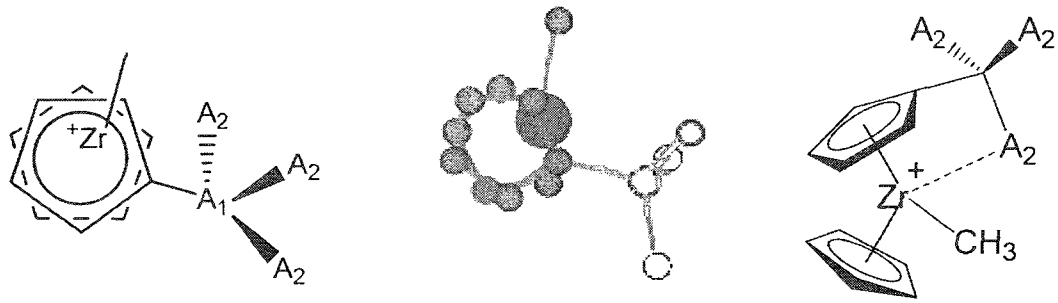

A_1- Si or C, A_2 – Me or F

Figure 3.7. Cp ligand substituent positions for positively charged catalysts, with respect to the remaining methyl ligand; view from above (a) where the two Cp rings are staggered, 3D view from above (b), side view (c).

For fluorous substituents, the mechanism of the Zr-F interaction can be easily explained by the donor-acceptor interaction common in organometallic compounds. In

these zirconocenium complexes, an occupied fluorine lone pair (donor) coordinates to the zirconium atom with formal electron configuration d^0 (acceptor). For ligands with the Si atom, where he alkyl group $(CH_2)_m$ (m=0,3) is also found relatively close to the metal center, the existence of agostic interactions is plausible.

For zirconocenium complexes with SiF_3 and -$SiMe_3$ substituents, only one rotational conformer is possible, where either the F or CH_3 group interacts with the metal center (complexes **1F(I) and 1C(II),** Figure 3.8). The same holds for substituents with CF_3. For fluorous substituents where the fluorine atom in the chain is separated from the Cp ring by an alkyl spacer, at least two conformers exist. The first is a conformer where the fluorine atom is in close proximity to the metal center (complexes **2F(IV n=0)** or **3F(IV n=1)** (Figure 3.8).

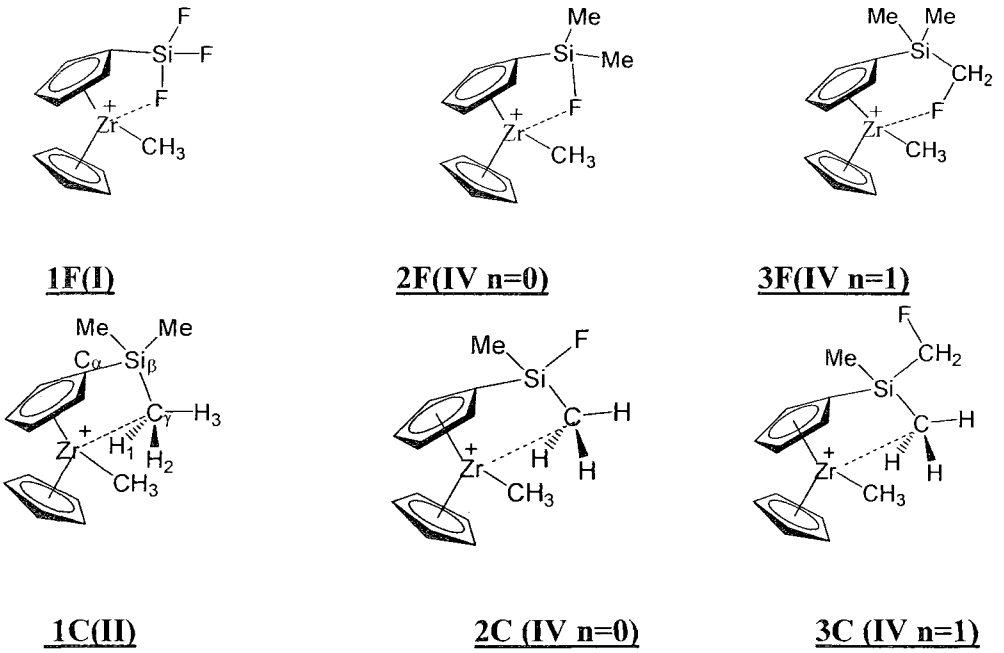

Figure 3.8. Molecular structures for the zirconocenium catalysts with CH_3 agostic interactions (**C**-conformers) and fluorine coordination (**F**-conformers).

and the second where the terminal CH_3 group is in close proximity to the zirconium atom (complexes **2C(IV n=0)** and **3C(IV n=0)**, Figure 3.8). They are denoted as **F**-conformers and **C**-conformers, respectively. In this study, optimized molecular geometries were found for all conformers illustrated in Figure 3.8.

3.3.2 Charge analysis

The calculated NBO charges for **C**– and **F**-conformers are plotted as a function of the substituent structure (Figure 3.9). In the zirconocenium catalysts, the charges on the metal are determined only by the type of substituent conformer (**F**- or **C**-) and their

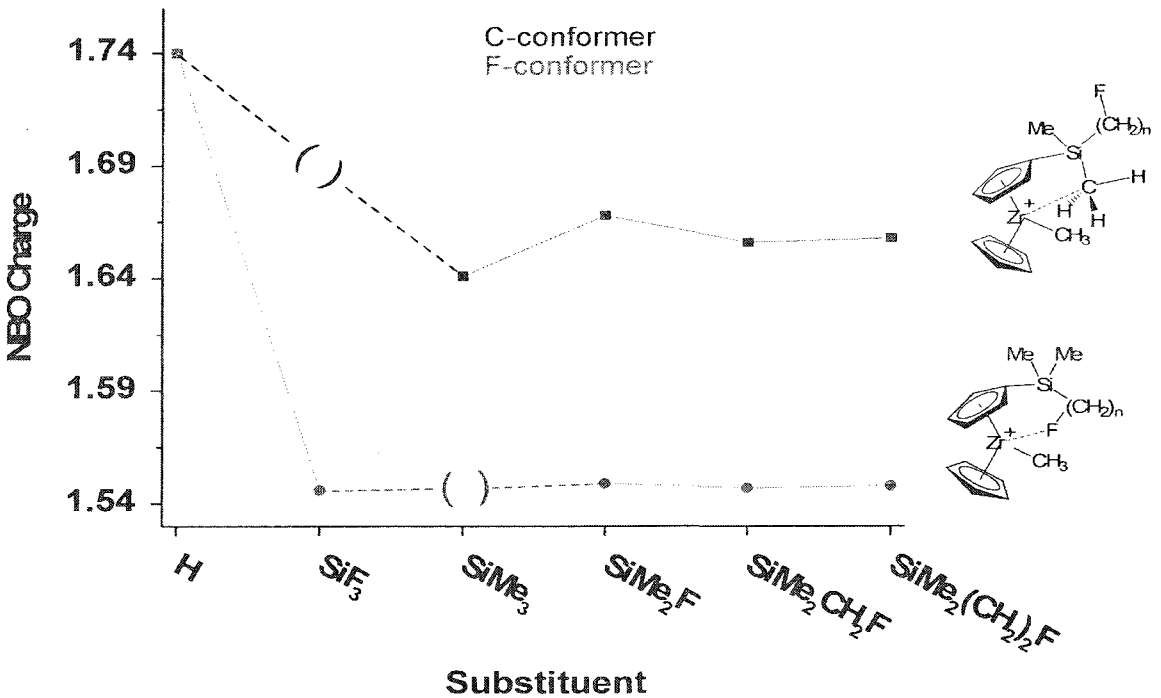

Figure 3.9. NBO Zr charges for n - alkyl substituents as a function of the substituent structure.

corresponding interactions with the metal. For all of the **F**–conformers the charge is on average +1.55 and for all of the **C**-conformers +1.65 on average. Compared to the unsubstituted complex (**V**), where the Zr charge is +1.74, the metal charges for **C**- and **F**-conformers are less positive. This means that intramolecular interactions partially compensate the positive charge of the zirconium atom in the active catalysts. The charge compensation is greater for F coordination to the metal in **F**-conformers than for terminal hydrocarbon group agostic interaction with Zr in **C**-conformers. This can be explained by stronger interaction of the fluorine atom with the metal center and therefore, a greater ability to compensate the positive charge of the zirconium, compared to the CH_3 group.

3.3.3 Energy analysis

Calculations of rotational conformations (around the C_α - Si bond) for the zirconocenium catalyst with the $SiMe_2F$ substituent show that the conformation without any intramolecular interaction is a transition state, 7 kcal/mol higher in energy than the complex with an agostic interaction (**2C**-conformer), and approximately 24 kcal/mol higher in energy than the complex with fluorine coordination (**2F**-conformer), Figure 3.10. Therefore, metal-substituent intramolecular interactions in zirconocenium catalysts are stabilizing interactions.

The calculated relative energies for other conformer pairs, complexes **IV (n=0-3)** are shown in Figure 3.11.

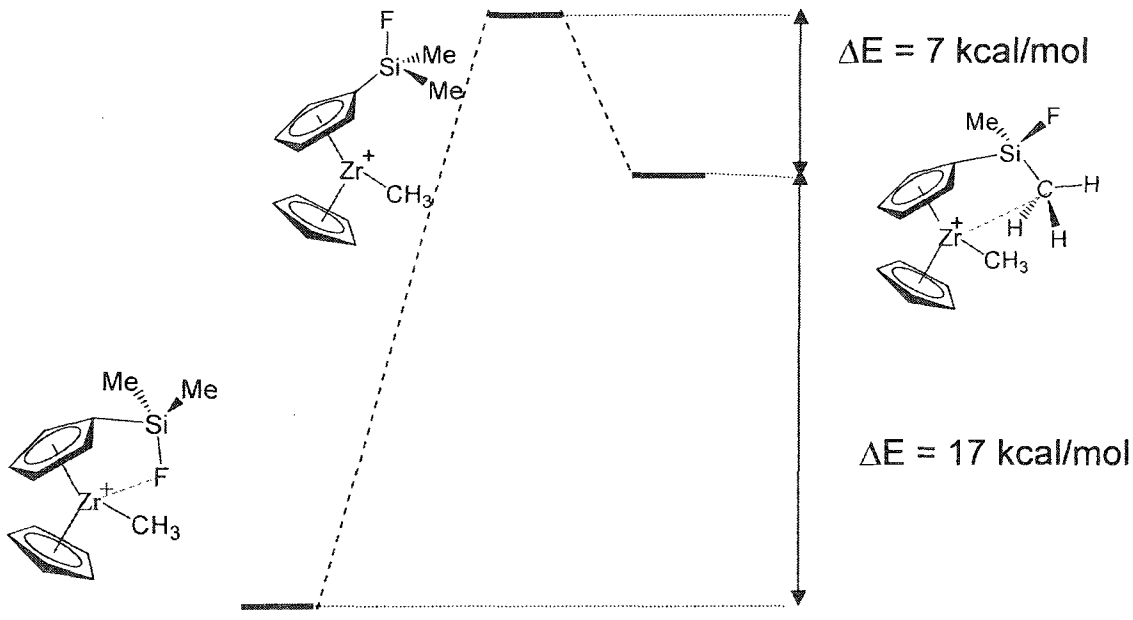

Figure 3.10. Calculated rotational conformation energy for the **2C/2F** conformers.

The energy analysis also indicates that calculated **F**-conformers are more thermodynamically stable than **C**-conformers with agostic interactions. Compared to agostc stabilization, the stabilization effect of F coordination for n = 1 is higher (23.7 kcal/mol) than for substituents with the shortest spacer with n=0 (17.2 kcal/mol), and it is the highest for the complexes with n = 2 (25.0 kcal/mol). For n>2, when the fluorine atom is separated from the Cp ring by a longer alkyl chains, the stabilizing effect of fluorine coordination becomes even less (only 13.1 kcal/mol) than that for the **C**-conformer with no carbons in the spacer (n=0). Therefore, for **F**-conformers, the 5- and 6-membered ring geometries [(Zr...C_α(Cp)...Si_β...C_γ and Zr...C_α(Cp)...Si_β...C_γ...C_δ)] are the most stable among complexes with a substituent spacer.

Thus, geometry, charge and energy analyses for zirconocenium catalysts with different, flexible, modified alkyl substituents offer strong evidence in favour of intramolecular interactions between the positively charged, coordinatively-unsaturated Zr

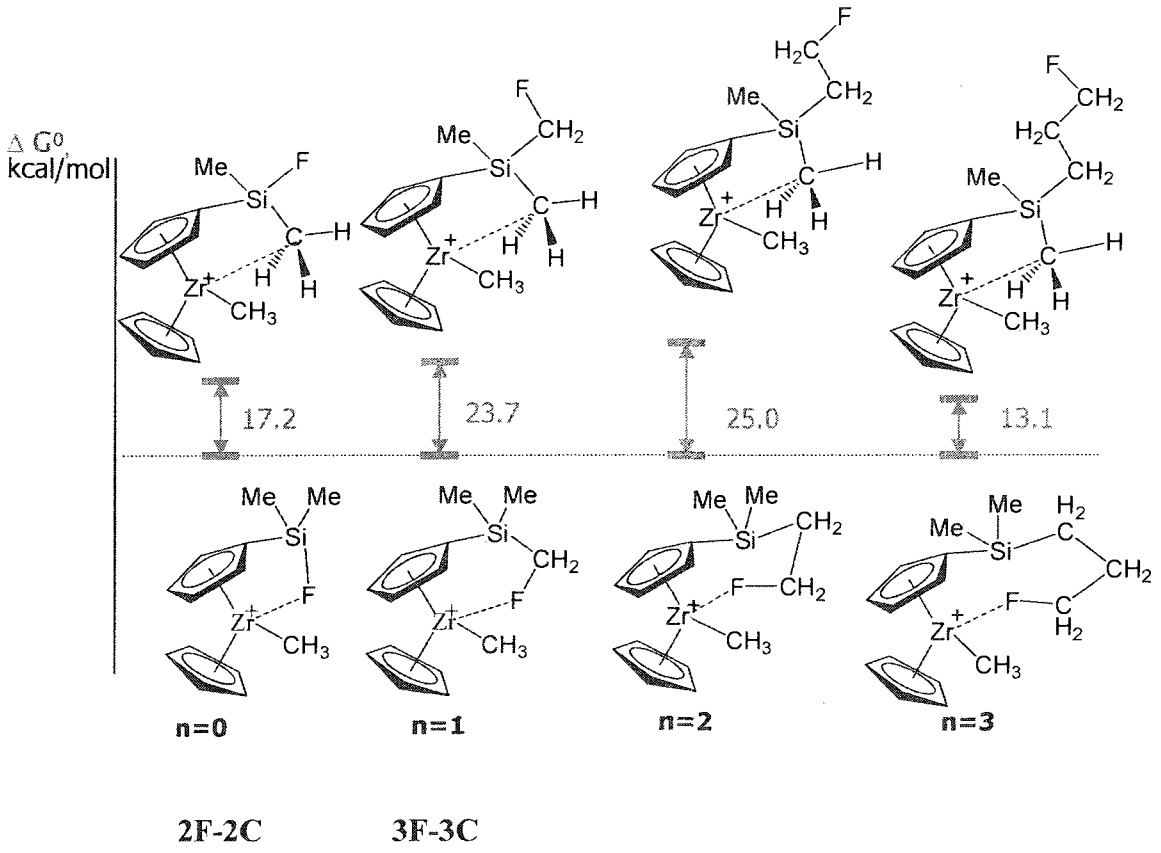

Figure 3.11. Stabilization energy for IV **(n = 0-3)**, fluorous substituents with different alkyl-likespacer length.

and atoms in the flexible substituent chain. These interactions cause an overall ligand geometry distortion, as well as charge compensation on the Zr atom, and an increase of the thermodynamic stability of the complexes. Depending on the nature of the substituent, two types of intramolecular interactions (Zr…C-H and Zr…F-C) are observed.

3.3.4 NBO analysis

To understand the nature of the interactions in zirconocenium catalysts, an NBO analysis was carried out. Due to the flexibility of the alkyl chain substituent, some atoms

can come in close proximity to the metal center; therefore, interaction between an electron-rich modified alkyl frame (both F- and Si-containing) and the positively charged, and coordinatively unsaturated central metal atom becomes possible. The interaction between filled and anti-bonding NBOs illustrates the deviation from Lewis structures and can be used as a measure of delocalization; therefore, it allows to evaluate the effect of hyperconjugative interactions. Stabilization energies due to delocalization are a quantitative measure for various ligand–metal interactions. For the molecules under consideration, only the interactions for which the stabilization energy is higher than 5 kcal/mol were analyzed.

The main hyperconjugative interactions predicted by second-order perturbation theory for structure **I** are shown in Figure 3.12. The C_γ - Si_β bond should be strongly polarized due to the higher electronegativity of carbon relative to silicon. The calculated natural charges also reveal that the silicon atom is significantly more positive (+ 1.84) than both the adjacent carbon atoms. For the C_α atom the charge is equal to -0.61; besides, according to the Lewis structure, an electron lone pair (p orbital in nature) is also located on that carbon. The C_γ charge is -1.23, which is larger in magnitude than normally calculated for carbons in alkyls (from -0.40 to -0.80). As a result, electron density from the p orbital of the C_α atom is transferred to the low energy Si–C_γ σ^* orbital. This can explain the angle distortions and a significant elongation of one of the Si–C_γ bonds. In this case the substituent acts as an acceptor of the electron density from the Cp ring and adopts a perpendicular conformation. The calculated stabilization energy for this interaction is 5.7 kcal/mol. NBO analysis also shows that the positive Zr ion center is stabilized by hyperconjugative overlap of both the C_α–Si σ and C_γ- Si σ bonds and the

practically vacant Zr d-orbitals that have the suitable symmetry (similar to the beta-silicon effect on carbenium ions in organic chemistry).[93] This stabilization is usually larger than for the unmodified alkyl substituents, with calculated stabilization energies of these interactions in the range of 5-8 kcal/mol.

Other predominant hyperconjugative interactions of the substituents with Zr for complex **I** involve electron transfer from the C_γ-H_1 and C_γ-H_2 σ-orbitals to the zirconium d-orbitals. These interactions stabilize the molecule by ~16-18 kcal/mol each. This symmetric electron density donation from the H-C σ bonds to Zr is consistent with a non-classical M - - η^3-H_2C agostic interaction.

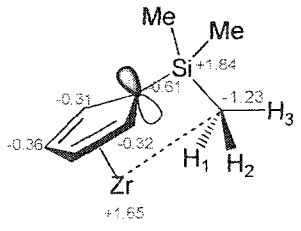

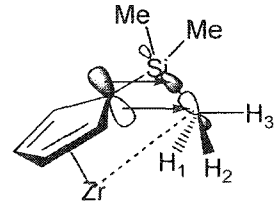

p_C - σ^*_{Si-C} 5.7

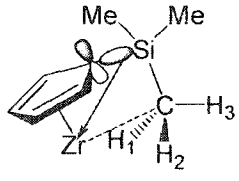

σ_{C-Si} - $d(1)_{Zr}$ 8.3
- $d(5)_{Zr}$ 5.8

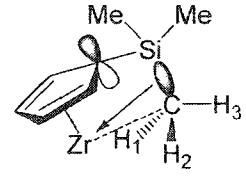

σ_{C-Si} - $d(1)_{Zr}$ 7.0
- $d(4)_{Zr}$ 6.9

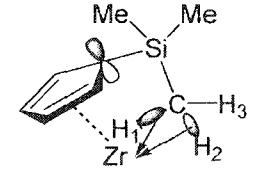

σ_{C-H1} - $d(4)_{Zr}$ 18.5
σ_{C-H2} - $d(4)_{Zr}$ 16.1

Figure 3.12. NBO Lewis structures, charge distribution (blue) and predominant hyperconjugative interactions in kcal/mol (red) for **I**.

The hyperconjugative interactions for the structure with the ^{t}Bu substituent have been discussed in Chapter 2. For the complex with the ^{t}Bu substituent, unlike structure **I**, the p-

orbital of the Cp ring is not localized on the C_α carbon attached to the alkyl and no significant interaction was found between the Cp ring and the substituent. There is also no interaction of alkyl the C-C bond electron density with the zirconium center stronger than 5 kcal/mol. In the ^{t}Bu substituted ligand similar to **I**, the observed key interactions are the electron density transfer from the C_γ-H_1/C_γ-H_2 σ bond orbitals to the zirconium d-orbitals; however these interactions are weaker than for complex **I**.

For fluorous complex **II**, the Lewis structures, charge distribution and predominant hyperconjugative interactions are shown in Figure 3.13.

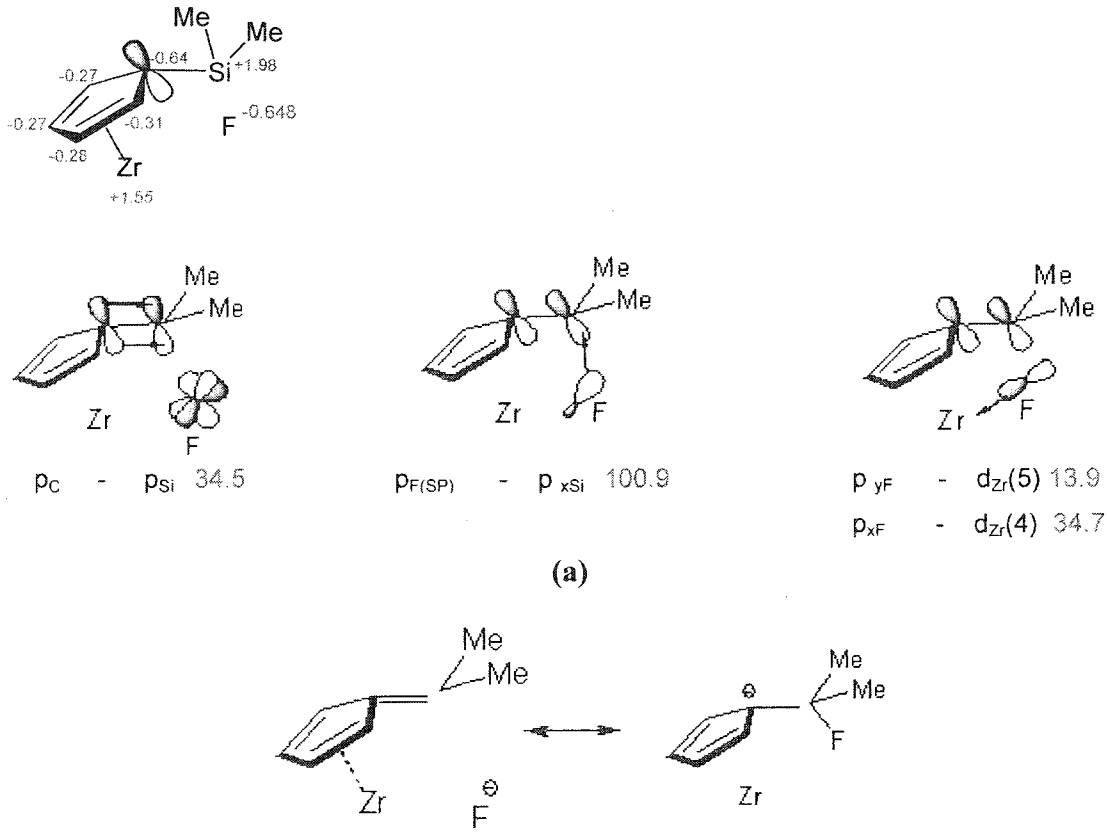

Figure 3.13. NBO Lewis structures, charge distribution (blue) and predominant hyperconjugative interactions with the substituent in kcal/mol (red) (a) and no-bond/double-bond resonance representation (b) for structure **IV** (n=0).

According to the NBO Lewis structures, the fluorine has a negative charge of -0.64 and it is not bonded to the silicon atom. Fluorine has four lone-pair-type orbitals which are hybridised, but still can be recognized as one mostly s-orbital and three mostly p_x, p_y, p_z-orbitals in nature. Because a bond was not found between F and Si in the NBO analysis, another lone-pair-type orbital with low occupancy appears on the Si atom, which is mostly p_x-orbtal in nature. In this complex, the NBO analysis reveals a strong hyperconjugative interaction between the Cp ring and the substituent (34.6 kcal/mol). In fact, electron density donation from the C_α p-orbital, to a vicinal Si p-orbital is associated with increasing the double bond character between the C_α-Si bond. At the same time the strongest hyperconjugative interaction is still between the F p- and Si p-orbitals (100.9 kcal/mol). This negative hyperconjugation interaction is illustrated by the no-bond/double-bond resonance for representation in Figure 3.13 b. Strong donor-acceptor interactions are also found between the two F donor p_x and p_y-orbitals and the practically vacant Zr d-orbitals. The highest stabilization energy for these interactions is 34.7 kcal/mol, which is higher than the corresponding energy for the agostic interactions in **I.**

For both Si and F modified alkyl substituents, the interaction with the metal is essentially electrostatic in nature and results in compensation of the highly positive charge on the metal via redistribution of electron density within the ligand skeleton, in order to favour an increased negative charge on the terminal groups, which can then coordinate to the metal (negative hyperconjugation). In both cases, the Cp ligand acts as electron density donor to the substituent. The fact that the calculated natural charges on the zirconium center changed from + 1.74 (Cp without substituent) to +1.64 (for **C**-conformers) and to +1.55 (for **F**-conformers) also confirms this findings.

3.3.5 AIM analysis

Figures 3.14 and 3.15 display the molecular graphs for the complexes **I**, **II**, **III** and the zirconocenium catalyst with the ^{t}Bu substituent, while Tables 3.3 and 3.4 collect data for the electron-density (ρ) and the Laplacian ($\nabla^2\rho$) at the bond critical points (BCP). The bond paths, connecting carbons and fluorines with the zirconium atom, clearly confirm the existence of intramolecular interactions between these atoms. In the complex with the ^{t}Bu substituent (Chapter 2) the agostic C-Zr interaction is close to vanishing or unstable, as can be inferred from the fact that the ring critical point almost coincides with the BCP. In structure **I**, this interaction is more stable, as can be judged from the ring critical point and the BCP positions, and the larger electron density at the BCP for **I** than for the complex with the ^{t}Bu substituent. The same conclusion about the interaction strength was drawn from the NBO analysis. In both complexes, the agostic interaction can be classified as a non-classical or C-agostic interaction. For structures **II** and **III**, with Zr-F fluorine coordination, the electron density values at the BCP are approximately the same as they are for the C-F or Si-F bonds, 0.33 e/Å^3 and 0.11 e/Å^3, respectively.

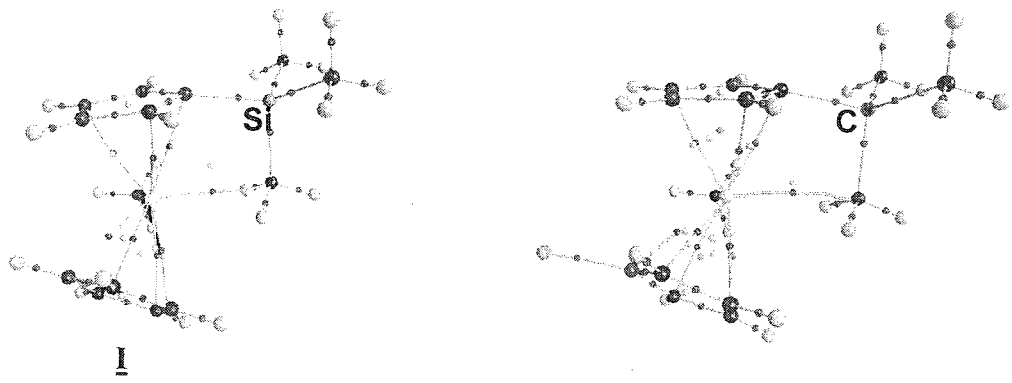

Figure 3.14. Molecular graph for zirconoceneum complexes (**I**) and the complex with the ^{t}Bu substituent.

Table 3.3. Electron-density (ρ) and Laplacian ($\nabla^2\rho$) at the BCP for **I** and the complex with the ^{t}Bu substituent.

Properties	Interactions			
	$C(CH_3)$-Zr	C(Cp) – Zr (av.)	$(C)C_\beta H_3$ – Zr	$(Si)C_\beta H_3$ – Zr
ρ(BCP), e/Å^3	0.655	0.330	0.105	0.115
$\nabla^2\rho$(BCP), e/Å^5	1.259	3.181	1.459	1.652

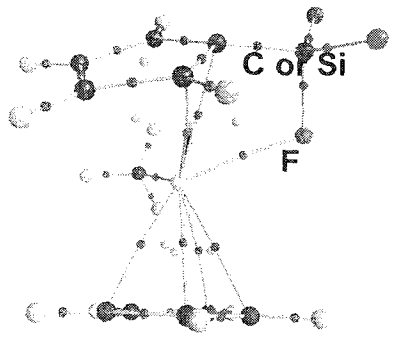

Figure 3.15. Molecular graph for **II** or **III**.

Table 3.4. Electron density (ρ) and Laplacian ($\nabla^2\rho$) at the BCP for **II** and **III**.

Properties	Interactions			
	(Si) F - Zr	F - Si	(C_β)F - Zr	F - C_β
ρ(BCP), e/Å^3	0.332	0.331	0.287	0.285
$\nabla^2\rho$(BCP), e/Å^5	5.812	3.181	4.982	2.621

The selected AIM charges are shown in Figure 3.16 for **I** and for the complex with the ^{t}Bu substituent. The electron density at the BCP for the Zr-C interaction is higher for **I** than for the complex with the ^{t}Bu substituent. The $C_\gamma H_3$ terminal group is overall more negative in **I** than in the complex with the ^{t}Bu substituents, therefore, the AIM charge analysis also supports the conclusion that the agostic interaction is stronger for **I**.

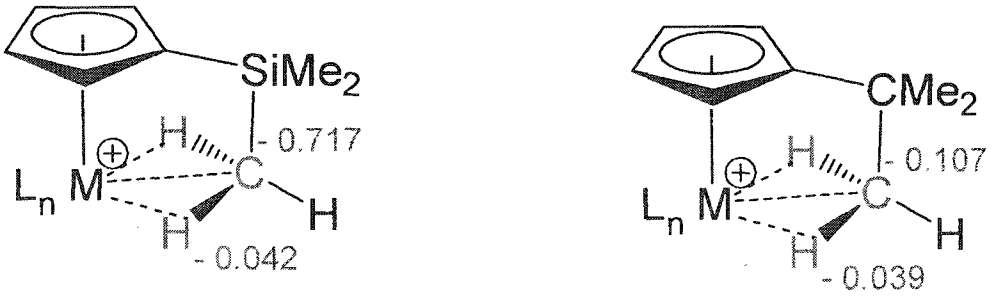

Figure 3.16. H and C charges for M - - η^3 –H_2C modes of agostic interactions for structure **I** and the ^{t}Bu substituents.

It is also worth mentioning that the zirconium atom is coordinated to the CF_3-substituted ligand in η^2-coordination mode. In general, in bent metallocenes some degree of the metal slippage is always present, and it is almost never η^5-coordination.[94] The mode of coordination depends on both how far the metal is from an imaginary line connecting the centers of the two Cp rings (the distance D, Figure 1.8, Chapter 1) and the amount of Cp ring electron density available for coordination to the metal. As can be seen from AIM molecular graphs, in all the zirconocenium complexes calculated here, the second unsubstitueted Cp ligand coordinates to the metal in η^4-coordination mode. The mode of coordination of another substituted Cp ligand depends on the substituent nature. For the shorter alkyls substituents such as methyl, ethyl and n-propyl, it is η^3-

coordination, while for longer n-butyl, it is η^4-coordination. Geometry analysis shows that the distance D is almost the same for all alkyl-substituted complexes. Therefore, an increase of the Cp electron density, compared to shorter alkyls, available for coordination with the metal can be assumed due to the electron donating nature of n-butyl. Strong electron withdrawing substituents and as CF_3 deplete the electron density of the Cp ring and the latter coordinates to the zirconium atom in η^2-coordination mode. The degree of substituent geometry distortion is also higher.

3.4. Conclusions

Using computational chemistry methods, intramolecular interactions were found for ziconocenium catalysts with modified alkyl substituents attached to the Cp ring. Both highly electropositive Si-containing and highly electronegative F-containing substituents act as electron withdrawing groups with respect to the Cp ring. Due to their flexibility, the substituent alkyl chains can move closer to the central metal and interact with it directly. These intramolecular interactions result in an increase in the thermodynamic stability of the zirconocenium catalysts, along with charge compensation on the zirconium atom. For complexes with fluorous substituents, the stabilization effect is stronger for F-coordinated conformers than for conformers with a C-agostic interaction. The energy of F coordination can be decreased by adding two or more CH_2 groups in the spacer alkyl chain.

From structural analysis it was found that ligand geometry distortion increases with the electron withdrawing ability of the substituent on the Cp ring. It was also shown that the stabilization energy calculated with second-order perturbation theory is greater for the

Zr-F coordination than for Zr-C agostic interaction. Although the electron density can not be directly compared for different interacting nuclei, the AIM electron density at the BCPs is also higher for the complexes with Zr-F coordination than for those with Zr-C intramolecular interactions. Based on this work, it can be concluded that the interaction strength for different substituents increases in the following order: $^{t}Bu<SiMe_3<CF_3< SiF_3$.

Therefore, for substituted zirconocenium catalysts, the charge on the metal center, and possibly its polymerization activity, cannot be predicted simply on the basis of the substituent electron-withdrawing or electron-donating ability with respect to the Cp ring only. Additional intramolecular interactions of flexible substituents with the central atom also have to be taken into account.

CHAPTER 4

Influence of intramolecular interactions on polymerization activity

4.1 Introduction

As was shown in Chapter 2, changing the length of the alkyl substituent on the cyclopentadienyl ligand will result in a variety of steric and electronic environments around the metal center. Longer alkyl substituents are somewhat stronger electron donors than hydrogen, and they will thus slightly increase the electron density on the Cp ring and result in more compensation of the electron deficiency around the metal center, compared to unsubstituted Cp. Furthermore, an increase in the length of the alkyl may result in different degrees of steric hindrance. Additional electronic and steric modifications may be expected if an agostic interaction is present between the metal and hydrogen on the alkyl substituent (Figure 1.13). Additional effects on the intramolecular interactions between the metal center, the Cp ring and alkyl substituents might be expected if alkyls are modified by introduction of heteroatoms such as Si and F (Chapter 3).

In an attempt to gain deeper insight into how alkyl substituents might affect polymerization, quantum chemical calculations based on density-functional theory (DFT) were performed on different monosubstituted zirconocene ethylene complexes. Our aim is to address the effect an alkyl substituent on the aromatic ligand may exert on the reactions that take place during polymerization. The polymerization behavior of a catalyst is intimately related to the structural and electronic environment of the active site. By pointing to certain structural and energetic features of model zirconocene cations, we attempt to contribute to the mechanistic understanding of these catalysts. Computational

results are used to explain experimental results for polymerizations activity. This work deals with only the first step of the polymerization mechanism – olefin molecule coordination.

4.2 Computational methodology

All geometries and energies discussed in this chapter are evaluated with DFT. The molecular geometry of ethylene-zirconocenium complexes was fully optimized at the B3LYP level of theory combined with the standard all-electron double-ζ quality 6-31G (d,p) basis set (and LANL2DZ pseudopotentials for Zr) using the Gaussian 98 software package.[75]. Vibrational frequencies and thermodynamic properties were calculated for all stationary points. Relative energies (ΔE) reported include zero-point corrections. For selected cases, enthalpies (ΔH°_{298}), entropies (ΔS°_{298}) and free energy changes (ΔG°_{298}) were also evaluated at 298 K under the rigid rotor-harmonic oscillator approximation. Results obtained in Chapters 2 and 3 using NBO analysis (provided as a routine within Gaussian 98) and AIM calculations (using the AIM2000 program package [76]) are also used in this chapter.

4.3 Results

4.3.1 Correlation of experimental polymerization activity with calculated catalyst properies

The experimental polymerization activity[26] of zirconocenium species **I**, **II**, **III**, **IV**, **V** from Chapter 2 and **V** from Chapter 3 is shown as a function of alkyl ligand substituent chain length (blue curve), along with the metal NBO charge (red curve) in Figure 4.1, and

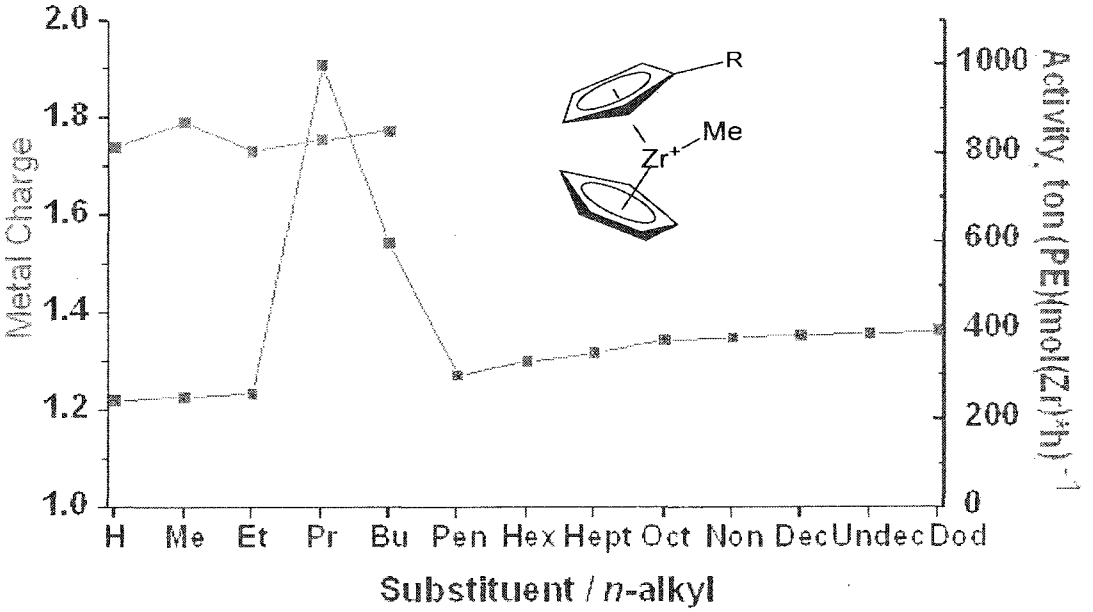

Figure 4.1. Metal charge as calculated by NBO (red) and observed polymerization activity (blue) as a function of ligand substituent chain length.

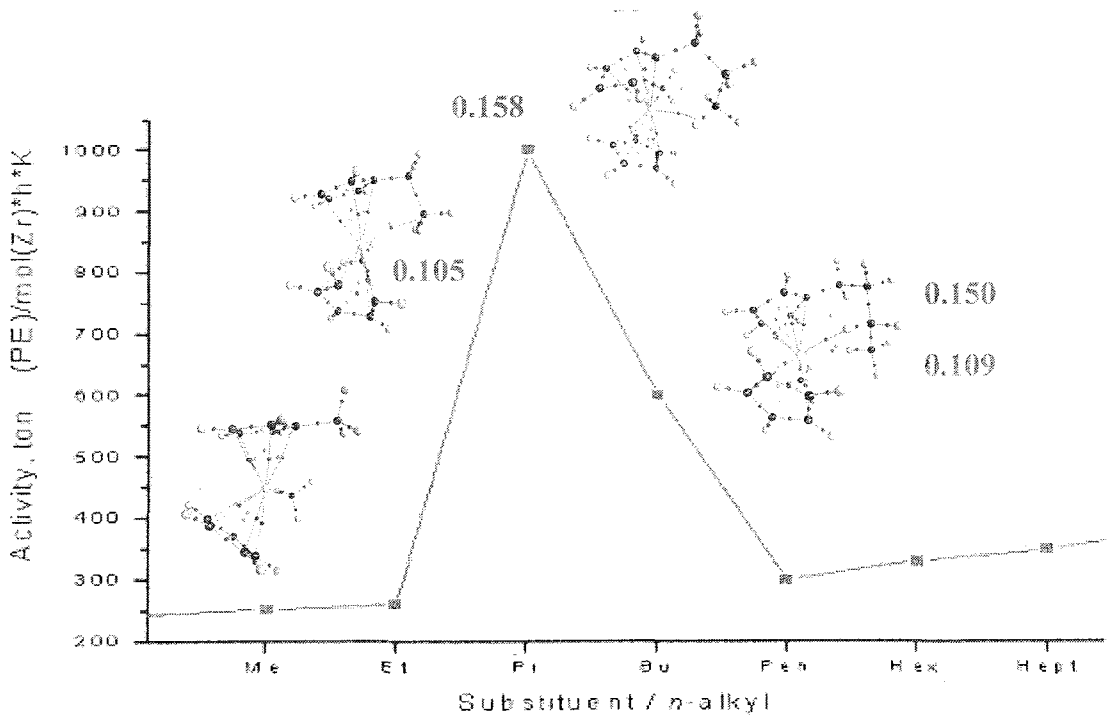

Figure 4.2. Catalytic activity (in blue) and electron density at the agostic interaction bond critical point (in red, e/Å^3) as a function of ligand substituent chain length.

along with the electron density at the bond critical point for the agostic interaction in Figure 4.2.

No obvious correlation can be found between the charge of the central metal and the polymerization activity. As was shown in Chapter 3, the metal charge is predominantly determined by the stabilization effect of the agostic interaction(s) between the flexible and relatively electron-rich alkyl chain fragments and the positively charged metal center. Thus, the metal charge analysis is not helpful in predicting the catalytic activity of zirconocenium species for olefin polymerization.

One might assume that the longer the hydrocarbon chain the less accessible the metal center, but a noticeable peak in the polymerization activity is observed for catalysts with n-propyl and n-butyl ligand substituents. This increase, on the other hand, might be explained by weak intramolecular interactions (Figure 4.2). The catalytic activity is the lowest for the unsubstituted zirconocenium species. Then a slight increase is observed for the catalyst with a methyl-substituted ligand (the NBO metal charge is also larger). The activity increases further, but modestly, for the catalyst with an ethyl-substituted ligand, for which a non-classical Zr...C agostic interaction was identified. The highest increase of catalytic activity for the catalysts with n-propyl and the n-butyl-substituted ligands coincides with the presence of classical Zr...H agostic interactions. The strongest single agostic interaction was observed for the catalyst with the n-propyl-substituted ligand, for which the polymerization activity is maximum. For n-butyl-substituted ligands, the two classical agostic interactions might be too strong for olefin complex formation, but still the activity is the second highest for the complexes investigated. Therefore, the relatively weak, but noticeable agostic interactions might play a role in the increase of catalytic

activity, compared to catalysts where there are no such interactions or, if present, the intramolecular interactions are much stronger. This catalytic activity increase might be achieved by weak ligand coordination to the metal center, preventing competitive solvent or co-catalyst binding to the zirconium, while allowing small olefin molecules to displace the substituent, since the interaction is not too strong. Formation of an olefin-catalyst complex is an essential step of polymerization according to the Z-N polymerization mechanism, and this issue is further addressed in the next section.

4.3.2 Analysis of the olefin-catalyst complex formation

The molecular structures of ethylene-zirconocenium complexes, along with selected geometrical parameters, are shown in Figure 4.3, while their formation/binding energies and free energies are shown in Figure 4.4. Ethylene binding is obviously thermodynamically less favourable when stabilizing effects on the metal center by ligand substituents are stronger. In other words, the larger the stabilizing effect of the intramolecular interaction, the weaker the olefin binds to the metal center. Weak olefin coordination might facilitate the next step of alkyl ligand migratory insertion and therefore increase the catalyst activity. The activity might be thought to be the highest for the catalyst with the fluorous ligand substituent, for which the ethylene-zirconocenium complex formation/binding energy is the lowest, but in fact, this is not the case. It has been reported that, if the olefin-catalyst formation/binding energy is less than 10 kcal/mol, no olefin binding actually occurs in the polymerization process;[42] it is also known that fluorous substituents very often irreversibly coordinate to the catalyst active center, deactivating it.[42, 56, 92]

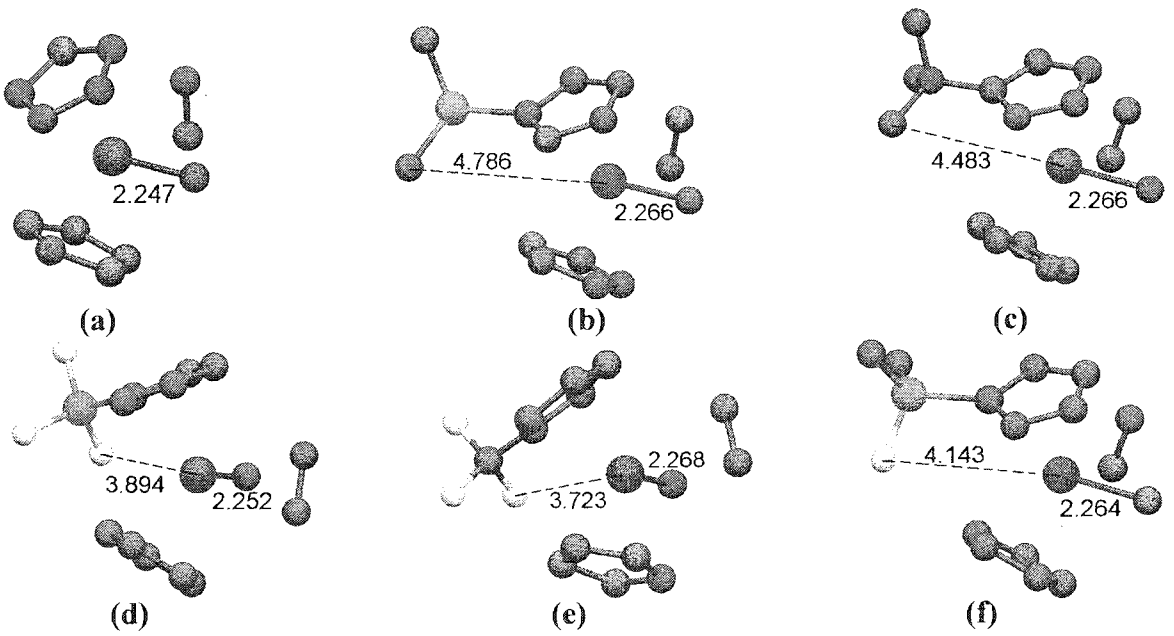

Figure 4.3. Molecular structures of the ethylene-zirconocenium complexes with unsubstituted (a), trimethylsilyl-substituted (b), ^{t}Bu-substituted (c), SiF_3-substituted (d), CF_3-substituted (e) and $Si(Me)_2F$-substituted (f) ligands on the Cp ring, along with selected interatomic distances (Å). (H – omitted, C in green, Zr in purple, Si in blue, F in yellow).

The electron-donating ability of the flexible ligands to the metal seems to be the most predominant factor in determining the formation/binding thermodynamics properties of the ethylene-zirconocenium complexes (Figure 4.4). The higher the electron-donating ability of the ligand substituent, the stronger its interaction with the positively charged metal center.

Prior to olefin-catalyst coordination, the ligand substituent has to be displaced from the metal coordination site. Therefore, the stronger the interaction between the ligand substituent and the metal center, the less thermodynamically favourable is the olefin-

catalyst complex formation, and even more so as temperature rises. Stabilizing effects due to agostic interactions for zirconocenium species with alkyl ligand substituents on the Cp ring are weak, and thus, the formation of the olefin adducts is thermodynamically favourable, even at 298 K. On the other hand, in the case of zirconocenium species with fluorous ligand substituents, the fluorine atom is too close to the metal, coordination to the metal center is too strong, and ethylene-zirconocenium complex formation under ambient conditions is not possible.

This means that, for catalysts with strong F-Zr intramolecular interactions, polymerization is not thermodynamically favorable at 298 K, and making these species effective catalysts requires "insulation" of the zirconium from the fluorine atom by

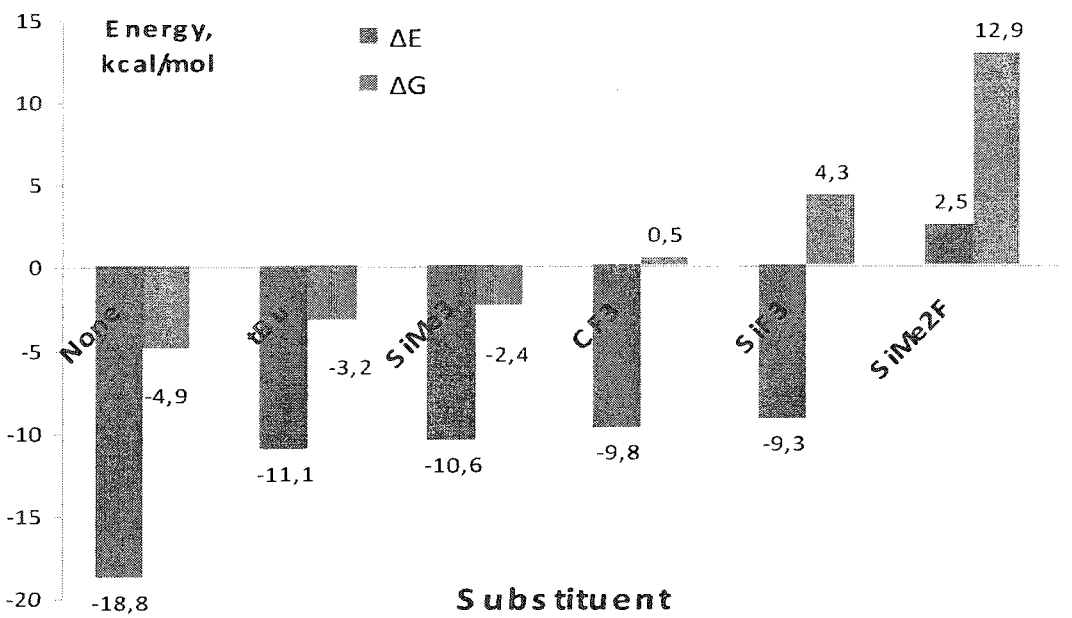

Figure 4.4. Ethylene-zirconocenium complex formation/binding energy at 0 K (in blue) and free energy at 298 K (in red).

adding alkyl or alkyl-like spacers between the Cp ring and the fluorous part of the ligand substituent.

Stabilization energies due to fluorine coordination to the metal center were shown in Figure 3.11 (Chapter 3) for fluorous ligand substituents with $(CH_2)_n$- spacers of varying chain length, relative to the strength of the C_γ agostic interaction. When there is no spacer (n=0), fluorine coordination to the metal center is ~17 kcal/mol thermodynamically more favourable than the agostic interaction. If a CH_2- spacer (n=1) is placed between the silicon and fluorine atoms, the stabilization energy increases and equals almost 24 kcal/mol. Further addition of a CH_2- group to the spacer (n=2) stabilizes the fluorine-coordination species by 25 kcal/mol, relative to the agostic interaction. For n=3, the stabilization energy of the fluorine-coordination species then falls to only 13 kcal/mol. For n=1 and 2, fluorine-coordination species adopt 5- and 6-membered ring structures ($Zr...C_\alpha(Cp)...Si_\beta...C_\gamma$ and $Zr...C_\alpha(Cp)...Si_\beta...C_\gamma...C_\delta$), respectively, and these conformations are the most stable of the structures with alkyl spacers. Hence, the number of carbon atoms in the alkyl spacer has to be more than two to effectively insulate the metal center from the fluorine so that polymerization can occur. These findings are supported by experimental data. [57-59]

4.4 Conclusion

In this chapter, the possible effects of intramolecular interactions in catalysts on α-olefin coordination polymerization were addressed. The experimental polymerization activity was found to be the highest for zirconocenium species that happen to exhibit classical agostic interactions, the strongest of the two types of agostic interaction, but still

a much weaker interaction than F coordination to the metal center. Analysis of ethylene-zirconocenium complex formation/binding thermodynamics revealed that, for zirconocenium species with the strongest agostic interaction, ethylene coordination is thermodynamically favourable at 298 K, but much less than for zirconocenium species exhibiting weaker, non-classical agostic interactions. The weaker the olefin binding, the easier the next step, migratory insertion of the methyl ligand, and as a result, the higher the polymerization activity. For short fluorous ligand substituents, olefin binding is not thermodynamically favourable at all at 298 K, and therefore polymerization is not efficient. This is in good agreement with several published experimental results.[42, 56, 92]

CHAPTER 5

General conclusions and outlook

This study was brought about by experimental observations in the coordination polymerization of α-olefins catalyzed with Group 4 metallocenes. The active species in this polymerization process is a zirconocenium complex where the metal is coordinatively unsaturated and positively charged. Its catalytic activity is to a large extent determined by the steric and electronic environments induced by the ligands. Experimental data has shown unambiguously that alkyl substituents on the Cp rings affect the polymerization activity of the catalyst and control the structural properties of the resulting polymer. Fast catalytic reactions are usually very difficult to monitor and rationalize, due to the difficulties in isolating short-lived active species experimentally. To shed some light onto the experimental findings, this work involves the modeling of zirconocenium catalysts, where the Cp rings bear alkyl substituents with various chain lengths or modified alkyl substituents containing highly electronegative F and/or electropositive Si atoms.

The first part of this work (Chapter 2) focused on the molecular geometries, energetics and electronic structure of zirconocenium catalysts with saturated hydrocarbon substituents of various lengths on the Cp ring. It was observed that, due to the chain flexibility, part of the longer substituents can move closer to the metal. In spite of the fact that alkyls are relatively poor metal ligands, the metal is so active that weak coordination of a saturated hydrocarbon fragment to the zirconium takes place. This kind of interaction is known as agostic. In addition, it was found that, depending on the chain length, two

types of agostic interaction were possible: classical for the longer chains and non-classical for the shorter chains. The intramolecular interactions between the alkyl ligand substituents and the metal center were analyzed using natural bond orbital (NBO) analysis and the quantum theory of atoms in molecules (AIM). According to established criteria, both classical and non-classical agostic interactions can be characterized as ionic, and the type of interaction is determined by the electron-donating ability of the alkyl ligand substituent with respect to the Cp ring, whether it acts as an electron donor or an electron acceptor. Depending on the role of the alkyl ligand substituent, the charge distribution on the terminal hydrocarbon fragment favours either the classical agostic interaction for longer chains or the non-classical agostic interaction for shorter chains.

The second part of this work (Chapter 3) focused on the investigation of the molecular geometries, energetics and electronic structure of zirconocenium complexes in which the alkyl ligand substituent was modified with F and Si atoms. Similarly to the situation with unmodified alkyl ligand substituents, flexible chains were found to coordinate to the electronically and sterically unsaturated zirconium. In spite of the difference in electronegativity between F and Si atoms, both F and Si-containing alkyl chains act as electron-withdrawing substituents with respect to the Cp ring. In case of the Si-containing alkyl ligand substituents, a non-classical agostic intramolecular interaction between the terminal hydrocarbon fragment and the metal center was identified. It was shown that coordination of the alkyl ligand substituent to the metal center via the F atom is different from an agostic interaction and is, in fact, much stronger than for zirconocenium species with unmodified alkyl or Si-modified alkyl ligand substituents.

Analysis of the energetics revealed that coordination of the terminal alkyl F is the strongest for alkyl ligand substituent chains containing one or two carbons.

Finally, in Chapter 4, the possible effects of intramolecular interactions in catalysts on α-olefin coordination polymerization were investigated. It was found that there is a correlation between the experimental polymerization activity and agostic interactions. The stronger the interaction, the higher the polymerization activity of the catalyst. In this case a long alkyl might act as a semilabile ligand protecting the active metal center from interactions with solvent or co-catalyst molecules which might compete with olefin binding.

According to the Cossee-Arlman homogenous Z-N polymerization reaction mechanism, the polymerization is a multi-stage process, in which olefin coordination to the zirconocenium is only the first step. In order to draw unambiguous conclusions about the relationship between agostic interactions and polymerization activity, all polymerization reaction steps should be investigated computationally. Given the size of the model systems; the computational cost of such analysis might be very high and might require a team of several researchers with powerful computational resources. Moreover, in practice, it is very difficult to compare polymerization activity data from different experimental sources. The many reported polymerization investigations were not performed under the same conditions, as different concentrations, solvents, reaction temperatures or pressures were used. Confirming that classical agostic intramolecular interactions between the metal center and ligand substituents may accelerate polymerization will require a specially designed set of experiments, all under the same

polymerization conditions, but with the different zirconocenium species investigated in this work.

References

(1) Bochmann, M. *J. Chem. Soc., Dalton Trans.* **1996**, 255.

(2) *Concise Encyclopedia of Polymer Science and Technology*; John Wiley & Sons: Hoboken; NJ, 2007.

(3) Kaminsky, W.; Laban, A. *Appl. Catal.,* **2001**, *222*, 47.

(4) Parshall, G.W.; Ittel, S.D. *Homogeneous Catalysis*, Wiley Interscience, New York, 1992.

(5) Moulijn, J.A.; Van Leeuwen, P.W.; Van Santen, R.A., Eds., Elsevier, Amsterdam, 1993.

(6) Brintzinger, H.H.; Fisher, D.; Mulhaupt, R.; Rieger, B.; Waymouth, R. M. *Angew. Chem., Int. Ed.* **1995**, *34*, 1143.

(7) Ziegler, K.; Holzkamp, E.; Breil, H.; Martin, H. *Angew. Chem.* **1955**, *67*, 426.

(8) Natta, G. *Angew. Chem.* **1956**, *68*, 393.

(9) Boor, J. J. *Catalysts and Polymerization*; Academic Press: New-York, 1979.

(10) Sinn, H.; Kaminsky, W. *Adv. Organomet. Chem.* **1980**, *18*, 99.

(11) Marks, T. J.; Stevens, J. C. *Topics in Catalysis*; Baltzer: Amsterdam, **1999**, 7, 45.

(12) Cossee, P. *J. Catal. Journal of Catalysis* **1964**, *3*, 80.

(13) Arlman, E. J.; Cossee, P. *J. Catal.* **1964**, *3*, 99.

(14) Chen, E. Y.-X.; Marks, T. J. *Chem. Rev.* **2000**, *100*, 1391.

(15) Bochmann, M. *Organometallics*; University Press: Oxford, 2001; Vol. 2.

(16) Hawrelak, E. J.; Deck, P. A. *Organometallics* **2003**, *22*, 3558.

(17) Dewar, M. J. S. *Bull. Soc. Chim. Fr.* **1951**, C71.

(18) Chatt, J. D., L. A. *J. Chem. Soc.* **1953**, 2939.

(19) Chatt, J.; Duncanson, L. A.; Venanzi, L. M. *J. Chem. Soc.* **1955**, 4456.

(20) Thomas, E. J.; Chien, J. C. W.; Rausch, M. D. **1999**, *18*, 1439.

(21) Ready, T. E.; Chien, J. C. W.; Rausch, M. D. *J. Organomet. Chem.* **1996**, *519*, 21.

(22) Kaminsky, W. *Catal. Today* **2000**, *62*, 23.

(23) Kukral, J.; Lehmus, P.; Feifel, T.; Troll, C.; Rieger, B. *Organometallics* **2000**, *19*, 3767.

(24) Resconi, L.; Piemontesi, F.; Franciscono, G.; Abis, L.; Fiorani, T. *J. Am. Chem. Soc.* **1992**, *114*, 1025.

(25) Stehling, U.; Diebold, J.; Kirsten, R.; Roell, W.; Brintzinger, H. H.; Juengling, S.; Muelhaupt, R.; Langhauser, F. *Organometallics* **1994**, *13*, 964.

(26) Thorshaug, K.; Stovneng, J. A.; Rytter, E.; Ystenes, M. *Macromolecules* **1998**, *31*, 7149.

(27) Janiak, C.; Versteeg, U.; Lange, K. C. H.; Weimann, R.; Hahn, E. *J. Organomet. Chem.* **1995**, *501*, 219.

(28) Kaminsky, W.; Engehausen, R.; Zoumis, K.; Spaleck, W.; Rohrmann, J. *Makromol. Chem.* **1992**, *193*, 1643.

(29) Spaleck, W.; Kueber, F.; Winter, A.; Rohrmann, J.; Bachmann, B.; Antberg, M.; Dolle, V.; Paulus, E. F. *Organometallics* **1994**, *13*, 954.

(30) Rappe, A. K.; Skiff, W. M.; Casewit, C. J. *Chem. Rev.* **2000**, *100*, 1435.

(31) Wilmes, G. M.; France, M. B.; Lynch, S. R.; Waymouth, R. M. *Organometallics* **2004**, *23*, 2405.

(32) Coates, G. W. *Chem. Rev.* **2000**, *100*, 1223.

(33) Smith, J. A.; Von Seyerl, J.; Huttner, G.; Brintzinger, H. H. *J. Organomet. Chem.* **1979**, *173*, 175.

(34) Tian, G.; Wang, B.; Dai, X.; Xu, S.; Zhou, X.; Sun, J. *J. Organomet. Chem.* **2001**, *634*, 145.

(35) Shapiro, P. J. *Coord. Chem. Rev.* **2002**, *231*, 67.

(36) Resconi, L.; Cavallo, L.; Fait, A.; Piemontesi, F. *Chem. Rev.* **2000**, *100*, 1253.

(37) Shaltout, R. M.; Corey, J. Y.; Rath, N. P. *J. Organomet. Chem.* **1995**, *503*, 205.

(38) Alt, H. G.; Koeppl, A. *Chem. Rev.* **2000**, *100*, 1205.

(39) Toto, M.; Cavallo, L.; Corradini, P.; Moscardi, G.; Resconi, L.; Guerra, G. *Macromolecules* **1998**, *31*, 3431.

(40) Lanza, G.; Fragala, I. L.; Marks, T. J. *Organometallics* **2002**, *21*, 5594.

(41) Chan, M. S. W.; Vanka, K.; Pye, C. C.; Ziegler, T. *Organometallics* **1999**, *18*, 4624.

(42) Lee, I. M.; Gauthier, W. J.; Ball, J. M.; Iyengar, B.; Collins, S. *Organometallics* **1992**, *11*, 2115.

(43) Piccolrovazzi, N.; Pino, P.; Consiglio, G.; Sironi, A.; Moret, M. *Organometallics* **1990**, *9*, 3098.

(44) Siemeling, U. *Chem. Rev.***2000**, *100*, 1495.

(45) Barthel-Rosa, L. P.; Gladysz, J. A. *Coord. Chem. Rev.* **1999**, *190*, 587.

(46) Smith, D. C., Jr.; Stevens, E. D.; Nolan, S. P. *Inorg. Chem.* **1999**, *38*, 5277.

(47) Soos, T.; Bennett, B. L.; Rutherford, D.; Barthel-Rosa, L. P.; Gladysz, J. A. *Organometallics* **2001**, *20*, 3079.

(48) Mitani, M.; Furuyama, R.; Mohri, J.; Saito, J.; Ishii, S.; Terao, H.; Nakano, T.; Tanaka, H.; Fujita, T. *J. Am. Chem. Soc.* **2003**, *125*, 4293.

(49) Merle, P. G.; Cheron, V.; Hagen, H.; Lutz, M.; Spek, A. L.; Deelman, B.-J.; Van Koten, G. *Organometallics* **2005**, *24*, 1620.

(50) Herrera, V.; de Rege, P. J. F.; Horvath, I. T.; Le Husebo, T.; Hughes, R. P. *Inorg. Chem. Commun.* **1998**, *1*, 197.

(51) Maldanis, R. J.; Chien, J. C. W.; Rausch, M. D. *J. Organomet. Chem.* **2000**, *599*, 107.

(52) Deck, P. A.; Jackson, W. F.; Fronczek, F. R. *Organometallics* **1996**, *15*, 5287.

(53) Briza, T.; Kvicala, J.; Paleta, O.; Cermak, J. *Tetrahedron* **2002**, *58*, 3841.

(54) Soula, R.; Broyer, J. P.; Llauro, M. F.; Tomov, A.; Spitz, R.; Claverie, J.; Drujon, X.; Malinge, J.; Saudemont, T. *Macromolecules* **2001**, *34*, 2438.

(55) Plenio, H. *Chem. Rev.* **1997**, *97*, 3363.

(56) Santamaria, C.; Beckhaus, R.; Haase, D.; Saak, W.; Koch, R. *Chem.--Eur. J.* **2001**, *7*, 622.

(57) Hughes, R. P.; Trujillo, H. A. *Organometallics* **1996**, *15*, 286.

(58) Cermak, J.; St'astna, L.; Sykora, J.; Cisarova, I.; Kvicala, J. *Organometallics* **2004**, *23*, 2850.

(59) Dinh, L. V.; Gladysz, J. A. *Chem. Commun.* **2004**, 998.

(60) Brookhart, M.; Green, M. L. H. *J. Organomet. Chem.* **1983**, *250*, 395.

(61) Scherer, W.; McGrady, G. S. *Angew. Chem., Int. Ed.* **2004**, *43*, 1782.

(62) Yao, W.; Eisenstein, O.; Crabtree, R. H. *Inorg. Chim. Acta* **1997**, *254*, 105.

(63) Brookhart, M.; Green, M. L. H.; Wong, L. L. *Prog. Inorg. Chem.* **1988**, *36*, 12.

(64) Baratta, W.; Herdtweck, E.; Rigo, P. *Angew. Chem., Int. Ed.* **1999**, *38*, 1629.

(65) Baratta, W.; Mealli, C.; Herdtweck, E.; Ienco, A.; Mason, S. A.; Rigo, P. *J. Am. Chem. Soc.* **2004**, *126*, 5549.

(66) Butts, M. D.; Bryan, J. C.; Luo, X.-L.; Kubas, G. J. *Inorg. Chem.* **1997**, *36*, 3341.

(67) King, W. A.; Luo, X.-L.; Scott, B. L.; Kubas, G. J.; Zilm, K. W. *J. Am. Chem. Soc.* **1996**, *118*, 6782.

(68) Rogers, R. D.; Atwood, J. L.; Gruening, R. *J. Organomet. Chem.* **1978**, *157*, 229.

(69) Grubbs, R. H.; Coates, G. W. *Acc. Chem. Res.* **1996**, *29*, 85.

(70) Laverty, D. T.; Rooney, J. J. *J. Chem. Soc., Faraday Trans.* **1983**, *79*, 869.

(71) Jensen, F. *Introduction to computational chemistry*; John Wiley & Sons Ltd: Baffins Lane, 1999.

(72) Kawamura-Kuribayashi, H.; Koga, N.; Morokuma, K. *J. Am. Chem. Soc.* **1992**, *114*, 2359.

(73) Deng, L.; Woo, T. K.; Cavallo, L.; Margl, P. M.; Ziegler, T. *J. Am. Chem. Soc.* **1997**, *119*, 6177.

(74) Talarico, G.; Blok, A. N. J.; Woo, T. K.; Cavallo, L. *Organometallics* **2002**, *21*, 4939.

(75) Frisch, M. J.; Trucks, G. W.; Schlegel, H. B.; Scuseria, G. E.; Robb, M. A.; Cheeseman, J. R.; Zakrzewski, V. G.; Montgomery, J. A. Jr.; Stratmann, R. E.; Burant, J. C.; Dapprich, S.; Millam, J. M.; Daniels, A. D.; Kudin, K. N.; Strain, M. C.; Farkas, O.; Tomasi, J.; Barone, V.; Cossi, M.; Cammi, R.; Mennucci, B.; Pomelli, C.; Adamo, C.; Clifford, S.; Ochterski, J.; Petersson, G. A.; Ayala, P. Y.; Cui, Q.; Morokuma, K.; Malick, D. K.; Rabuck, A. D.; Raghavachari, K.; Foresman, J. B.; Cioslowski, J.; Ortiz, J. V.; Stefanov, B. B.; Liu, G.; Liashenko, A.; Piskorz, P.; Komaromi, I.; Gomperts, R.; Martin, R. L.; Fox, D. J.; Keith, T.; Al-Laham, M. A.; Peng, C. Y.; Nanayakkara, A.; Gonzalez, C.; Challacombe, M.; Gill, P. M. W.; Johnson, B.; Chen, W.; Wong, M. W.; Andres, J. L.; Gonzalez, C.; Head-Gordon, M.; Replogle E. S.; Pople J. A. *Gaussian 98, Revosion A.7;* Gaossian Inc., Pittsburgh, PA, 1998.

(76) Konig, F. B.; Schonbohm, J.; Bayles, D. *J. Comput. Chem.* **2001**, *22*, 545.

(77) Godbout, N.; Salahub, D. R.; Andzelm, J.; Wimmer, E. *Can. J. Chem.* **1992**, *70*, 560.

(78) Batsanov, S. S. *Izv. Akad. Nauk, Ser. Khim.* **1995**, 2349.

(79) Taddei, F. *J. Chem. Inf. Comput. Sci.* **1998**, *38*, 476.

(80) Portmann, S.; Luthi, H. P. *Chimia* **2000**, *54*, 766.

(81) Schleyer, P.v.R.; Allinger, N. L., Kollmann P.A. *Encyclopedia of Computational Chemistry*; Wiley-VCH: Chichester, 1998.

(82) Becke, A. D. *J. Chem. Phys.* **1993**, *98*, 5648.

(83) Miehlich, B.; Savin, A.; Stoll, H.; Preuss, H. *Chem. Phys. Lett.* **1989**, *157*, 200.

(84) Lee, C.; Yang, W.; Parr, R. G. *Phys. Rev. B: Condens. Matter* **1988**, *37*, 785.

(85) Vosko, S. H.; Wilk, L.; Nusair, M. *Can. J. Phys.* **1980**, *58*, 1200.

(86) Hay, P. J.; Wadt, W. R. *J. Chem. Phys.* **1985**, *82*, 270.

(87) Hehre, W. J.; Ditchfield, R.; Pople, J. A. *J. Chem. Phys.* **1972**, *56*, 2257.

(88) Reed, A. E.; Curtiss, L. A.; Weinhold, F. *Chem. Rev.* **1988**, *88*, 899.

(89) Bader, R. F. W. *Atoms in Molecules: A Quantum Theory*; Clarendon: Oxford, UK, 1990.

(91) Simons, G.; Zandler, M.E.; Talaty, E.R. *J. Am. Chem. Soc.* **1976**, *98*, 7869.

(92) Ziegler, T. *Organometallics* **1998**, *17*, 933.

(93) Lambert, J. B. *Tetrahedron* **1990,** *46*, 2677.

(94) Veiros, L. F. *Organometallics* **2000**, *19(26),* 5549

Appendix A

Short description of computational methods used in this study

A proper description of the energy and geometry is necessary to predict various properties of molecules. A geometry optimization is a many-iteration process performed to find a stable atomic arrangement on the potential energy surface which is the mathematical relationship between the molecular geometries and their corresponding energies. A stable arrangement on the potential energy surface is a point where the forces are zero and is called a stationary point. A geometry optimization does not indicate the nature of the stationary point, that is, whether it is a minimum or a saddlepoint. For this purpose, a frequency calculation has to be performed for the optimized geometry, taking the second derivative of the energy with respect to atomic positions in order to determine whether the observed geometry is a minimum (no imaginary frequencies) or a transition state (one imaginary frequency). Since molecules always have some vibrational motion even at zero temperature, it is necessary to add the zero-point vibrational energy correction to the total energy of the optimized geometry. Theoretical methods have also been developed to analyze the calculated electronic structures and provide insight into the bonding scheme of molecules. These methods analyze electron wave functions and/or density.[81]

A.1 Quantum chemistry computational methods for molecular geometry and energy calculations

A computational method that does not rely on experimental values is called an *ab initio* method. The Hartree-Fock method is the simplest *ab initio* method where the

electron–electron interaction is considered in an average fashion, i.e. an electron experiences the interaction with all remaining electrons via an average field. As a result of this, the Hartree-Fock method is not accurate enough for most purposes. Higher-level *ab initio* methods for calculations taking electron-electron interaction, the so-called electron correlation, into consideration explicitly were also developed.

Another important approach that includes electronic correlation is known as density-functional theory (DFT). In DFT the energy of the electronic system is expressed in terms of the electron density.

A.2 Methods of determining partial atomic charges

The atomic charge distribution in molecules is often used to explain structure and reactivity. Despite its usefulness, the concept of a partial atomic charge is somewhat arbitrary, because atomic charges are not measurable properties and they depend on the method used to delimit atoms (in reality, atoms in molecules have no clear boundaries). As a consequence, there are many methods for estimating partial charges; based on various partitioning schemes to define the atomic subspace in a molecule. These methods include, but are not restricted to, population analysis based on atomic and molecular orbitals (Mulliken population analysis and Natural charges) and partitioning of electron density distributions (Atoms-in-molecules quantum theory).

A.3 Quantum chemical methods for analyzing the chemical bonds

A.3.1 Natural bond orbital analysis

Molecular orbitals (MO) are generally delocalised over the whole molecule, and usually bear no resemblance to "conventional" σ, π bonds, or lone-pair orbitals, so they cannot be used to support familiar chemical reasoning. Overlap of hybrid orbitals to produce localized bonds, proposed by Pauling and used by most chemists ever since, is not just a figment of our collective imagination: the calculated electron density *can* also be described in these terms. In natural bond orbital (NBO) analysis [88] The atomic basis set is transformed into an equal number of natural atomic orbitals (NAOs), and the MOs into an equal number of natural bond orbitals (NBOs) (Figure A.1). These additional transformations are not computationally expensive. This analysis was devised by F. Weinhold at University of Wisconsin, during the 1980s. NBO analysis is available in the Gaussian package. NBO analysis transforms a given wave function into localized form, corresponding to the one-center (lone pair) and two-center ("bond") elements of the Lewis structure representation. The process involves the following steps:

- input AO basis sets ⟶ NAOs
  - Basis functions are transformed to natural atomic orbitals
- NAOs ⟶ NHOs
  - NAOs are combined into natural hybrid orbitals, so as to describe the atom combination to the molecular electron density
  - The NHOs form orthogonal sets on each A and B atom as

$\sigma_{AB} = C_A h_A + C_B h_B$ (Lewis or bond orbitals)

$\sigma^*_{AB} = C_A h_A - C_B h_B$ (non-Lewis or antibonding orbitals),

where h_A, h_B are valence hybrids orbital and C_A, C_B are coefficients

- NHOs ⟶ NBOs
  - NHOs overlap to produce NBOs

The total number of orbitals remains the same:

No. of basis functions = no. of MOs = no. of NAOs = no. of NBOs

Each set consists of normalized linear combinations of MOs, which also form a valid set of solutions to Schroedinger's equation for the molecule. Because there is not a one-to-one correspondence between occupied or virtual MOs and NBOs, the NBOs are not restricted to either occupied or empty, as MOs are and in fact NBOs have fractional occupancy between 0 and 2. Many NBOs contain nearly 2 electrons: these correspond to classical Lewis-type core, bonding or lone pair orbitals. Some of the remaining NBOs are not practically empty: usually these are antibonding orbitals.

NBO analysis can be used to calculate the stabilization energy arising from orbital delocalization. This is done by examining all possible interactions between 'filled' (donor) Lewis-type NBOs and 'empty' (acceptor) non-Lewis-type NBOs, and estimating their energetic importance by 2nd-order perturbation theory. Since these interactions lead to loss of occupancy from the localized NBOs of the idealized Lewis structure into the empty non-Lewis orbitals (and thus, to departure from the idealized Lewis structure description), they are referred to as 'delocalization' corrections to the natural Lewis structure (Figure A.2).

A.3.2 Atoms-in-molecules quantum theory

The electron density $\rho(r)$ of a molecule– i.e. the probability of finding an electron of the molecule at a given point in space, can be calculated or determined experimentally and provides information about the electron distribution within the molecule, which may allow for an understanding of molecular properties. The quantum theory of "atoms in molecules" (AIM) analyses of its topology of $\rho(r)$, $\nabla\rho(r)$ and $\nabla^2\rho(r)$.[89] The topology is described by the number and kinds of critical points. Critical points (CP) are the points where the first derivative of $\rho(r)$ vanishes ($\nabla\rho(r) = 0$), thus they determine the positions of extremes as maxima, minima or saddle points. Each CP is labelled by rank (ω) and signature (σ) as (ω, σ). For example (3,-3) CP with three negative curvatures and occurs at nuclear positions. A (3,-1) CP has two negative curvatures and one positive, is found between every pair of interacting nuclei is referred to as a bond critical point (BCP) in a minimum geometry. Connecting all (3, -1) to their respective (3, -3) CPs produces a

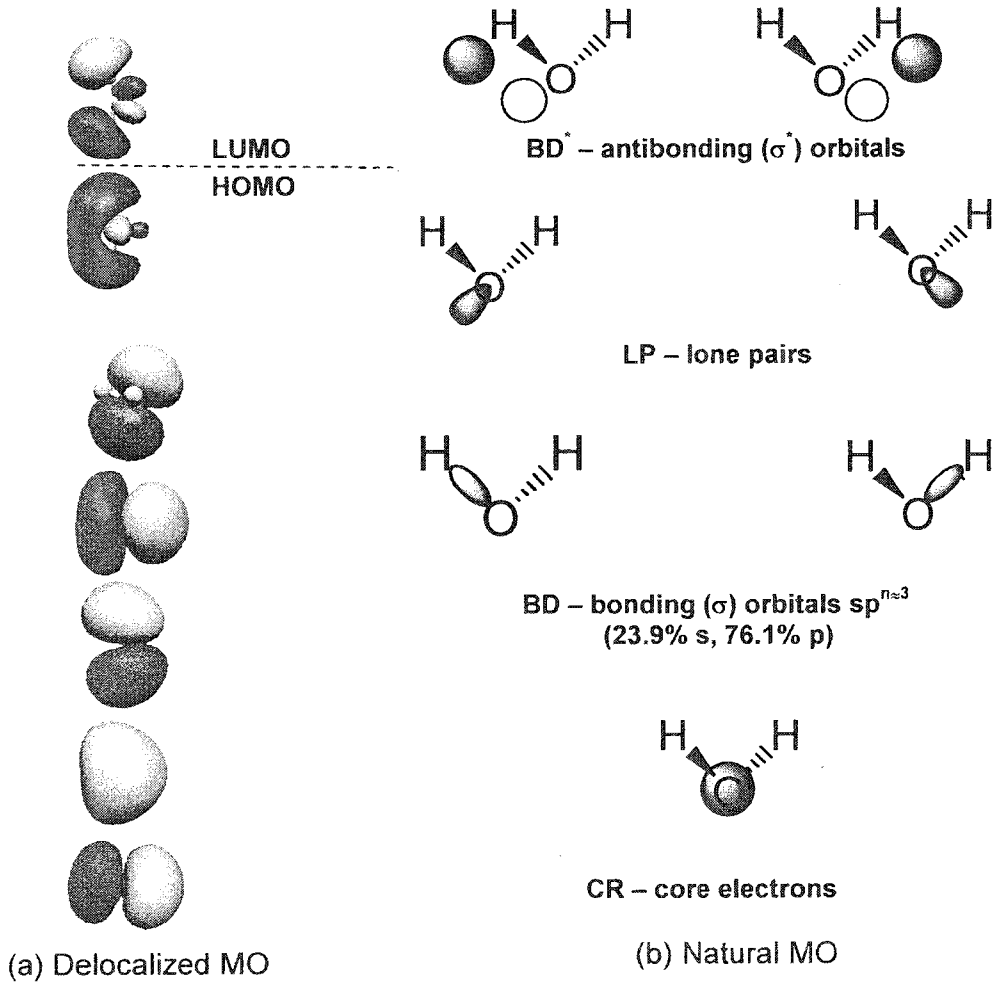

Figure A.1. Delocalized MOs (a) and natural MOs (b)for the water molecule.

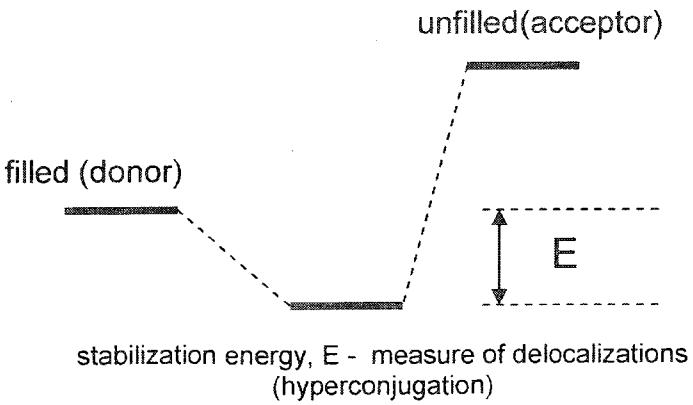

Figure A. 2. NBO second-order perturbation approach for bond delocalization energies.

molecular graph. Figure A.3 displays BCPs of the water molecule. Gradient vectors that terminate at a BCP span the interatomic surface. The atom is then defined as the union of a (3, -3) CP and its basin (Ω), the area enclosed by interatomic surfaces. Integration of $\rho(r)$ over a basin determines, for example, an atom's volume, energy and charge. It was proposed to use AIM to find and characterize agostic interactions. The sign of the Laplacian of the electron density $\nabla^2\rho$ at the BCP defines the shared or closed-shell interaction. If the Laplacian is negative then it is defined as shared interaction and if it is positive then it is defined as a closed-shell interaction. Covalent bonds typically correspond to shared interaction, while other types of interactions are closed-shell interactions. The value of ρ at the BCP for ionic bonds is usually 10 times weaker than for covalent and approximately of the order 10^{-1} e/Å^3.

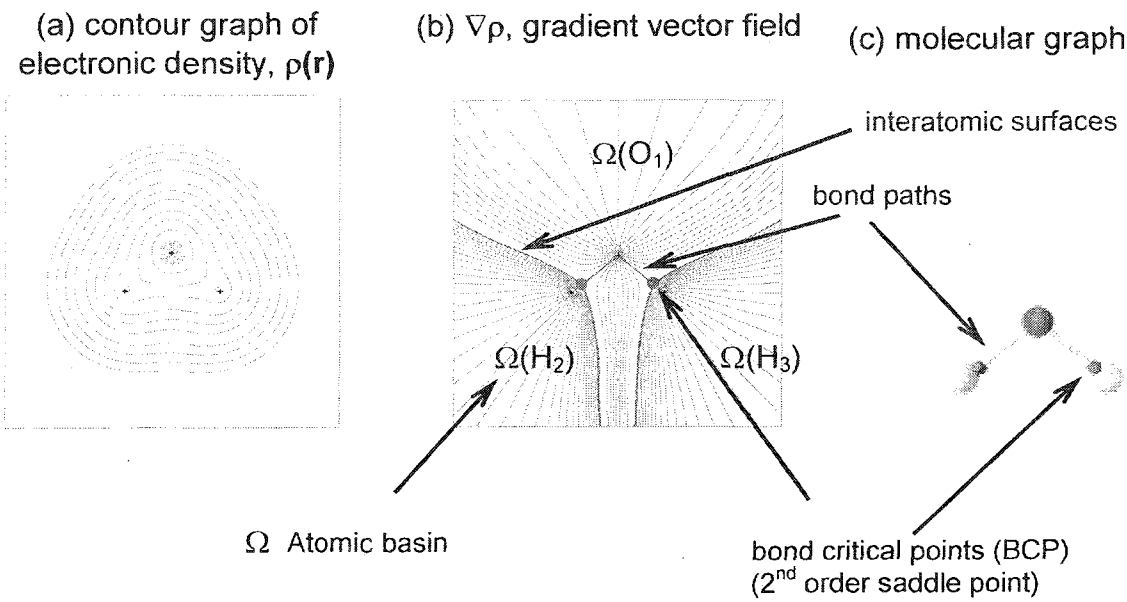

Figure A.3. Contour diagram and molecular graph for the water molecule.

Appendix B

Supplemental information related to CHAPTER 2

Table B1. Geometry of the structure in **Figure 2.3.**

B3LYP/6-31G(d,p)

Atomic Number	Coordinates (Angstroms) X	Y	Z
6	-1.173308	-1.138162	0.000104
6	-2.525406	-0.714748	-0.000033
6	-2.540842	0.702792	0.000001
6	-1.197206	1.155591	0.000112
6	-0.338264	0.018618	0.000248
6	1.187812	0.006524	0.000000
6	1.724378	-0.731700	-1.260266
6	1.724765	-0.728789	1.261746
6	1.761570	1.443352	-0.001753
1	-0.830711	-2.171393	0.000404
1	-3.397596	-1.365508	-0.000408
1	-3.426175	1.335173	-0.000117
1	-0.881730	2.195375	-0.000020
1	2.826705	-0.779833	-1.271340
1	1.387444	-0.215340	-2.167268
1	1.331378	-1.754117	-1.297343
1	2.827128	-0.776752	1.272878
1	1.331971	-1.751216	1.301214
1	1.387858	-0.210479	2.167653
1	2.861951	1.427514	-0.001805
1	1.420466	1.993946	0.883019
1	1.420316	1.991765	-0.887830

E = -350.6821908 hartrees

ν = 33.9726, 144.7987, 212.0046, 237.5774, 282.8360, 286.2746, 333.8472, 341.5893, 342.3973, 443.2067, 471.1628, 580.9224, 628.8884, 635.5185, 670.9425, 692.5104, 761.2685, 791.9701, 818.0127, 881.8339, 913.1820, 934.6720, 942.2064, 974.5476, 1058.2228, 1068.4770, 1077.4061, 1083.8654, 1102.5919, 1201.0975, 1229.4641, 1238.4069, 1298.3479, 1323.0610, 1398.2946, 1415.5619, 1417.0223, 1426.3823, 1444.5035, 1473.2475, 1514.4701, 1525.5362, 1525.6319, 1530.4317, 1534.6703, 1537.3544, 1555.2729, 2975.7356, 2985.9905, 3011.4969, 3075.0461,

3077.7868, 3087.5326, 3107.7204, 3113.8667, 3116.5213, 3137.3190, 3152.8119, 3171.3532, 3193.0567 cm^{-1}

File name (in my CERMM directory): Ligand2.log

Table B2. Zr. geometry of **I**.

B3LYP/6-31G(d,p) on lighter elements and DZVP DeMon DFT orbitals on

Atomic Number	Coordinates (Angstroms) X	Y	Z
6	1.290135	-1.064325	1.493108
6	2.073024	0.059634	1.091261
6	2.374332	-0.070327	-0.290601
6	1.765802	-1.289426	-0.740389
6	1.128634	-1.912175	0.361223
6	3.230320	0.851067	-1.114255
1	0.941966	-1.270897	2.497812
1	2.399548	0.866616	1.733104
1	1.833501	-1.693292	-1.744859
1	0.610900	-2.861893	0.345004
1	2.928879	0.866830	-2.166316
1	4.270749	0.506673	-1.087197
1	3.215874	1.873947	-0.729695
6	-2.554560	0.857598	-0.663804
6	-2.260575	-0.329125	-1.400960
6	-2.070513	-1.386445	-0.476465
6	-2.221541	-0.851812	0.837407
6	-2.544741	0.532694	0.713465
1	-2.766641	1.832392	-1.084494
1	-2.227831	-0.414975	-2.481430
1	-1.862532	-2.418761	-0.724441
1	-2.179344	-1.415577	1.760700
1	-2.743939	1.216524	1.528054
40	-0.156779	0.213238	-0.083917
6	0.052272	2.320293	0.689102
1	1.029314	2.747078	0.430331
1	-0.732968	2.977294	0.298999
1	-0.021834	2.352610	1.786562

E = - 4006.7936048 hartrees

ν = 15.7755, 34.0867, 62.1696, 24.2355, 40.4762, 88.1474, 99.4851, 113.3596, 133.0286, 165.7375, 176.9271, 217.0694, 243.8953, 260.3377, 281.4664, 290.4018, 307.8436, 361.8566, 383.1476, 386.1359, 436.5140, 469.3823, 485.8906, 497.2434, 545.3418, 592.4854, 597.6745, 601.6035, 653.4628, 678.9537, 703.8617, 822.3311, 835.7112, 842.7113, 847.9809, 850.2656, 851.5502, 854.5860, 859.9475, 862.7480, 909.2328, 928.2853,

938.0016, 939.1582, 942.4423, 1036.4578, 1043.3203, 1058.0545,
1072.2944, 1090.0205, 1091.6138, 1094.0757, 1145.6057, 1186.4353,
1212.4463, 1256.5227, 1297.7934, 1339.1415, 1377.2969, 1401.1739,
1406.9639, 1418.2258, 1425.2663, 1439.2685, 1444.5175, 1467.8757,
1475.0324, 1482.6980, 1516.3182, 3025.3991, 3099.1198, 3120.8828,
3242.3814, 3248.3365, 3254.7114, 3256.6572, 3263.4073, 3265.5603,
3270.6771, 3276.2976, 3277.2778 cm^{-1}

File name (in my CERMM directory): Chain1BS.log

Table B3. Geometry of **IIa**.

B3LYP/6-31G(d,p) on lighter elements and LanL2DZ on Zr

Atomic Number	Coordinates (Angstroms) X	Y	Z
6	0.484595	2.445880	-0.232311
6	0.301976	1.853318	-1.507392
6	1.051843	0.648431	-1.534836
6	1.710644	0.482699	-0.281660
6	1.333214	1.599116	0.523894
6	2.989446	-1.567426	-1.059010
6	2.808864	-0.526278	0.062377
6	4.137701	0.259189	0.203463
6	2.524406	-1.253937	1.393491
1	0.043949	3.372350	0.108484
1	-0.302748	2.244796	-2.314897
1	1.130828	-0.019376	-2.381756
1	1.668281	1.790004	1.534124
1	3.268261	-1.092287	-2.005009
1	2.080836	-2.152284	-1.230102
1	3.787920	-2.267625	-0.792603
1	4.085335	0.987615	1.018239
1	4.966127	-0.426514	0.415555
1	4.372174	0.802570	-0.717561
1	3.357586	-1.919047	1.647197
1	1.615325	-1.860195	1.333869
1	2.398657	-0.546891	2.218760
40	-0.912021	0.334554	0.154343
6	-0.781801	0.329861	2.436197
6	-2.583178	1.891420	0.012024
1	-0.554349	1.341065	2.797531
1	-1.756019	0.038684	2.849854
1	-0.031764	-0.346914	2.863127
1	-2.833926	2.173627	-1.019089
1	-3.501523	1.522697	0.484493
1	-2.279738	2.807441	0.534484
6	-0.883183	-2.136500	-0.513711

6	-1.614096	-1.461478	-1.533239
6	-2.834267	-1.013248	-0.968769
6	-2.853946	-1.400173	0.395337
6	-1.656177	-2.103200	0.674842
1	0.074458	-2.622799	-0.633752
1	-1.305294	-1.336822	-2.562712
1	-3.605795	-0.455630	-1.481420
1	-3.639761	-1.178625	1.105126
1	-1.374223	-2.524042	1.630175

E = -670.7964724 hartrees

ν = 26.1767, 37.8443, 65.4853, 97.3239, 124.5995, 133.6733, 140.6140, 148.1487, 164.9107, 181.0822, 208.9833, 214.9668, 225.7441, 232.6769, 241.5324, 261.3864, 263.1059, 279.7869, 291.3272, 297.2066, 322.9174, 336.3501, 345.5002, 370.0564, 441.4077, 454.5262, 465.2425, 467.5424, 519.2847, 546.0324, 578.2107,595.4393, 598.8221, 603.7714, 641.6446, 655.2027, 681.3398, 808.5187, 810.4958, 813.9206, 816.6072, 822.3762, 825.0034, 853.9368, 856.6189, 864.0086, 883.7624, 895.4981, 910.4844, 911.8971, 926.0891, 935.1409, 945.6185, 966.1885, 1038.6335, 1043.5010, 1046.2528, 1054.2755, 1069.0720, 1075.3253, 1088.8923, 1089.9343, 1092.6820, 1154.4373, 1188.0580, 1188.9515, 1196.9543, 1217.8692, 1229.5099, 1276.9987, 1298.7920, 1306.4895, 1382.9448, 1408.8586, 1410.9811, 1412.4471, 1414.0219, 1431.3543, 1445.4920, 1454.6270, 1458.3204, 1460.0692, 1463.9012, 1466.3858, 1485.6114, 1488.1034, 1493.7600, 1497.6957, 1500.8951, 1513.7845, 1517.7327, 1520.6354, 1536.0466, 3015.4492, 3017.0186, 3039.7528, 3044.6258, 3052.0798, 3090.5861, 3092.2200, 3101.1645, 3101.5908, 3110.0689, 3113.1209, 3119.1775, 3123.0730, 3126.2607, 3128.1135, 3244.1291, 3245.1739, 3247.8727, 3253.0256, 3259.7538, 3261.3421, 3266.1323, 3271.4796, 3275.5548

File name (in my CERMM directory): No25tBuNeu.log

Table B4. Zr .geometry of **IIb**.

B3LYP/6-31G(d,p) on lighter elements and DZVP DeMon DFT orbitals on

Atomic Number	Coordinates (Angstroms) X	Y	Z
6	2.037244	-1.925583	-0.355411
6	2.606339	-1.358734	0.823192

6	3.126989	-0.084168	0.490483
6	2.852915	0.155381	-0.886598
6	2.192316	-0.995347	-1.411773
1	1.594026	-2.911143	-0.436199
1	2.657802	-1.831353	1.796207
1	3.640445	0.588231	1.163687
1	3.157299	1.026509	-1.452280
1	1.885233	-1.139216	-2.439159
6	-1.748871	0.494630	-0.482884
6	-0.968717	0.403373	-1.677114
6	-0.113826	1.539314	-1.744658
6	-0.362714	2.341921	-0.599922
6	-1.364839	1.703092	0.172725
6	-2.602781	-0.625395	0.121210
6	-1.615413	-1.511112	0.925976
6	-3.275000	-1.468593	-0.977684
6	-3.676369	-0.062977	1.070704
1	-1.024131	-0.380999	-2.420438
1	0.564201	1.776314	-2.553776
1	0.112572	3.285874	-0.366170
1	-1.768351	2.078488	1.101743
1	-2.099757	-2.384515	1.375162
1	-0.828976	-1.953247	0.276704
1	-1.165953	-0.968387	1.779607
1	-3.879441	-2.261037	-0.526671
1	-2.547564	-1.948603	-1.640367
1	-3.934700	-0.848878	-1.591382
1	-4.273829	-0.878653	1.488317
1	-4.352031	0.609811	0.535239
1	-3.242320	0.488631	1.910614
40	0.609395	0.115943	0.213721
6	0.936871	1.197726	2.178843
1	1.549066	0.605273	2.867618
1	1.451557	2.157092	2.030993
1	-0.015812	1.430922	2.669184

E = -4124.7471585 hartrees

ν = 31.2685, 39.1516, 79.0870, 86.4782, 132.8482, 139.9060, 142.8226, 203.6836, 227.3691, 228.9255, 244.0818, 250.5397, 261.3842, 280.7733, 287.4606, 311.8071, 331.9426, 343.0452, 359.6901, 360.1516, 374.8485, 445.7215, 463.6144, 465.9903, 482.8127, 572.0623, 576.0644, 582.9622, 589.1906, 681.5879, 694.7587, 809.2019, 827.9900, 835.5236, 842.6281, 846.6387, 850.5196, 851.6375, 852.7473, 858.9250, 884.8724, 921.9912, 922.6073, 923.3206, 925.9396, 926.7347, 941.5803, 965.7562, 1015.3107, 1035.3974, 1043.7238, 1045.7418, 1069.7438, 1074.3589, 1088.5750, 1091.1033, 1094.2431, 1145.1361, 1178.2289, 1211.2715, 1217.3766, 1229.5200, 1275.7516, 1294.1485, 1298.3709, 1378.4464, 1381.5020, 1399.9524, 1406.8296, 1422.3790, 1427.7453, 1445.5781, 1447.6060, 1448.7989, 1455.3668, 1473.7706, 1483.6521, 1492.4751, 1496.7230,

1499.1338, 1501.4084, 1520.8734, 1525.2000, 1532.0352, 2896.4391,
2970.5231, 3025.3224, 3054.0108, 3057.9719, 3095.6104, 3104.3565,
3116.5075, 3123.3955, 3126.7897, 3137.7843, 3141.3821, 3239.0045,
3251.0942, 3252.5047, 3255.7188, 3259.3909, 3267.4751, 3269.5551,
3277.7830, 3279.6737 cm^{-1}

File name (in my CERMM directory): No25BStBu.log

Table B5. Geometry of **III.**

B3LYP/6-31G(d,p) on lighter elements and DZVP DeMon DFT orbitals on Zr .

Atomic Number	Coordinates (Angstroms) X	Y	Z
6	1.327735	-2.049000	0.276716
6	2.113064	-0.941844	0.686217
6	2.223745	-0.035980	-0.409157
6	1.496126	-0.596629	-1.500045
6	0.940101	-1.836997	-1.074435
6	2.751832	1.378508	-0.337355
6	1.622878	2.310800	0.144140
1	1.082004	-2.912096	0.881893
1	2.560466	-0.809638	1.662256
1	1.400164	-0.163534	-2.488487
1	0.374567	-2.524626	-1.689024
1	3.108643	1.703044	-1.319078
1	3.599469	1.439410	0.350932
1	1.299547	2.072339	1.172576
1	1.919903	3.363249	0.173156
1	0.755641	2.296629	-0.548331
6	-2.499130	1.093314	0.340866
6	-2.025238	1.306955	-0.987655
6	-1.912754	0.046925	-1.624210
6	-2.308205	-0.952861	-0.685839
6	-2.691916	-0.298032	0.520275
1	-2.701616	1.862122	1.076192
1	-1.820047	2.269339	-1.441839
1	-1.601704	-0.127005	-2.645797
1	-2.375280	-2.015433	-0.880758
1	-3.062901	-0.778432	1.415046
40	-0.190315	0.011962	0.220934
6	-0.341932	-0.279732	2.462126
1	0.620545	-0.099009	2.955090
1	-1.094583	0.382378	2.904555
1	-0.630046	-1.309789	2.714377

E = - 4046.1131546 hartrees

ν = 30.2690, 32.9929, 88.1605, 91.0521, 118.0496, 127.0215, 137.9892,

216.6737, 239.7673, 251.2042, 266.8168, 269.1134, 289.8080, 321.3221,
357.0936, 360.3823, 433.1689, 450.0616, 480.0675, 589.2141, 595.0471,
598.5162, 626.3063, 676.0961, 687.2792, 785.9167, 837.8694, 838.4314,
846.4026, 847.6343, 850.9685, 852.6749, 855.6878, 860.8915, 893.4912,
920.9579, 927.1312, 929.5198, 933.9786, 975.6576, 1034.8751, 1038.9826,
1043.6806, 1049.6262, 1067.4574, 1078.1671, 1089.4373, 1091.2313,
1094.7500, 1144.7799, 1210.8606, 1244.6625, 1256.3311, 1297.1339,
1297.6514, 1353.3580, 1395.1149, 1398.6800, 1399.7461, 1407.4669,
1428.9059, 1440.2731, 1443.3321, 1461.6650, 1473.3327, 1483.6988,
1491.8116, 1504.7910, 1516.8878, 1521.2086, 2916.3763, 2998.1579,
3022.2790, 3083.1208, 3092.4169, 3116.9502, 3120.8952, 3131.6358,
3237.6110, 3241.3817, 3250.8648, 3252.2295, 3255.6005, 3262.0108,
3266.4454, 3270.1572, 3276.5439 cm^{-1}

File name (in my CERMM directory): chain2CBS.log

Table B6. Geometry of **IV.**

B3LYP/6-31G(d,p) on lighter elements and DZVP DeMon DFT orbitals on Zr

Atomic Number	Coordinates (Angstroms) X	Y	Z
6	0.550928	-2.365082	0.226729
6	1.552871	-1.567979	0.844529
6	2.090907	-0.681217	-0.128229
6	1.420929	-0.958896	-1.365534
6	0.489673	-2.001841	-1.147790
6	3.157145	0.360446	0.112681
6	2.827484	1.749070	-0.469511
6	1.391871	2.209920	-0.164613
1	-0.025631	-3.146605	0.705411
1	1.859608	-1.627982	1.879361
1	1.614674	-0.476508	-2.316511
1	-0.150751	-2.449253	-1.896180
1	4.106863	0.010444	-0.310138
1	3.319119	0.447480	1.192760
1	3.531322	2.479879	-0.060135
1	2.976037	1.760636	-1.554687
1	1.101073	1.997041	0.880288
1	1.253753	3.286873	-0.295732
1	0.672242	1.783383	-0.899545
6	-2.483047	1.380504	0.263816
6	-2.082332	1.344480	-1.103563
6	-2.156111	0.002098	-1.550140
6	-2.601140	-0.797818	-0.455395

6	-2.820293	0.062673	0.657904
1	-2.544027	2.264424	0.886025
1	-1.804200	2.200399	-1.706735
1	-1.941025	-0.349275	-2.550527
1	-2.802482	-1.860781	-0.486260
1	-3.179387	-0.236707	1.632873
40	-0.321682	0.005934	0.182595
6	-0.348186	0.134228	2.451745
1	0.660732	0.269197	2.860001
1	-0.975062	0.966407	2.791380
1	-0.749763	-0.779920	2.908772

E =- 4085.4366862 hartrees

ν = 34.4815, 48.8707, 94.8340, 108.3761, 132.2933, 152.6039, 167.3600, 168.7918, 201.8962, 230.0557, 258.5611, 275.9567, 292.0643, 322.3953, 336.7611, 344.4266, 373.3208, 414.5348, 466.0451, 477.8805, 485.6900, 594.4293, 595.4503, 600.1908, 617.9684, 660.0166, 677.5690, 794.9449, 838.7237, 840.2242, 846.2329, 847.5881, 851.5985, 853.3806, 856.2457, 858.3083, 872.9951, 896.3374, 903.1349, 925.6970, 932.0317, 935.6795, 940.7388, 1033.6407, 1036.0110, 1043.8867, 1051.6808, 1065.5030, 1081.9725, 1089.0835, 1091.4266, 1093.1029, 1096.9050, 1145.9780, 1213.2468, 1236.4859, 1253.0323, 1272.0614, 1289.4742, 1298.3463, 1362.2472, 1367.4119, 1381.1668, 1401.0933, 1407.2498, 1408.3085, 1430.6781, 1447.3133, 1448.2235, 1465.9873, 1474.7947, 1484.3400, 1491.3439, 1502.2091, 1506.0075, 1521.7465, 1549.5248, 2870.3452, 2987.0009, 3023.5536, 3053.7586, 3070.3632, 3093.3179, 3096.2761, 3113.9182, 3117.5091, 3123.3743, 3235.9241, 3240.2060, 3249.5184, 3251.5220, 3257.0136, 3265.0075, 3266.5335, 3272.6272, 3275.8519 cm^{-1}

File name (in my CERMM directory): chain3BS.log

Table B7. Geometry of **V**

B3LYP/6-31G(d,p) on lighter elements and DZVP DeMon DFT orbitals on Zr

Atomic Number	Coordinates (Angstroms) X	Y	Z
6	-0.273728	2.517733	0.323174
6	-1.378309	1.794926	0.842331
6	-1.937897	1.001681	-0.197440
6	-1.162470	1.248810	-1.375465
6	-0.150243	2.190704	-1.054538
6	-3.131511	0.087104	-0.063192

6	-2.958125	-1.287922	-0.737350
6	-1.636530	-1.999695	-0.402406
6	-1.320017	-2.156489	1.091538
1	0.344116	3.215889	0.872320
1	-1.742988	1.842940	1.859521
1	-1.340865	0.826067	-2.356520
1	0.570420	2.606632	-1.745502
1	-4.009876	0.581275	-0.496114
1	-3.356144	-0.039554	1.001220
1	-3.792608	-1.933749	-0.442737
1	-3.026358	-1.183359	-1.825811
1	-1.624858	-2.992244	-0.865631
1	-0.811879	-1.493231	-0.964454
1	-2.166556	-2.617860	1.609961
1	-1.172971	-1.205175	1.635890
1	-0.450742	-2.796965	1.266498
6	2.406257	-1.521221	0.187073
6	1.865122	-1.563531	-1.129247
6	2.009639	-0.279513	-1.708508
6	2.655006	0.559746	-0.750536
6	2.915153	-0.217038	0.410605
1	2.458676	-2.349473	0.882487
1	1.437231	-2.433238	-1.612484
1	1.715422	0.004600	-2.710152
1	2.956930	1.586954	-0.906301
1	3.414935	0.124866	1.305571
40	0.390890	0.065378	0.196855
6	0.812021	0.359186	2.426430
1	-0.106274	0.515065	3.002579
1	1.333251	-0.514563	2.834471
1	1.449344	1.233113	2.606197

E = - 4124.7513554 hartrees

ν = 39.4665, 61.0692, 99.4302, 125.8394, 133.7751, 142.1938, 167.1106, 178.5910, 209.5258, 240.1375, 249.5072, 260.4001, 267.2002, 276.5027, 294.5266, 322.6109, 330.6801, 344.9469, 362.2107, 392.3486, 465.1899, 511.3957, 549.6523, 592.7972, 597.1974, 602.2225, 614.5283, 668.4352, 689.8355, 746.2366, 814.6773, 840.4450, 841.7037, 845.2856, 849.5804, 852.0148, 852.4609, 857.1006, 861.2668, 870.1985, 899.3665, 928.5655, 931.3749, 933.4348, 938.3756, 954.7202, 979.3832, 1036.9830, 1045.5594, 1064.9522, 1069.2625, 1077.3074, 1084.2344, 1090.5345, 1093.3363, 1096.0753, 1106.8816, 1147.7980, 1206.6008, 1216.9585, 1247.8679, 1257.0604, 1279.5821, 1295.8652, 1299.7000, 1348.4069, 1376.2565, 1386.3507, 1403.9273, 1409.7918, 1410.6829, 1433.8774, 1435.1596, 1454.6274, 1459.8895, 1464.4804, 1477.4168, 1482.9495, 1485.5994, 1501.0031, 1506.7083, 1522.8301, 1534.7044, 1537.6559, 2813.5297, 2965.1495, 3031.4263, 3055.4010, 3062.6161, 3086.0302, 3090.9188, 3096.2564, 3107.6481, 3110.7153, 3118.8142, 3134.9688, 3242.2354,

3242.9359, 3252.0668, 3254.0504, 3257.9012, 3263.1384, 3266.8441, 3271.8231, 3280.9748 cm^{-1}

File name (in my CERMM directory): chain2BS.log

Appendix C

Supplemental information related to CHAPTER 3

Table C1. Geometry of **I**.

B3LYP/6-31G(d,p)on lighter elements and for Zr a DZVP DeMon DFT orbitals

Atomic Number	Coordinates (Angstroms) X	Y	Z
6	2.061888	-1.940228	-0.642320
6	2.565115	-1.654797	0.661212
6	3.202658	-0.390740	0.618635
6	3.061967	0.126199	-0.699932
6	2.367576	-0.844261	-1.483724
1	1.558425	-2.850960	-0.944283
1	2.499493	-2.304452	1.525161
1	3.705775	0.096149	1.441997
1	3.472417	1.059594	-1.062686
1	2.138610	-0.766055	-2.538160
6	-1.490086	0.890278	-0.537923
6	-0.644190	0.867813	-1.697078
6	0.350129	1.872707	-1.559967
6	0.134724	2.533550	-0.319920
6	-0.993488	1.940319	0.297570
14	-2.648062	-0.501814	0.017849
6	-1.361378	-1.678136	0.840563
6	-3.440458	-1.362572	-1.447731
6	-3.874542	0.099669	1.301200
1	-0.747338	0.202944	-2.546358
1	1.112054	2.120372	-2.287530
1	0.715735	3.359103	0.071185
1	-1.404147	2.232901	1.254460
1	-1.833279	-2.601516	1.195623
1	-0.589307	-2.063457	0.143952
1	-0.888537	-1.260415	1.748857
1	-4.027373	-2.226329	-1.117637
1	-2.703743	-1.723177	-2.173338
1	-4.120169	-0.683559	-1.972945
1	-4.480385	-0.730354	1.679862
1	-4.558322	0.835406	0.865182
1	-3.383730	0.568101	2.160543
40	0.733068	0.077114	0.207178
6	1.052657	0.835352	2.324348
1	1.505617	0.054627	2.946583
1	1.717811	1.707374	2.361905
1	0.105119	1.143615	2.781010

E = -4376.1724771 hartrees

ν = 30.6694, 34.4111, 83.8099, 87.7997, 111.0390, 126.4840, 137.2733, 151.6430, 156.1590, 159.8547, 184.7232, 195.0165, 222.5322, 225.9945, 227.7989, 246.4961, 254.8812, 263.7984, 291.1928, 303.5127, 328.6470, 337.3387, 377.8925, 422.0392, 474.5762, 497.0507, 580.1044, 590.9945, 595.7500, 600.7414, 637.6416, 679.7299, 685.5336, 690.2824, 712.4118, 721.7692, 787.3202, 839.5737, 842.9280, 849.5359, 851.6337, 852.0951, 853.5659, 857.8157, 861.7100, 862.8676, 870.5162, 877.9518, 908.4938, 916.4179, 926.4107, 937.8931, 938.3653, 1035.0216, 1045.0231, 1069.1226, 1073.1918, 1089.4679, 1092.7787, 1095.7380, 1146.2765, 1193.9454, 1214.3235, 1230.0298, 1289.6787, 1298.7209, 1326.2119, 1333.5067, 1352.1329, 1401.1252, 1408.0939, 1411.1797, 1446.2238, 1448.4486, 1449.6560, 1463.3549, 1464.3546, 1465.7804, 1474.7331, 1475.3923, 1481.7372, 1485.0895,1486.2234, 1492.5787, 2926.9268, 2998.5017, 3026.0514, 3049.5209, 3051.6776, 3102.3531, 3102.8829, 3114.0721, 3126.0470, 3129.6467, 3131.4971, 3132.6849, 3238.6506, 3239.5889, 3250.0292, 3250.5792, 3255.0875, 3260.8042, 3266.6313, 3268.6623, 3278.4035 cm^{-1}

File name (in my CERMM directory): No25BS.log

Table C2. Geometry of **II**.

B3LYP/LANL2DZ for Zr and B3LYP/6-31G (d,p) for the rest elements

Atomic Number	Coordinates (Angstroms) X	Y	Z
6	1.854466	-1.905073	-0.423657
6	2.491737	-1.363739	0.729620
6	3.030908	-0.098337	0.384162
6	2.701615	0.159369	-0.976206
6	1.983737	-0.968057	-1.478526
1	1.361100	-2.867785	-0.483620
1	2.567388	-1.843984	1.697481
1	3.595017	0.552778	1.037348
1	3.002041	1.028063	-1.548467
1	1.627443	-1.095652	-2.492200
6	-1.829809	0.520091	-0.471456
6	-1.061030	0.579729	-1.669319
6	-0.299824	1.776408	-1.611012
6	-0.604677	2.445335	-0.392629
6	-1.545927	1.670130	0.320295
6	-2.376928	-0.741525	0.079576
9	-3.216684	-0.620146	1.081107
9	-1.169180	-1.402636	0.695213

9	-2.799478	-1.620859	-0.800721
1	-1.073940	-0.142928	-2.474400
1	0.354904	2.145432	-2.389371
1	-0.198213	3.395400	-0.071853
1	-1.972420	1.900180	1.286943
40	0.513683	0.149523	0.226695
6	0.954856	1.194034	2.178069
1	1.577665	0.568649	2.826209
1	1.472670	2.153961	2.052410
1	0.012355	1.407556	2.697827

E = -4304.5152827 hartrees

ν = 24.2355, 40.4762 , 88.1474, 99.4851, 113.3596,133.0286, 165.7375, 176.9271, 217.0694, 243.8953, 260.3377, 281.4664, 290.4018 307.8436 361.8566, 383.1476, 386.1359, 436.5140, 469.3823, 485.8906, 497.2434, 545.3418, 592.4854, 597.6745, 601.6035, 653.4628, 678.9537, 703.8617, 822.3311, 835.7112, 842.7113, 847.9809, 850.2656, 851.5502, 854.5860, 859.9475, 862.7480, 909.2328, 928.2853, 938.0016, 939.1582, 942.4423, 1036.4578, 1043.3203, 1058.0545, 1072.2944, 1090.0205, 1091.6138, 1094.0757, 1145.6057, 1186.4353, 1212.4463, 1256.5227, 1297.7934, 1339.1415, 1377.2969, 1401.1739, 1406.9639, 1418.2258, 1425.2663, 1439.2685 1444.5175 1467.8757, 1475.0324, 1482.6980, 1516.3182, 3025.3991, 3099.1198, 3120.8828, 3242.3814, 3248.3365, 3254.7114, 3256.6572, 3263.4073, 3265.5603, 3270.6771, 3276.2976, 3277.2778 cm^{-1}

File name (in my CERMM directory): Chain1BSF.log

Table C3. Geometry of **III**.

B3LYP/6-31G (d,p) on lighter elements, for Zr a DZVP DeMon DFT orbitals

Atomic Number	Coordinates (Angstroms) X	Y	Z
6	1.824710	-1.976208	-0.638922
6	2.410887	-1.687716	0.627171
6	3.110413	-0.458972	0.520484
6	2.929907	0.032273	-0.802901
6	2.144144	-0.917698	-1.523959
1	1.238754	-2.854649	-0.881637
1	2.348292	-2.308849	1.512229
1	3.679929	0.019636	1.304859
1	3.369223	0.934101	-1.209887
1	1.864393	-0.852250	-2.567202
6	-1.579657	0.959734	-0.529283

6	-0.718594	1.001986	-1.677135
6	0.244594	2.019048	-1.462083
6	-0.008417	2.613125	-0.193861
6	-1.123987	1.968450	0.382271
14	-2.467749	-0.540471	-0.009562
9	-1.125577	-1.386142	0.568756
9	-3.060294	-1.454146	-1.149994
9	-3.440278	-0.403932	1.223194
1	-0.802506	0.382305	-2.561253
1	1.007399	2.326961	-2.165267
1	0.545943	3.432125	0.245902
1	-1.558141	2.196341	1.346686
40	0.658176	0.107973	0.226671
6	1.064627	0.830986	2.326099
1	1.526895	0.035162	2.920349
1	1.725932	1.705182	2.375362
1	0.118896	1.119544	2.802010

E = -4556.0994219 hartrees

ν = 20.8192 , 34.3001, 83.3845, 89.4470, 97.5472, 122.6704, 134.7891, 163.3212, 202.6273, 204.5113, 218.1276, 223.5586, 240.4591, 249.3142, 272.3377, 291.1391, 321.2828, 342.6003, 355.7649, 390.3275, 470.9588, 485.1065, 509.1953, 572.0223, 575.3966, 582.1899, 603.7401, 639.3487, 696.6522, 821.1198, 843.2453, 850.4930, 852.5119, 860.6577, 861.8171, 865.4849, 871.0891, 875.4098, 917.8824, 928.1036, 930.1743, 934.0821, 941.1774, 953.9909, 1035.3891, 1045.0242, 1071.6344, 1082.5470, 1104.1213, 1106.0912, 1113.0484, 1134.4266, 1219.2458, 1239.9167, 1256.5834, 1307.5662, 1360.4350, 1394.6991, 1397.1083, 1402.0981, 1445.6661, 1453.8980, 1457.0559, 1462.95751, 466.9854, 1469.0313, 3006.8875, 3101.3290, 3110.5351, 3263.8882, 3269.1259, 3271.3045, 3275.6581, 3278.8116, 3285.1207, 3289.3554, 3301.4598, 3305.6069 cm^{-1}

File name (in my CERMM directory): No26BS.log

Table C4. Geometry of the structure in **Figure 3.4 (a).**

B3LYP/LANL2DZ for Zr and B3LYP/6-31G (d,p) for the rest elements

Atomic Number	Coordinates (Angstroms) X	Y	Z
6	-0.023129	2.621127	-0.143259
6	-0.166071	2.076372	-1.446718
6	0.686119	0.950428	-1.537895
6	1.371960	0.770448	-0.291947

6	0.912502	1.827153	0.559616
6	2.580498	-1.460426	1.560980
14	2.840956	-0.366787	0.037815
6	3.153322	-1.436479	-1.493433
6	4.355589	0.729405	0.340607
1	-0.548846	3.482708	0.245737
1	-0.818788	2.450071	-2.225056
1	0.811993	0.330162	-2.416354
1	1.235849	1.998523	1.577817
1	1.749530	-2.160907	1.432154
1	2.368199	-0.857894	2.450657
1	3.482800	-2.047442	1.767968
1	3.368653	-0.816986	-2.370861
1	4.019310	-2.088170	-1.332006
1	2.303239	-2.079790	-1.743302
1	5.252894	0.125433	0.517767
1	4.212014	1.373698	1.214881
1	4.552415	1.379465	-0.518485
40	-1.142788	0.302724	0.164334
6	-0.992205	0.285992	2.444204
6	-3.010695	1.616040	0.001243
1	-0.954031	1.317139	2.819351
1	-1.876971	-0.196365	2.878355
1	-0.110056	-0.236041	2.836496
1	-3.300190	1.850229	-1.031788
1	-3.866626	1.122765	0.478301
1	-2.841447	2.570748	0.514721
6	-0.747792	-2.121769	-0.569726
6	-1.602127	-1.545658	-1.552962
6	-2.860146	-1.301475	-0.947100
6	-2.780582	-1.712319	0.407505
6	-1.481061	-2.228501	0.639247
1	0.269533	-2.451231	-0.727394
1	-1.345313	-1.353933	-2.586407
1	-3.722724	-0.860975	-1.427372
1	-3.569979	-1.628597	1.142640
1	-1.110419	-2.618593	1.577239

E = -922.2226957 hartrees

ν = 27.1537, 41.9943, 58.9219, 79.0277, 116.5683, 124.0837, 131.0573,
132.4572, 139.3688, 141.3132, 154.2924, 158.0773, 172.0590, 177.4863,
200.1148, 204.3607, 213.9243, 226.3779, 228.8160, 237.1861, 248.1703,
267.2343, 276.5840, 306.8236, 317.8864, 349.4634, 415.3106, 444.9459,
464.1831, 509.0988, 539.1981, 595.4136, 597.3304, 602.1508, 618.5563,
629.3096, 641.4999, 666.1754, 688.4855, 692.6514, 696.7688,
778.0945, 785.5283, 814.5187, 820.1747, 822.5121, 823.0459,
828.7975, 853.4886, 855.5400, 865.3603, 870.2749, 874.4328,
879.5473, 881.5732, 905.4908, 912.6281, 914.6745, 921.7522,
1039.4262, 1044.7407, 1068.9959, 1073.0600, 1090.1235, 1091.3970,
1093.5859, 1153.9992, 1186.0093, 1194.4063, 1204.1977, 1229.9201,

1299.4888, 1308.8497, 1311.8432, 1320.9103, 1350.0669, 1409.2312,
1411.8315, 1413.7173, 1454.6002, 1456.8097,1458.9833, 1461.8190,
1465.3134, 1468.1182, 1470.4467, 1471.9093, 1480.3191, 1481.5070,
1485.9231, 1488.3440, 1489.4840, 1491.6971, 3015.2579, 3016.8358,
3040.2967, 3043.9565, 3045.1390, 3090.7539, 3093.0885, 3097.7478,
3100.6052, 3115.3457, 3117.1081, 3119.0666, 3122.4514, 3123.8365,
3131.0801, 3236.0712, 3244.6691, 3246.1011, 3247.8974, 3252.2695,
3261.2781, 3265.1168, 3266.8766, 3275.8513 cm^{-1}

File name (in my CERMM directory): No25neu.log

Table C5. Geometry of the structure in **Figure 3.4 (b).**

B3LYP/LANL2DZ for Zr and B3LYP/6-31G (d,p) for the rest elements

Atomic Number	Coordinates (Angstroms) X	Y	Z
6	-0.081618	2.710524	-0.069212
6	-0.214055	2.208957	-1.393697
6	0.665529	1.118160	-1.538767
6	1.348203	0.915919	-0.291250
6	0.879394	1.932176	0.604146
9	2.351864	-1.219204	1.311158
14	2.650048	-0.314066	0.025496
9	2.783211	-1.298370	-1.231978
9	4.086979	0.337207	0.272822
1	-0.633737	3.540062	0.351335
1	-0.881924	2.593815	-2.153072
1	0.808684	0.527187	-2.433569
1	1.200022	2.069234	1.627474
40	-1.080945	0.276050	0.174020
6	-0.890000	0.233230	2.443514
6	-3.033226	1.446484	0.005111
1	-0.949245	1.256597	2.837733
1	-1.705488	-0.346443	2.892174
1	0.053726	-0.201421	2.796959
1	-3.390513	1.586353	-1.023316
1	-3.822425	0.918208	0.555251
1	-2.920758	2.442106	0.451301
6	-0.478087	-2.024232	-0.784228
6	-1.541160	-1.519816	-1.585575
6	-2.712891	-1.483629	-0.786295
6	-2.370234	-1.944863	0.510131
6	-0.992498	-2.284059	0.511612
1	0.537049	-2.194501	-1.115699
1	-1.474319	-1.241878	-2.629582
1	-3.690406	-1.151421	-1.105997
1	-3.041015	-2.015252	1.355922

1		-0.427171	-2.657514	1.354367

E = -1102.1597378 hartrees

ν = 26.4975, 36.5900, 45.1729, 77.3269, 109.3072, 121.6699, 127.4444, 132.4003, 143.4621, 158.6820, 170.2033, 207.0051, 219.8773, 226.5477, 238.1716, 254.6158, 269.9201, 272.9970, 289.1761, 305.4145, 318.4800, 379.7481, 386.5526, 449.7801, 469.4422, 503.1034, 520.3737, 547.3179, 595.0103, 598.4728, 599.5468, 622.8848, 643.3341, 662.2981, 815.4331, 818.0328, 821.9051, 828.2498, 831.5136, 841.6014, 854.1147, 855.3178, 865.4074, 889.7884, 910.0529, 920.6911, 924.1188, 933.6683, 976.9843, 987.3821, 1039.5994, 1046.6519, 1073.0292, 1079.8637, 1090.5966, 1093.3526, 1095.4465, 1152.8835, 1192.3157, 1200.3105, 1231.9755, 1239.1595, 1301.9494, 1354.8179, 1407.9429, 1411.1745, 1413.2031, 1453.8927, 1455.0252, 1461.1553, 1463.2443, 1475.5341, 1484.3655, 1489.1081, 1493.3813, 3015.6307, 3017.0834, 3092.5797, 3093.2984, 3100.2165, 3102.5568, 3244.0362, 3246.3175, 3250.2762, 3255.3397, 3262.4265, 3263.0332, 3269.3360, 3272.3206, 3276.9305 cm^{-1}

File name (in my CERMM directory): No26neu.log

Table C6. Geometry of the structure in **Figure 3.3 (a).**

B3LYP\6-31G(d,p)

Atomic Number	Coordinates (Angstroms) X	Y	Z
6	0.701657	-0.000172	-0.029610
6	1.563737	1.144202	-0.006632
6	2.894888	0.710101	0.027745
6	2.894876	-0.710405	0.027944
6	1.563735	-1.144543	-0.006359
14	-1.120705	0.000050	-0.001465
6	-1.855599	1.539911	-0.868753
6	-1.922328	-0.009794	1.744392
6	-1.856585	-1.529551	-0.886074
1	1.233498	2.181044	-0.021167
1	3.776383	1.348668	0.037539
1	3.776372	-1.348971	0.037970
1	1.233585	-2.181440	-0.020615
1	-2.951307	1.569638	-0.802960
1	-1.471327	2.462875	-0.418643
1	-1.578305	1.557266	-1.928692
1	-3.020822	-0.009274	1.706181

1	-1.605037	0.868334	2.319426
1	-1.605564	-0.894828	2.309043
1	-2.952451	-1.558879	-0.822594
1	-1.474082	-2.457746	-0.445274
1	-1.577366	-1.535882	-1.945636

E = -602.2191777 hartrees

ν = 19.4862, 92.5642, 103.8940, 130.5906, 144.2654, 166.6250, 184.0437, 195.0982, 207.0311, 278.3174, 303.3331, 424.6610, 612.2937, 617.1867, 641.0273, 641.1610, 643.1290, 660.1902, 672.6191, 691.8184, 763.5396, 768.4740, 772.5896, 799.2280, 853.3491, 855.2520, 861.1630, 865.1190, 923.1533, 1062.9191, 1070.3035, 1078.7091, 1220.0136, 1229.1770, 1277.7796, 1283.0760, 1292.6841, 1348.1491, 1407.5882, 1469.8840, 1475.4645, 1476.5544, 1482.2173, 1482.3284, 1488.1590, 1493.5831, 1496.0214, 3007.8501, 3017.3352, 3019.4488, 3082.2677, 3088.8925, 3091.8118, 3100.2776, 3105.5248, 3106.9097, 3131.3489, 3142.9234, 3157.3380, 3174.2285 cm^{-1}

File name (in my CERMM directory): LigandtMeSi1.log

Table C7. Geometry of the structure in **Figure 3.3 (b).**

B3LYP/6-31G(d,p)

Atomic Number	Coordinates (Angstroms) X	Y	Z
6	-0.338248	0.019025	-0.000309
6	-1.170439	-1.132343	-0.000023
6	-2.517288	-0.711688	-0.000050
6	-2.532824	0.700252	0.000213
6	-1.194384	1.150545	-0.000225
6	1.184286	0.006501	0.000118
6	1.718520	-0.727812	-1.254987
6	1.718017	-0.726369	1.256113
6	1.757866	1.436147	-0.000775
1	-0.827538	-2.166084	-0.000249
1	-3.389121	-1.363936	-0.000486
1	-3.418086	1.333775	0.000185
1	-0.878731	2.190988	-0.000555
1	2.819621	-0.777705	-1.272453
1	1.330033	-1.750512	-1.296103
1	1.382694	-0.215983	-2.163564
1	2.819072	-0.777063	1.273286
1	1.328220	-1.748439	1.298456
1	1.382733	-0.212935	2.163950

1	2.857156	1.423600	-0.001053
1	1.420735	1.989788	0.882170
1	1.420173	1.988947	-0.884022

E =-350.7841256 hartrees

ν = 35.1770, 142.6675, 211.0591, 236.5358, 286.3764, 289.5166, 328.2812, 336.6434, 337.3039, 433.5861, 461.2722, 576.3663, 601.4756, 612.9736, 653.9938, 681.7018, 743.7918, 771.5199, 812.2913, 859.6651, 905.3650, 921.8089, 929.5888, 949.1931, 1038.2989, 1048.2432, 1061.9911, 1071.8282, 1079.2359, 1188.9418, 1212.8793, 1222.3127, 1271.9356, 1313.5636, 1384.3615, 1389.3804, 1400.6850, 1418.6742, 1426.2191, 1472.8882, 1482.6750, 1493.6697, 1499.6792, 1505.5734, 1506.2804, 1522.9846, 1533.0042, 2973.1105, 2983.3780, 3010.3000, 3071.7553, 3074.4011, 3082.6830, 3103.3783, 3108.4502, 3110.8591, 3125.3636, 3139.0571, 3155.7990, 3173.7388 cm^{-1}

File name (in my CERMM directory): LigandtBu.log

Table C8. Geometry of the structure in **Figure 3.3 (c).**

B3LYP/6-31G

Atomic Number	Coordinates (Angstroms) X	Y	Z
6	-2.855327	-0.716817	0.035560
6	-2.841802	0.713821	0.029836
6	-1.512554	1.144358	-0.012766
6	-0.672829	-0.023612	-0.044257
6	-1.534341	-1.173564	-0.003778
9	1.898036	-1.186158	-0.931017
14	1.111265	-0.005232	-0.004039
9	1.791778	1.453539	-0.529293
9	1.951551	-0.219290	1.458067
1	-3.742521	-1.342461	0.056817
1	-3.717085	1.356094	0.045249
1	-1.160943	2.169595	-0.036425
1	-1.208312	-2.207915	-0.016476

E = - 782.0081644 hartrees

ν = 12.4589, 92.4267, 105.9980, 210.4340, 246.3157, 276.4054, 324.6670, 358.7104, 474.0928, 630.0322, 633.4722, 685.5915, 719.5913, 777.1367, 818.9470, 827.4996, 858.0325, 866.1123, 882.3219, 939.3726, 1069.3312,

1099.0998, 1104.0003, 1244.5625, 1253.6098, 1366.8719, 1410.6810, 1491.7164, 1510.6461, 3177.5295, 3194.9266, 3215.0973, 3228.1367 cm^{-1}

File name (in my CERMM directory): ligandSiF.log

Table C9. Geometry of **IV n=0 F**-conformer

B3LYP/LanL2DZ on Zr B3LYP/6-31G (d,p) for the rest elements

Atomic Number	Coordinates (Angstroms) X	Y	Z
6	0.342110	1.808638	-1.722892
6	0.089029	2.588274	-0.545913
6	-1.064712	2.051154	0.099924
6	-1.540117	0.923659	-0.663989
6	-0.661108	0.788356	-1.802846
9	-1.042331	-1.211078	0.738650
14	-2.590118	-0.461100	0.015231
6	-3.649124	-0.086244	1.500064
6	-3.195518	-1.751647	-1.182942
40	0.690364	0.136694	0.231654
6	1.158785	1.159065	2.171553
1	1.111469	2.001016	-2.458438
1	0.652876	3.452580	-0.221035
1	-1.502706	2.432041	1.012835
1	-0.758397	0.067329	-2.604363
1	-4.600326	0.368723	1.192799
1	-3.888476	-1.005793	2.047826
1	-3.161522	0.602923	2.198072
1	-3.416515	-2.690785	-0.661218
1	-2.467950	-1.967487	-1.973030
1	-4.123624	-1.421764	-1.668742
1	0.241840	1.597209	2.593590
1	1.564503	0.428443	2.886699
1	1.893635	1.973622	2.080402
6	2.961429	-0.153057	-0.823384
6	2.133088	-1.193176	-1.381408
6	1.807264	-2.105251	-0.329993
6	2.429348	-1.636015	0.876834
6	3.162294	-0.445459	0.567164
1	3.427343	0.651999	-1.376276
1	1.854487	-1.292177	-2.421972
1	1.209379	-3.002583	-0.425826
1	2.385318	-2.122256	1.842948
1	3.770154	0.124511	1.255436

E = - 942.0958338 hartrees

ν = 27.3434, 38.5459, 85.5524, 97.3481, 101.8956, 111.5184, 118.1715, 130.9382, 137.3951, 163.7201, 192.0983, 200.4353, 217.6949, 225.4044,

231.6831, 244.6726, 268.9678, 290.1239, 323.4854, 334.2678, 348.6941,
396.5333, 432.0233, 474.6261, 492.7270, 514.1227, 577.7821, 581.5659,
584.9190, 650.9526, 696.3559, 697.2336, 763.8952, 836.0502, 836.7923,
849.4358, 850.6216, 858.1915, 862.4133, 864.4514, 870.4553, 872.5573,
878.2274, 905.0400, 916.2449, 921.4726, 928.4320, 938.0170, 948.1013,
959.2727, 1036.6773, 1044.4435, 1071.1299, 1077.9887, 1103.4948,
1105.2252, 1108.6148, 1135.8127, 1200.5827, 1236.3000, 1244.7755,
1307.1168, 1357.4301, 1384.3600, 1391.8015, 1397.5790, 1400.1600,
1403.5040, 1438.7772, 1459.4704, 1463.7472, 1466.6914, 1467.1464,
1473.2317, 1475.9799, 1481.0804, 1486.4430, 1493.6886, 3008.6131,
3052.3465, 3053.8509, 3102.4060, 3111.0256, 3140.4527, 3142.3912,
3158.0329, 3160.1656, 3263.3145, 3264.2421, 3268.3314, 3269.9172,
3278.9937, 3280.4998, 3288.3503, 3297.3010, 3305.0706 cm^{-1}

File name (in my CERMM directory): No29.log

Table C10. Geometry of **IV n=0 C-** conformer

B3LYP/LanL2DZ on Zr B3LYP/6-31G (d,p) for the rest elements

Atomic Number	Coordinates (Angstroms) X	Y	Z
6	-0.303465	2.270888	-0.572521
6	-0.380093	2.189525	0.874343
6	-1.373279	1.288996	1.215625
6	-1.959115	0.762523	-0.016901
6	-1.231865	1.399839	-1.115653
9	-0.236163	-1.595454	-1.161649
6	-2.959044	-0.196318	-0.136842
6	-3.670558	-0.758108	1.044569
6	-3.347462	-0.750072	-1.465714
1	0.354936	2.925784	-1.127519
1	0.218248	2.767801	1.566258
1	-1.673370	1.034789	2.221403
1	-1.418701	1.248572	-2.169922
1	-4.727816	-0.463602	0.984802
1	-3.666830	-1.854098	0.992488
1	-3.275590	-0.438226	2.007155
1	-2.632385	-1.555886	-1.698605
1	-3.282715	-0.020088	-2.274373
1	-4.348249	-1.185728	-1.445949
40	0.514192	-0.243014	0.006498
6	0.165701	-1.293873	1.967728
1	-0.901402	-1.535893	2.053462
1	0.714794	-2.242778	1.929062

1	0.470648	-0.771952	2.880247
6	2.749017	0.968619	0.391452
6	2.616036	0.772416	-1.017018
6	2.670351	-0.621502	-1.272704
6	2.810306	-1.288144	-0.028002
6	2.868267	-0.303135	1.000987
1	2.790569	1.923399	0.899275
1	2.542985	1.549704	-1.766295
1	2.590459	-1.095918	-2.242068
1	2.873593	-2.359562	0.113215
1	2.999826	-0.496582	2.056192

E =-942.0673098 hartrees

ν = 26.6632, 42.8436, 72.9675, 90.7028, 105.3780, 122.3046, 136.5329, 155.6539, 167.0454, 168.9546, 194.7277, 214.2398, 224.0780, 235.4803, 241.9439, 245.0813, 265.4170, 273.2315, 328.6780, 376.3472, 464.7064, 477.9867, 484.1122, 568.4242, 576.6505, 582.2369, 583.1322, 587.2412, 636.0692, 647.3999, 657.1146, 811.7851, 831.3405, 839.0581, 841.6828, 842.9820, 851.4006, 852.4369, 857.7099, 868.8237, 916.4317, 920.7024, 925.1507, 941.8066, 948.4520, 956.4358, 983.9479, 1035.8933, 1046.8032, 1048.7088, 1078.5512, 1090.0163, 1093.0497, 1104.7876, 1111.9328, 1148.8286, 1174.8526, 1199.4759, 1217.1198, 1294.1096, 1299.7455, 1359.8065, 1394.0829, 1398.9372, 1403.0778, 1406.2312, 1414.7119, 1447.0956, 1453.0847, 1457.1724, 1466.8165, 1467.3315, 1476.1868, 1483.0004, 1487.7331, 1508.2645, 1546.1465, 1606.2018, 3015.9915, 3027.0890, 3037.8696, 3087.3241, 3102.9867, 3120.2315, 3126.8942, 3169.2778, 3184.6999, 3249.1637, 3252.1821, 3257.0288, 3261.1432, 3264.4547, 3268.7543, 3276.3056, 3279.5665, 3287.2972 cm^{-1}

File name (in my CERMM directory): No29F-Cag.log

Table C11. Geometry of **IV n=1 F** conformer

B3LYP/LanL2DZ on Zr B3LYP/6-31G (d,p) for the rest elements

Atomic Number	Coordinates (Angstroms) X	Y	Z
6	-0.356805	1.970641	1.428968
6	-0.144302	2.555162	0.150950
6	0.957014	1.897881	-0.447752
6	1.448261	0.892991	0.445586
6	0.617712	0.952215	1.611396
6	4.306585	0.415374	-0.743981

14	2.814690	-0.356525	0.091046
6	3.234303	-1.350510	1.625510
6	1.948187	-1.508922	-1.207236
9	0.480820	-1.536626	-0.876402
40	-0.875648	0.111187	-0.219776
6	-1.380102	0.887105	-2.278764
1	-1.100066	2.277491	2.152951
1	-0.714026	3.366057	-0.284015
1	1.359340	2.128921	-1.425625
1	0.729015	0.344114	2.500418
1	4.031325	1.001521	-1.626492
1	5.026568	-0.347936	-1.057682
1	4.821534	1.085359	-0.047602
1	2.362023	-1.861783	2.046026
1	3.986810	-2.113422	1.399746
1	3.649902	-0.703066	2.404718
1	2.221907	-2.565334	-1.193522
1	1.967291	-1.141619	-2.235347
1	-0.455915	1.164290	-2.801263
1	-1.885197	0.103839	-2.856334
1	-2.028456	1.771213	-2.293825
6	-3.131456	0.209183	0.888398
6	-2.374934	-0.744241	1.634371
6	-2.138424	-1.860908	0.797335
6	-2.745727	-1.604754	-0.464798
6	-3.378368	-0.336767	-0.400516
1	-3.507345	1.153488	1.260545
1	-2.059667	-0.640448	2.664082
1	-1.591613	-2.755471	1.068898
1	-2.746127	-2.272695	-1.316957
1	-3.946069	0.132285	-1.191523

E = -981.3471177 hartrees

ν = 17.5171, 39.9966, 54.0632, 95.1994, 109.4052, 128.1836, 133.0200, 143.0523, 149.4683, 152.6460, 155.8543, 174.7746, 195.0237, 206.9481, 221.2570, 245.8582, 250.8814, 274.3649, 291.8755, 302.2601, 316.9831, 335.5491, 345.0552, 390.9285, 415.4106, 473.5669, 511.0285, 580.2757, 585.5789, 591.0213, 613.2039, 630.9581, 673.0820, 685.3370, 706.0404, 712.6388, 773.9505, 787.5851, 834.8929, 838.0642, 839.9429, 841.8687, 846.1668, 850.2620, 852.3946, 853.6276, 862.6143, 864.3677, 880.5178, 891.5809, 916.7661, 919.4832, 926.6649, 928.5898, 1038.1943, 1045.6030, 1067.8128, 1074.7800, 1090.9988, 1092.5897, 1096.0973, 1148.1806, 1193.4475, 1200.4691, 1215.5755, 1233.2324, 1300.2091, 1309.8766, 1324.4294, 1331.3356, 1353.8339, 1403.1209, 1408.3341, 1411.8026, 1448.4492, 1449.7114, 1452.7644, 1461.8832, 1462.9762, 1469.1112, 1474.2263, 1476.2526, 1478.3939, 1486.1368, 1488.7390, 3024.1947, 3050.1885, 3051.2180, 3103.2216, 3105.9079, 3111.5314, 3127.7496, 3129.9411, 3131.4957, 3133.4050, 3178.8722, 3243.4213, 3243.8192,

3248.6164, 3250.9279, 3257.2275, 3258.5269, 3267.0994, 3269.2530, 3280.1736 cm^{-1}

File name (in my CERMM directory): No30Fag-fr.log

Table C12. Geometry of **V**.

B3LYP/LanL2DZ on Zr B3LYP/6-31G (d,p) for the rest elements

Atomic Number	Coordinates (Angstroms) X	Y	Z
6	0.000341	2.436429	0.103944
6	2.521614	0.371931	-0.586650
6	2.264043	0.547975	0.795365
6	1.698928	-0.662904	1.291996
6	1.657632	-1.603544	0.217694
6	2.153783	-0.961389	-0.941484
6	-1.657599	-1.603111	0.220298
6	-2.152931	-0.963438	-0.940568
6	-2.521296	0.370566	-0.588715
6	-2.264870	0.549448	0.793150
6	-1.699832	-0.660280	1.292636
40	0.000027	0.231955	-0.300633
1	-0.892155	2.889160	-0.346630
1	0.893693	2.889306	-0.344669
1	-0.000915	2.723212	1.163188
1	2.955094	1.110071	-1.250620
1	2.460502	1.442104	1.370380
1	1.432474	-0.864359	2.321518
1	1.327347	-2.631243	0.284379
1	2.261069	-1.412113	-1.921884
1	-1.327092	-2.630582	0.289360
1	-2.259341	-1.416195	-1.920123
1	-2.954542	1.107193	-1.254530
1	-2.462041	1.444669	1.366210
1	-1.434058	-0.859545	2.322760

E =-473.393185

ν = 22.3715, 44.8822, 96.1957, 249.8640, 252.8466, 273.2899, 283.7769, 319.4429 363.8779, 578.6770, 581.1621, 587.8802, 687.2387, 833.9128, 838.1652, 839.7649, 846.2959, 847.0097, 848.0127, 850.7037, 852.3594, 855.5086, 860.2113, 914.0927, 924.8286, 925.8881, 927.8042, 1032.2956 1034.3830,1043.0061,1044.9720,1084.3976, 1088.5391, 1090.9652,1094.5834 1142.8741, 1144.3430, 1211.9766, 1297.0087 cm^{-1}

File name (in my CERMM directory): No1-3.log

Table C13. Geometry of **IV n=1 C** conformer

B3LYP/LanL2DZ on Zr B3LYP/6-31G (d,p) for the rest elements

Atomic Number	Coordinates (Angstroms) X	Y	Z
6	3.454399	-2.221324	-0.063071
6	0.917478	1.074252	1.545012
6	-0.254234	0.975779	2.333470
6	-0.600281	-0.400361	2.435491
6	0.351592	-1.146401	1.693760
6	1.305049	-0.236824	1.121201
14	2.495588	-0.628485	-0.288632
6	1.275377	-0.707272	-1.767548
6	3.592323	0.902311	-0.567915
9	2.716006	1.993173	-0.782450
1	4.109185	-2.159210	0.812199
1	2.790561	-3.080190	0.080418
1	4.079924	-2.429530	-0.937575
1	1.419672	1.989365	1.266207
1	-0.780460	1.799933	2.798162
1	-1.424952	-0.807314	3.005974
1	0.360911	-2.225788	1.597311
1	1.746424	-1.079904	-2.684193
1	0.436370	-1.415245	-1.617187
1	0.898516	0.291970	-2.049750
1	4.225575	1.139401	0.294785
1	4.243028	0.811892	-1.445566
40	-0.845717	0.155251	-0.045592
6	-0.823146	2.335601	-0.600913
1	0.232444	2.617584	-0.711243
1	-1.337100	2.509388	-1.551793
1	-1.258241	3.014422	0.141468
6	-3.259797	-0.249262	0.447450
6	-2.730517	-1.523000	0.076024
6	-2.390349	-1.465558	-1.296400
6	-2.705552	-0.161028	-1.778970
6	-3.267835	0.579458	-0.709732
1	-3.657090	0.014419	1.418986
1	-2.634260	-2.385255	0.722322
1	-1.985322	-2.279883	-1.885312
1	-2.572570	0.190586	-2.794563
1	-3.633273	1.595319	-0.761220

E = -981.3092881 hartrees

ν = 38.0137, 45.4301, 59.3921, 83.4392, 102.3910, 110.8497, 121.0956, 132.2280, 139.0356, 143.3190, 152.0030, 181.0882, 188.8328, 214.4261, 226.2634, 246.0425, 251.3714, 258.4011, 275.7750, 286.4165, 309.7459,

335.5933, 368.4126, 379.0108, 421.7415, 471.2851, 510.2475, 581.6715,
583.7712, 590.7426, 592.9056, 635.7861, 678.8059, 698.6058, 705.0966,
716.5189, 766.9918, 800.8326, 835.7649, 837.9735, 845.9197, 849.7463,
850.8807, 852.6431, 855.5725, 859.4474, 862.3530, 872.9197, 911.9413,
915.3665, 920.7793, 930.1483, 946.1977, 1009.4647, 1035.3524, 1045.4076,
1068.9209, 1074.5091, 1088.8514, 1093.0873, 1095.7809, 1145.9046,
1196.5643, 1214.1411, 1226.8485, 1233.0129, 1286.8110, 1299.3120,
1325.0373, 1327.7682, 1348.5377, 1400.8030, 1407.4421, 1410.6158,
1449.9470, 1450.6943, 1453.2137, 1464.3276, 1467.2149, 1473.5798,
1475.5035, 1481.2846, 1483.7443, 1485.5379, 1493.9733, 2935.8597,
3012.5825, 3028.3208, 3050.5039, 3053.5964, 3102.7243, 3106.6696,
3107.8416, 3124.7789, 3129.0323, 3133.3679, 3235.3902, 3239.9748,
3251.1479, 3252.0392, 3256.9188, 3264.2141, 3267.3150, 3280.4780,
3284.5582 cm^{-1}

File name (in my CERMM directory): No30Cag.log

Table C 14. Geometry of **IV n=2 F** conformer.

B3LYP/LanL2DZ on Zr B3LYP/6-31G (d,p) for the rest elements

Atomic Number	Coordinates (Angstroms) X	Y	Z
6	-0.380050	-2.472444	0.513203
6	0.735637	-1.729596	0.976981
6	1.335591	-1.042981	-0.122725
6	0.564873	-1.405556	-1.282876
6	-0.467163	-2.291750	-0.895174
14	2.919517	-0.010435	-0.083830
6	2.548066	1.722708	-0.836737
6	1.494897	2.563722	-0.182206
6	4.228423	-0.815612	-1.165750
6	3.487392	0.189881	1.699922
9	0.173337	1.839185	-0.212559
1	-1.022229	-3.100897	1.117401
1	1.072050	-1.692383	2.003652
1	0.756543	-1.082889	-2.299935
1	-1.192068	-2.752825	-1.552730
1	3.481025	2.299330	-0.745093
1	2.352776	1.647784	-1.913094
1	1.649208	2.746409	0.881312
1	1.240829	3.486261	-0.704324
1	5.150155	-0.223757	-1.172910
1	4.478114	-1.814214	-0.792997
1	3.893191	-0.924069	-2.202490

1	4.397999	0.796728	1.748594
1	3.726337	-0.782884	2.142611
1	2.737737	0.666303	2.341074
6	-3.072598	1.463553	0.111626
6	-2.703351	1.258776	-1.245405
6	-2.854403	-0.118657	-1.541297
6	-3.328461	-0.768342	-0.361766
6	-3.475785	0.215143	0.652618
1	-3.064997	2.409925	0.636957
1	-2.363989	2.022814	-1.933974
1	-2.678068	-0.586867	-2.500560
1	-3.587196	-1.815299	-0.273479
1	-3.832274	0.043151	1.658520
40	-0.981731	-0.025459	0.150387
6	-1.008485	0.271651	2.392496
1	0.024904	0.389254	2.744484
1	-1.563246	1.184115	2.637864
1	-1.448347	-0.547201	2.972836

E = - 1020.6741048 hartrees

ν = 21.5814, 31.5942, 48.0908, 95.1251, 106.3532, 116.0586, 123.1976, 130.9523, 138.1819, 147.0056, 156.8789 164.7014, 173.2423, 186.6608, 211.5350, 232.2352, 245.6590, 257.3683, 264.1724, 269.6227, 284.3288, 313.5149, 321.9191, 330.3045, 365.7945, 408.2533, 450.9968, 471.7558, 525.1848, 581.7093, 583.2528, 589.7818, 589.9796, 627.0603, 663.1958, 682.5939, 698.5645, 704.8113, 746.8868, 779.1623, 800.6741, 835.6246, 839.9595, 845.5904, 846.2644, 851.2669, 852.3319, 853.5963, 862.3390, 864.0999, 873.9693, 904.1784, 915.1478, 918.2218, 928.2137, 930.9262, 982.9681, 1023.5157, 1039.1199, 1045.8004, 1070.9646, 1072.6152, 1091.3130, 1093.9425, 1095.9320, 1148.9050, 1177.6829, 1194.3934, 1199.8764, 1211.8454, 1229.6837, 1300.8781, 1319.8660, 1321.5693, 1329.4472, 1349.0674, 1394.9143, 1404.5632, 1410.0699, 1414.3164, 1447.0022, 1451.8452, 1454.6152, 1457.2984, 1462.7554, 1469.2722, 1475.3286, 1477.6361, 1479.9493, 1485.9446, 1487.6961, 1516.3354, 3023.8881, 3035.9184, 3045.5265, 3048.7939, 3088.0063, 3101.8574, 3119.1844, 3119.4254, 3120.7328, 3126.1130, 3127.2391, 3131.7170, 3191.3807, 3231.0682, 3243.4319, 3248.4824, 3252.4085, 3259.6747, 3263.5975, 3266.3601, 3271.8346, 3278.7886 cm^{-1}

File name (in my CERMM directory): No24Fag-2.log

Table C15. Geometry of **IV n=2 C** conformer.

B3LYP/LanL2DZ on Zr B3LYP/6-31G (d,p) for the rest elements

Atomic Number	Coordinates (Angstroms) X	Y	Z
6	-0.592534	-1.725456	-1.673732
6	-0.294069	-2.444764	-0.484825
6	0.760746	-1.768501	0.176469
6	1.128918	-0.612433	-0.581955
6	0.279850	-0.604857	-1.736796
6	3.482486	0.371697	1.266862
14	2.111832	0.870299	0.057928
6	2.666362	1.998913	-1.330516
6	0.723904	1.772983	1.055866
6	4.390070	-0.717523	0.698931
9	4.549475	-0.511760	-0.678079
1	-1.324639	-2.006720	-2.419432
1	-0.773941	-3.357141	-0.154551
1	1.202402	-2.077752	1.114430
1	0.307008	0.123996	-2.537683
1	3.064892	0.047183	2.227713
1	4.063230	1.279291	1.475283
1	1.837878	2.296395	-1.982023
1	3.110640	2.914845	-0.925786
1	3.425582	1.501703	-1.939518
1	1.107901	2.695839	1.506526
1	0.329272	1.204140	1.917759
1	-0.110467	2.157234	0.434000
1	5.385392	-0.708099	1.153658
1	3.951772	-1.712345	0.832840
6	-3.679570	0.084271	0.617758
6	-3.478283	-0.341140	-0.725317
6	-2.878264	0.736534	-1.445167
6	-2.684325	1.806347	-0.540192
6	-3.163821	1.398155	0.740294
1	-4.140393	-0.495033	1.405201
1	-3.796264	-1.286323	-1.146233
1	-2.637669	0.741403	-2.499907
1	-2.269158	2.776724	-0.785129
1	-3.170633	2.002745	1.638797
40	-1.170709	-0.121002	0.216040
6	-1.452920	-1.115595	2.225731
1	-0.482805	-1.354523	2.677067
1	-2.002153	-0.455433	2.907064
1	-2.011710	-2.058201	2.169580

E = -1020.6324714 hartrees

ν = 21.5111, 28.6451, 40.9553, 67.1002, 80.3992, 86.4481, 108.2904, 125.1552, 129.1020, 139.6205, 152.1430, 171.7188, 180.1623, 208.8438, 214.9888, 224.9049, 235.0295, 247.0959, 260.9674, 262.9328, 282.4477, 296.1947, 321.5851, 331.2592, 371.8552, 420.5513, 472.3631, 487.1364, 493.8803, 576.8857, 578.7968, 584.3289, 591.0838, 646.1170, 661.9717, 683.0051, 695.5302, 698.2290, 719.8559, 823.8624, 829.1239, 833.2136,

841.7521, 847.1772, 850.1540, 851.2310, 852.0479, 853.3954, 861.0420, 872.3196, 900.7093, 909.6882, 921.4728, 926.3605, 928.2896, 955.8078, 994.6741, 1034.1587, 1044.5153, 1069.0930, 1070.9379, 1076.0053, 1088.2113, 1091.3055, 1095.4746, 1146.3377, 1195.1893, 1208.9555, 1213.3821, 1227.7800, 1236.1746, 1290.5510, 1298.1517, 1309.8475, 1324.3868, 1355.4759, 1400.5452, 1407.4208, 1410.5215, 1420.9326, 1446.3280, 1451.4073, 1452.2577, 1460.4463, 1464.1361, 1469.6918, 1473.8197, 1479.4459, 1485.2827, 1487.3845, 1494.0148, 1531.4256, 2923.4443, 2998.3372, 3027.8208, 3047.2552, 3052.4554, 3062.3631, 3092.4557, 3096.0148, 3103.5207, 3114.1792, 3118.8108, 3122.8661, 3154.1585, 3239.7060, 3243.8944, 3250.3456, 3250.6764, 3255.0993, 3259.0980, 3266.8032, 3268.6264, 3279.6915 cm^{-1}

File name (in my CERMM directory): No24C1.log

Table C16. Geometry of **IV n=3 F** conformer.

B3LYP/LanL2DZ on Zr B3LYP/6-31G (d,p) for the rest elements

Atomic Number	Coordinates (Angstroms) X	Y	Z
6	-0.890745	-2.836628	-0.098884
6	0.289852	-2.385291	0.544304
6	1.006167	-1.511796	-0.332963
6	0.231913	-1.452128	-1.542462
6	-0.916762	-2.271384	-1.402692
14	2.732542	-0.791560	0.011315
6	3.023956	0.826832	-0.981803
6	1.915851	1.857747	-1.262792
6	1.199316	2.402389	-0.058916
6	4.016847	-2.033534	-0.581375
6	2.914819	-0.486874	1.863507
9	1.972609	2.768627	0.945420
9	0.349287	1.354066	0.529389
9	0.337884	3.373191	-0.340663
1	-1.625241	-3.514218	0.318076
1	0.593995	-2.663072	1.544089
1	0.495800	-0.909058	-2.442468
1	-1.670843	-2.447103	-2.158253
1	3.858332	1.336251	-0.483503
1	3.418861	0.528490	-1.959840
1	2.332330	2.740804	-1.763014
1	1.147629	1.462796	-1.935004
1	3.894041	-2.270738	-1.643111
1	5.030747	-1.643175	-0.439562
1	3.943333	-2.971112	-0.020872

1	2.738347	-1.404166	2.435393
1	3.938356	-0.166178	2.086966
1	2.240242	0.284186	2.247103
6	-2.982595	1.479316	0.456403
6	-2.506121	1.577509	-0.881715
6	-2.847685	0.383562	-1.560505
6	-3.539875	-0.459547	-0.638798
6	-3.642002	0.232528	0.599090
1	-2.880019	2.235461	1.224489
1	-1.973561	2.420942	-1.302680
1	-2.646104	0.160296	-2.599724
1	-3.972404	-1.425871	-0.862869
1	-4.132135	-0.130434	1.491354
40	-1.184662	-0.325739	0.208547
6	-1.457374	-0.748343	2.406243
1	-0.459537	-0.902693	2.838060
1	-1.919319	0.113674	2.900037
1	-2.053344	-1.632799	2.657886

E = -1258.4633956 hartrees

ν = 21.2516, 38.7548, 58.7782, 61.3322, 87.2816, 96.5229, 111.5420, 120.2156, 127.2400, 138.5323, 145.8232, 150.3267, 151.7825, 163.4562, 171.3147, 181.6062, 202.1788, 221.3254, 234.4414, 246.9339, 255.4429, 274.4783, 283.5990, 313.7748, 325.0741, 336.1681 355.2415, 367.8900, 400.3899, 447.4018, 471.2588, 512.5020, 517.0504, 533.0757, 582.2448, 584.3627, 586.3740, 592.1920, 614.2873, 631.8594, 676.9142, 687.8522, 697.8141, 702.2489, 703.2129, 783.3880, 825.0202, 836.2028, 840.2156, 843.6210, 845.9150, 849.8092, 851.4798, 854.1666, 857.7225, 862.9975, 878.6463, 900.4563, 906.1036, 916.8408, 919.9878, 927.6327, 932.2303, 971.6065, 1036.7614, 1045.5834, 1046.6118, 1068.9701, 1071.5257, 1090.7050, 1092.9840, 1094.8575, 1148.2650, 1171.6465, 1192.5246, 1212.1693, 1223.4022, 1230.5489, 1270.5006, 1299.6104, 1312.0455, 1320.1513, 1329.3526, 1347.8582, 1362.9118, 1402.3269, 1410.3482, 1415.3114, 1419.6082, 1447.9475, 1450.4873, 1453.2659, 1463.8730, 1467.0658, 1475.6667, 1477.1602, 1477.7108, 1479.7878, 1486.1112, 1487.2493, 1491.9633, 3025.1378, 3047.1899, 3050.7550, 3051.9588, 3062.5531, 3093.3182, 3104.2153, 3110.6200, 3120.7163, 3122.1148, 3125.6806, 3131.0686, 3135.1269, 3235.8198, 3246.2939, 3247.3517, 3251.9499, 3259.4291 3263.0020, 3267.2638, 3269.4086, 3280.1987 cm^{-1}

File name (in my CERMM directory): No4CH2F.log

Table C17. Geometry of **IV n=3 C** conformer.

B3LYP/LanL2DZ on Zr B3LYP/6-31G (d,p) for the rest elements

Atomic Number	Coordinates (Angstroms) X	Y	Z
6	2.640792	2.163804	0.280165
6	1.310304	2.338182	0.729533
6	0.402516	2.014758	-0.332936
6	1.215449	1.640482	-1.448284
6	2.586630	1.716208	-1.069322
14	-1.473059	1.735846	-0.170406
6	-1.341817	0.039985	0.763373
6	-2.553894	-0.763940	1.276656
6	-3.454337	-1.262077	0.164266
6	-2.202655	1.612187	-1.894871
6	-2.292242	3.027291	0.912943
9	-2.728891	-1.878858	-0.808551
9	-4.124177	-0.246531	-0.426651
9	-4.355784	-2.137661	0.622535
1	3.538485	2.342425	0.857579
1	1.029347	2.665763	1.722651
1	0.852124	1.354129	-2.427244
1	3.437425	1.530727	-1.711987
1	-1.823839	3.109645	1.899195
1	-0.809329	-0.666615	0.082991
1	-0.712292	0.240255	1.651245
1	-2.227477	-1.643495	1.840115
1	-3.163590	-0.155856	1.950885
1	-1.870550	0.714491	-2.426343
1	-3.293678	1.584944	-1.865106
1	-1.902795	2.485302	-2.484489
1	-2.238997	4.011868	0.436477
1	-3.351727	2.794475	1.063843
6	1.604778	-2.703807	0.297121
6	0.974326	-2.350346	-0.933605
6	1.919862	-1.658675	-1.727792
6	3.139425	-1.580105	-0.988832
6	2.946711	-2.253109	0.251120
1	1.148863	-3.255943	1.109548
1	-0.046727	-2.582272	-1.212986
1	1.757847	-1.281312	-2.728515
1	4.070786	-1.159046	-1.344420
1	3.691858	-2.392794	1.021640
40	1.514900	-0.147242	0.260266
6	2.335409	-0.178040	2.361253
1	1.915069	0.641587	2.955685
1	2.091413	-1.130779	2.847297
1	3.426748	-0.069006	2.406262

E = -1258.4387971 hartrees

ν = 14.3553, 24.1025, 29.4966, 38.6779, 55.5942, 73.4039, 77.3931,

103.0641, 111.6871, 132.4303, 134.5893, 139.8984, 143.1407, 145.3217,
147.6544, 201.2118, 210.0547, 220.4849, 244.2486, 252.7222, 259.5923,
282.7693, 288.6727, 310.8842, 324.5800, 336.9028, 366.5725, 378.2020,
421.1039, 457.0458, 471.3651, 486.7601, 523.4721, 536.6015, 573.0870,
579.1211, 585.0913, 590.1445, 624.7602, 642.4606, 686.7493, 695.6121,
707.4294, 717.4935, 787.6645, 813.7700, 835.7511, 842.2767, 845.9250,
846.2147, 850.9360, 851.0551, 855.9544, 857.4454, 863.5088, 872.4293,
878.8188, 898.0330, 905.5937, 919.3744, 926.0037, 928.0812, 933.8407,
1031.8436, 1034.9971, 1044.9583, 1061.4955, 1071.3121, 1076.9761,
1089.7515, 1091.2283, 1094.9033, 1145.4091, 1164.7313, 1191.0798,
1214.3679, 1228.6685, 1232.1657, 1255.2199, 1267.2546, 1299.7677,
1324.9534, 1329.0323, 1336.7393, 1351.8986, 1400.3925, 1404.1679,
1409.1064, 1422.0000, 1443.2160, 1444.5829, 1447.5267, 1460.3808,
1467.8604, 1471.4979, 1473.5822, 1474.7083, 1484.0883, 1485.5563,
1491.2137, 1494.5493, 2838.6305, 2959.7577, 3023.5751, 3049.9366,
3055.8201, 3081.0536, 3098.2384, 3110.7274, 3127.6575, 3128.4791,
3130.0011 3131.6371, 3158.5270, 3240.1387, 3244.2058, 3246.7128,
3251.6240, 3256.0035, 3257.6772, 3267.8113, 3269.1813, 3278.6071

File name (in my CERMM directory): No4-1CH2C.log

Table C18. Geometry of the structure **Figure 3.10** (TS highest energy).

B3LYP/LanL2DZ on Zr B3LYP/6-31G (d,p) for the rest elements

Atomic Number	Coordinates (Angstroms) X	Y	Z
6	0.320159	1.807520	-1.599266
6	0.098508	2.519067	-0.388164
6	-1.003157	1.920373	0.270128
6	-1.490253	0.834359	-0.526194
6	-0.657661	0.775188	-1.687669
6	-1.539725	-1.648867	1.075073
14	-2.675891	-0.482051	0.095273
9	-3.634601	0.231388	1.182317
6	-3.664863	-1.319904	-1.234442
1	1.061075	2.048742	-2.349791
1	0.665207	3.371507	-0.037457
1	-1.414298	2.232312	1.222192
1	-0.761555	0.082889	-2.513840
1	-0.660649	-2.013009	0.506077
1	-2.047499	-2.578652	1.356613
1	-1.214680	-1.195972	2.022507

1	-4.331405	-2.071290	-0.798689
1	-3.025546	-1.825160	-1.966740
1	-4.282471	-0.591549	-1.769166
6	3.289326	-0.307350	0.265325
6	2.888034	-0.132853	-1.088951
6	2.071370	-1.246100	-1.455776
6	1.956798	-2.088200	-0.322939
6	2.690690	-1.499141	0.748454
1	3.937899	0.352162	0.824011
1	3.216476	0.658774	-1.748993
1	1.651253	-1.430542	-2.435551
1	1.427921	-3.033110	-0.284111
1	2.808238	-1.911087	1.742968
40	0.783789	0.120924	0.230946
6	1.337514	1.096182	2.164840
1	0.979209	2.101450	2.388241
1	0.688667	0.389081	2.738928
1	2.344033	0.981045	2.567790

E = -942.0656528 hartrees

ν = -53.3098, 32.9880, 38.5912, 73.3710, 82.0933, 102.5292, 124.6584, 133.1605, 142.9321, 158.1236, 188.7659, 198.3224, 217.6753, 231.9025, 249.6583, 254.9032, 264.6320, 289.3923, 306.7145, 333.3551, 339.7503, 379.1170, 395.5083, 432.3832, 568.0842, 577.6856, 585.0521, 589.1373, 607.9425, 645.6579, 682.3455, 700.9309, 727.9765, 790.1993, 808.5453, 836.8530, 841.0089, 844.0606, 850.2397, 851.4591, 853.4102, 853.8179, 859.3691, 863.8704, 905.0749, 913.8787, 922.5350, 929.9505, 933.8507, 950.3200, 1035.7756, 1043.2706, 1065.9756, 1073.2318, 1088.3394, 1090.5599, 1097.2917, 1144.5472, 1200.3272, 1217.6328, 1233.0763, 1298.8151, 1305.4952, 1331.4188, 1356.9723, 1389.7057, 1400.1096, 1404.1693, 1410.4254, 1444.4325, 1453.3063, 1462.2747, 1468.8702, 1470.6352, 1474.4688, 1482.6919, 1486.7246, 1490.1814, 2858.7813, 2937.2919, 3052.1370, 3058.1628, 3107.2710, 3127.3166, 3129.2841, 3140.1659, 3183.6036, 3240.2021, 3246.4616, 3250.1290, 3253.7920, 3258.9853, 3261.0558, 3268.1240, 3272.3171, 3282.1938 cm^{-1}

File name (in my CERMM directory): None29.log

Appendix D

Supplemental information related to CHAPTER IV

Table D1. Olefin complex geometry in **Figure 4.3 (a).**

B3LYP/LanL2DZ on zirconium B3LYP/6-31G(d,p) on lighter elements

Atomic Number	Coordinates (Angstroms) X	Y	Z
6	-0.003224	0.653889	2.286343
40	0.000495	0.082412	0.112768
1	-0.901704	1.249726	2.509126
1	0.891540	1.255451	2.509173
1	-0.000463	-0.198533	2.981372
6	2.590785	0.266014	0.128857
6	2.245597	-0.841983	0.960793
6	1.631537	-1.841234	0.132610
6	1.638106	-1.359123	-1.226232
6	2.223738	-0.059859	-1.226646
1	3.107919	1.159906	0.451103
1	2.433141	-0.924611	2.021876
1	1.323065	-2.826885	0.452819
1	1.310571	-1.909375	-2.097430
1	2.417397	0.544936	-2.103408
6	-1.628386	-1.372049	-1.223285
6	-2.217324	-0.074206	-1.233470
6	-2.590809	0.258140	0.118579
6	-2.245626	-0.844251	0.958237
6	-1.625640	-1.846412	0.138424
1	-1.294799	-1.925978	-2.089668
1	-2.407922	0.525788	-2.114362
1	-3.111105	1.152803	0.433502
1	-2.436652	-0.921027	2.019012
1	-1.314468	-2.829031	0.465795
6	-0.690990	2.776790	-0.542453
6	0.672467	2.779020	-0.558725
1	-1.271672	2.721666	-1.459773
1	-1.242823	2.964490	0.375990
1	1.231150	2.725743	-1.489849
1	1.245643	2.970056	0.345787

E =- 551.9136298 hartrees

ν = 29.1617, 40.1493, 62.4238, 85.5264, 106.5036, 149.6560, 154.6631, 178.0434, 188.8528, 212.6980, 235.0782, 240.9403, 241.6955, 265.4426, 272.0862, 311.1509, 346.6898, 395.5604, 488.3404, 520.1532, 574.3880, 580.6383, 582.7292, 588.5574, 701.2110, 832.4083, 841.6743, 847.2787, 850.7692, 853.4129, 858.4745, 859.5292, 862.4493, 864.4588, 867.3844, 880.9282, 924.9633, 937.4789, 941.2137, 945.7009, 1024.1162, 1032.7858, 1035.0185, 1043.5498, 1046.7849, 1049.5104, 1054.7096, 1098.3004, 1103.5801, 1106.0266, 1110.7001, 1138.0721, 1139.8092, 1237.7626, 1253.2418, 1306.3133, 1308.1921, 1373.9839, 1396.1568, 1400.2028, 1402.4249, 1407.7160, 1457.3350, 1458.6201, 1466.3700, 1471.2303, 1471.5309, 1476.6237, 1490.6171, 1631.1938, 3004.3035, 3102.2130, 3105.1597, 3160.9241, 3177.5358, 3259.5922, 3262.2159, 3266.5690, 3271.9344, 3275.3238, 3281.7052, 3284.7734, 3289.7168, 3292.5615, 3294.5128, 3307.0336, 3309.0039 cm^{-1}

File name (in my CERMM directory): No10-4.log

Table D2. Olefin complex geometry in **Figure 4.3 (b).**

B3LYP/LanL2DZ on zirconium B3LYP/6-31G(d,p) on lighter elements

Atomic Number	Coordinates (Angstroms) X	Y	Z
6	2.894872	-0.920385	-1.254343
40	1.097378	-0.171344	-0.120339
1	2.933923	-2.019016	-1.244171
1	3.805447	-0.520123	-0.780482
1	2.919644	-0.604548	-2.307676
6	2.630494	1.935949	0.145633
6	2.026594	2.012596	-1.145459
6	0.609285	2.161920	-0.963779
6	0.343325	2.188906	0.449064
6	1.592357	2.053524	1.132173
1	3.690756	1.849609	0.342692
1	2.547729	1.990697	-2.092448
1	-0.116795	2.320428	-1.747922
1	-0.616772	2.361495	0.912089
1	1.737355	2.114297	2.202278
6	-1.426724	-0.694938	-0.374885
6	-0.840333	-1.845332	0.253928
6	0.077099	-2.479722	-0.656333
6	0.072549	-1.730458	-1.870334
6	-0.822333	-0.621242	-1.692402
14	-2.988574	0.222671	0.238305
6	-4.436231	-0.951443	-0.099670

6	-2.847853	0.540476	2.103552
6	-3.220648	1.828273	-0.739669
1	-1.103048	-2.220151	1.236084
1	0.627347	-3.394191	-0.476900
1	0.626307	-1.965319	-2.768542
1	-1.090850	0.086777	-2.465211
1	-4.520002	-1.191699	-1.167154
1	-5.384277	-0.493513	0.213138
1	-4.327834	-1.896379	0.448081
1	-3.776623	0.992770	2.475859
1	-2.028242	1.220974	2.368520
1	-2.704230	-0.395126	2.661181
1	-4.171151	2.297060	-0.452184
1	-3.276537	1.636501	-1.819594
1	-2.432291	2.570217	-0.565484
6	1.959291	-1.977254	1.953247
6	2.360580	-0.742529	2.368948
1	1.066826	-2.448802	2.354428
1	2.579356	-2.581536	1.294477
1	1.800216	-0.191685	3.121162
1	3.324720	-0.332416	2.077042

E = - 674.9688716 hartrees

ν = 23.0118, 33.0599, 58.5878, 65.9729, 74.7574, 79.1871, 104.4738, 114.9732, 119.7585, 132.4529, 139.6128, 142.1253, 147.3104, 160.0118, 173.5060, 180.9823,201.9684, 209.0134, 215.1534, 229.9670, 238.2677, 245.5154, 253.5651, 264.8163, 294.9365, 316.5819, 326.0636, 359.1904, 387.0915, 410.7065, 482.6805, 523.6741, 577.7017, 579.5900, 588.6183, 615.2680, 630.3895, 701.2340, 715.4225, 722.3275, 770.4354, 828.2895, 836.3257, 842.5237, 847.1234, 850.8992, 853.3475, 861.0674, 864.1728, 866.1051, 869.4485, 883.2712, 900.3126, 902.8984, 926.3163, 934.5523, 936.5593, 942.4599, 948.2027, 949.7394, 1022.3540, 1037.6234, 1039.4539, 1046.2733, 1051.7474, 1063.9052, 1073.9307, 1104.1108, 1104.8338, 1109.5933, 1140.2819, 1180.3657, 1109.5933, 1140.2819, 1180.3657, 1233.6361, 1236.2246, 1253.9453, 1307.5250, 1344.3924, 1359.4100, 1364.2733, 1372.6113, 1376.6749, 1401.3070, 1404.6952, 1408.8609, 1425.0063, 1459.7279, 1464.4328, 1469.8183, 1476.8148, 1477.5637, 1487.4280, 1488.1977, 1491.3180, 1493.6757, 1502.1062, 1505.8612, 1508.6690, 1631.9771, 3004.6616, 3039.0150, 3042.1351, 3045.1222, 3098.4376, 3111.8703, 3126.9310, 3129.9226, 3131.2890, 3135.4101, 3140.6907, 3141.3647, 3160.6254, 3179.0055, 3247.6331, 3262.8744, 3266.2533, 3268.5996, 3272.4955, 3278.7108, 3289.5912, 3295.5813, 3296.0429, 3297.2131, 3313.6070 cm^{-1}

File name (in my CERMM directory): No10-25-2.log

Table D3. Olefin complex geometry in **Figure 4.3 (c).**

B3LYP/LanL2DZ on zirconium B3LYP/6-31G(d,p) on lighter elements

Atomic Number	Coordinates (Angstroms) X	Y	Z
6	2.512567	-1.071583	-1.405599
40	0.864665	-0.185700	-0.126450
1	2.427233	-2.162670	-1.456093
1	3.486168	-0.812756	-0.970147
1	2.525764	-0.704229	-2.438097
6	2.652281	1.692206	0.122083
6	1.986200	1.906520	-1.107461
6	0.627573	2.218718	-0.822404
6	0.460634	2.206340	0.592509
6	1.713342	1.885926	1.173347
1	3.699605	1.447288	0.238890
1	2.434578	1.851482	-2.089865
1	-0.126328	2.489595	-1.547651
1	-0.440538	2.461319	1.130741
1	1.928881	1.855020	2.232961
6	-1.743198	-0.462640	-0.277214
6	-1.212221	-1.667995	0.258012
6	-0.397602	-2.303447	-0.725500
6	-0.398617	-1.488946	-1.879712
6	-1.190719	-0.339642	-1.595770
6	-2.911508	0.328145	0.314383
6	-4.186543	-0.508034	0.014911
6	-2.781129	0.489287	1.843023
6	-3.082044	1.708576	-0.348284
1	-1.454389	-2.080174	1.229194
1	0.101082	-3.257866	-0.620153
1	0.110567	-1.696050	-2.810350
1	-1.425532	0.441904	-2.305113
1	-4.322052	-0.652710	-1.061218
1	-5.070310	0.010083	0.400417
1	-4.139045	-1.493827	0.487058
1	-3.655643	1.013969	2.238626
1	-1.895276	1.068361	2.124466
1	-2.730482	-0.478013	2.352954
1	-3.963216	2.206616	0.065959
1	-3.240472	1.622687	-1.427745
1	-2.226995	2.368252	-0.178722
6	1.641925	-2.159044	1.801773
6	2.230739	-1.029403	2.243635
1	0.725678	-2.531174	2.247958
1	2.119878	-2.790141	1.057506
1	1.805712	-0.456111	3.062697
1	3.208454	-0.722744	1.883325

E = -709.2805905 hartrees

ν = 15.2757, 29.0746, 68.8548, 80.4478, 92.6365, 100.5803, 108.0633, 139.8797, 144.7581, 178.3231, 184.7548, 193.3411, 198.9062, 229.2588, 230.7110, 249.4275, 251.9476, 262.7871, 269.4526, 277.7815, 284.8866, 312.2090, 337.5560, 345.4923, 352.8244, 371.2852, 386.2221, 444.9487, 466.8894, 468.7049, 515.6271, 574.2137, 581.6168, 583.2243, 593.3569, 661.8160, 701.3545, 814.2983, 833.0491, 834.1052, 837.9891, 843.4975, 847.0142, 849.2811, 852.4799, 853.9696, 863.8198, 880.3387, 917.1264, 920.9558, 926.2759, 931.5925, 935.2956, 946.3744, 965.4484, 1000.5753, 1026.7916, 1038.7478, 1039.4233, 1044.6609, 1047.2684, 1064.6570, 1066.7800, 1078.3247, 1092.0029, 1092.7418, 1098.1794, 1151.3242, 1179.4256, 1213.3050, 1216.6322, 1221.1463, 1248.1748, 1276.0781, 1295.2606, 1300.0084, 1372.9104, 1375.7905, 1406.4922, 1410.6360, 1414.7877, 1417.0080, 1433.5840, 1448.1440, 1450.9227, 1452.5086, 1460.7210, 1477.5212, 1480.6911, 1486.9102, 1491.9287, 1495.2197, 1500.5159, 1509.7481, 1517.7586, 1523.6299, 1534.8078, 1656.4899, 3027.0326, 3047.5329, 3051.4527, 3061.9779, 3104.4546, 3114.9204, 3118.3551, 3125.9208, 3126.2149, 3130.5795, 3131.9227, 3139.0139, 3163.5479, 3172.5531, 3244.7575, 3250.6611, 3254.3313, 3258.3694, 3261.6635, 3263.4747, 3271.1526, 3275.0928, 3276.9339, 3279.6558, 3287.2368 cm^{-1}

File name (in my CERMM directory): No10-25tBu.log

Table D4. Olefin complex geometry in **Figure 4.3 (d).**

B3LYP/LanL2DZ on zirconium B3LYP/6-31G(d,p)on lighter elements

Atomic Number	Coordinates (Angstroms) X	Y	Z
6	0.827882	-0.162367	2.311757
40	0.982029	-0.119940	0.078974
1	1.634062	0.449571	2.743612
1	0.916978	-1.190059	2.694015
1	-0.121006	0.249143	2.686764
6	0.242002	-2.626318	-0.224909
6	-0.773363	-1.980670	0.530856
6	-1.366856	-0.959255	-0.296258
6	-0.741083	-1.043609	-1.603548
6	0.256754	-2.047879	-1.548958
14	-2.835042	0.056678	0.101839
9	-3.103220	1.103086	-1.163930
9	-4.214506	-0.804100	0.390596

9	-2.572639	0.998585	1.452186
1	0.833537	-3.467790	0.109078
1	-1.060146	-2.219675	1.545202
1	-1.011923	-0.456937	-2.470936
1	0.879756	-2.362360	-2.377553
6	0.011648	2.023517	-0.859160
6	1.226881	1.785447	-1.582585
6	2.321009	1.968224	-0.672508
6	1.778408	2.307529	0.614847
6	0.356728	2.341333	0.502756
1	-0.981107	2.061904	-1.286565
1	1.305766	1.591145	-2.644425
1	3.368913	1.961704	-0.936674
1	2.347760	2.537374	1.505278
1	-0.342994	2.589533	1.289338
6	3.840282	-0.576687	0.147857
6	3.228302	-1.789720	0.272362
1	4.270491	-0.258585	-0.798634
1	4.034464	0.054050	1.012983
1	3.170303	-2.478382	-0.566883
1	2.926305	-2.171929	1.245974

E = -854.8996402 hartrees

ν = 27.1607, 33.5123, 46.3622, 69.3070, 83.7669, 98.9093, 109.7654, 111.4412, 134.9462, 144.5355, 148.0373, 175.5783, 193.6500, 208.3821, 224.8615, 234.5136, 241.3522, 248.6679, 259.4248, 268.7912, 276.3081, 297.2983, 329.6820, 358.5426, 378.7668, 415.9400, 468.8130, 492.3037, 533.2949, 575.8092, 580.0155, 583.6729, 625.6362, 685.1954, 751.0515, 847.1400, 850.8562, 859.7363, 860.3567, 861.7698, 863.9296, 866.1230, 875.0189, 878.4884, 887.3295, 902.2619, 917.9719, 943.8936, 947.3408, 956.7771, 971.9177, 1027.8286, 1038.5141, 1048.0982, 1050.4018, 1058.3277, 1063.9861, 1088.8755, 1105.2643, 1111.4561, 1117.8230, 1138.7159, 1227.7959, 1240.6154, 1250.6116, 1259.8965, 1312.8111, 1355.8031, 1374.0023, 1312.8111, 1355.8031,1374.0023, 1398.3790, 1404.3058, 1406.5414, 1457.4653, 1462.0314, 1462.5587, 1472.9628, 1476.8239, 1477.8185, 1492.1229, 1629.7320, 3008.0477, 3105.7282, 3108.2767, 3156.9534, 3174.0411, 3259.7333, 3260.8604, 3266.8106, 3273.7442, 3278.1950, 3284.2081,3286.4420, 3290.2470, 3293.0425, 3299.6019, 3306.8501 cm^{-1}

File name (in my CERMM directory): No10-26-2.log

Table D5. Olefin complex geometry in **Figure 4.3 (f).**

B3LYP/LanL2DZ on zirconium B3LYP/6-31G(d,p) on lighter elements

Atomic Number	Coordinates (Angstroms) X	Y	Z
6	0.750127	-0.277545	2.319883
40	0.776296	-0.129891	0.056461
1	1.602937	0.258948	2.751656
1	0.802208	-1.328580	2.630501
1	-0.158639	0.144691	2.764283
6	-0.229600	-2.479122	-0.249864
6	-1.152936	-1.761062	0.541101
6	-1.672454	-0.705373	-0.259265
6	-1.099553	-0.804980	-1.563291
6	-0.196363	-1.886376	-1.550670
6	-2.816858	0.182448	0.135103
9	-2.994505	1.174296	-0.766930
9	-3.958097	-0.513295	0.213504
9	-2.603578	0.756285	1.342206
1	0.306695	-3.365395	0.060592
1	-1.434650	-1.979201	1.561219
1	-1.336285	-0.169188	-2.404714
1	0.394433	-2.224053	-2.393624
6	0.002865	2.205074	-0.394948
6	0.849983	1.868180	-1.493072
6	2.171825	1.761186	-1.002082
6	2.148191	2.029658	0.399089
6	0.814183	2.318031	0.768867
1	-1.057834	2.402355	-0.452968
1	0.543681	1.756668	-2.524673
1	3.051962	1.560413	-1.598931
1	3.006279	2.051501	1.057841
1	0.470456	2.583319	1.758817
6	3.541545	-0.910333	0.099138
6	2.849035	-2.067566	0.086550
1	3.997380	-0.513776	-0.802691
1	3.769463	-0.400979	1.031190
1	2.727022	-2.643638	-0.826235
1	2.508723	-2.526315	1.011027

E = - 1140.6314237 hartrees

ν = 26.1229, 39.6670, 47.4035, 76.0184, 93.2069, 103.5540, 109.1816, 141.6361, 146.7752, 179.5214, 180.0890, 200.7648, 209.6681, 224.7247, 244.9103, 255.1070, 267.6508, 286.7715, 305.5198, 344.4561, 372.7482, 397.1112, 408.5149, 429.9424, 472.5274, 529.2221, 537.6227, 573.8756, 592.6490, 596.3574, 598.4152,675.2254, 686.4816, 733.6817, 834.4187, 842.6576, 845.7765, 847.7481, 850.6325, 852.4786, 855.3679, 862.8157,876.0725, 905.0004, 912.5770, 933.7496, 935.3696, 943.7274, 1000.5390, 1032.4237, 1036.8610, 1047.7606, 1049.1048, 1066.5742,

1073.7852, 1089.9701, 1093.2946, 1095.8153, 1145.3693, 1150.8612,
1185.9988, 1214.6094, 1225.0458, 1249.9291, 1267.8396, 1300.5411,
1345.7774, 1372.7030, 1401.7579, 1406.0073, 1410.6749, 1426.3493,
1448.1183, 1457.4382, 1473.2509,1475.7426,1479.3803,1489.7188,1532.7967,
1656.4792, 3024.5611, 3106.1693, 3114.5644, 3161.0782, 3171.5951,
3242.6992, 3247.7215, 3251.4814, 3258.2523, 3263.9752, 3267.2596,
3273.6067, 3274.9847,3276.4343, 3281.4410, 3289.2142 cm^{-1}

File name (in my CERMM directory): No10-26-3.log

Table D6. Olefin complex geometry in **Figure 4.3 (g).**

B3LYP/LanL2DZ on zirconium B3LYP/6-31G(d,p) on lighter elements

Atomic Number	Coordinates (Angstroms) X	Y	Z
6	2.855346	-0.886039	-1.290895
40	1.066219	-0.160682	-0.107673
1	2.934633	-1.978239	-1.261634
1	3.767070	-0.454062	-0.858698
1	2.841472	-0.591446	-2.346393
6	2.528832	1.982171	-0.138831
6	1.721865	2.005891	-1.301456
6	0.363287	2.123834	-0.891264
6	0.332820	2.169106	0.529239
6	1.673212	2.086953	0.993006
1	3.608240	1.915877	-0.118682
1	2.079563	1.959314	-2.321281
1	-0.499234	2.220806	-1.533961
1	-0.555254	2.306181	1.128920
1	1.992898	2.167544	2.023067
6	-1.416155	-0.770457	-0.333085
6	-0.814698	-1.869714	0.345148
6	0.108246	-2.518632	-0.523576
6	0.082210	-1.842059	-1.766345
6	-0.827455	-0.759000	-1.648576
14	-2.930991	0.202251	0.241755
6	-4.409689	-0.276478	-0.789352
6	-3.186208	-0.008961	2.081545
9	-2.596587	1.773827	-0.060520
1	-1.049689	-2.183304	1.355526
1	0.693759	-3.399246	-0.293208
1	0.654206	-2.102211	-2.645980
1	-1.096974	-0.084511	-2.451459
1	-4.228281	-0.097182	-1.853877
1	-5.288393	0.307740	-0.496863
1	-4.655112	-1.336633	-0.665123
1	-4.034799	0.598314	2.413291
1	-2.313418	0.302439	2.665141

1	-3.414326	-1.049487	2.337580
6	2.053574	-1.828276	1.980369
6	2.461624	-0.596176	2.347233
1	1.183805	-2.293898	2.432227
1	2.644293	-2.440029	1.303740
1	1.929352	-0.028969	3.105578
1	3.399714	-0.180675	1.990149

E = -1020.6886172 hartrees

ν = 15.7193, 27.0694, 50.8789, 76.5998, 84.5761, 95.1506, 104.3519, 119.7503, 134.9584, 142.0781, 143.8489, 145.8167, 162.3990, 177.4088, 186.2000, 209.3817, 217.7397, 224.5788, 241.1419, 253.8833, 260.4503, 268.3315, 274.1757, 306.3351, 322.0872, 338.4463, 361.3496, 380.5246, 430.4337, 465.8989, 508.4147, 580.4682, 583.6594, 591.5659, 620.8211, 661.0521, 687.3631, 707.3094, 766.0074, 799.1992, 818.2384, 838.0641, 845.4143, 847.3848, 847.7556, 850.1047, 852.6062, 857.2276, 858.0609, 862.1402, 871.4172, 903.0507, 909.8065, 919.3108, 925.9805, 933.6147, 938.1211, 991.9171, 1020.9692, 1035.1895, 1040.7530, 1056.0043, 1067.7968, 1079.5708, 1085.3533, 1092.2260, 1097.9124, 1150.5510, 1194.6862, 1208.6502, 1233.5215, 1248.5309, 1292.2558, 1326.5803, 1331.5463, 1350.4396, 1370.5524, 1406.0624, 1407.0311, 1412.8567, 1447.3916, 1450.6062, 1459.7683, 1462.0429, 1467.3667, 1473.8432, 1474.1976, 1478.7194, 1481.4435, 1483.8477, 1494.5803, 1654.9477, 3026.4528, 3047.8871, 3051.3570, 3104.8052, 3117.7610, 3124.0520, 3129.5520, 3131.3233, 3134.3811, 3161.3376, 3170.4099, 3236.9612, 3248.4391, 3248.7355, 3255.0789, 3255.6664, 3262.2504, 3272.1000, 3272.8253, 3275.7258, 3280.9365, 3292.4443 cm^{-1}

File name (in my CERMM directory): No10-29.log

Appendix E

Natural charges and second order perturbation stabilization energies

Legend for donor and acceptor orbitals

BD(1) A1-A2	σ type NBO between Atom #1 and Atom #2
BD(2) A1-A2	π type NBO between Atom #1 and Atom #2
LP(#) A1	Lone pair(s)-type orbital on Atom #1
BD*(1) A1-A2	σ^* type natural anti-bonding orbital between Atom #1 and Atom #2
BD*(2) A1-A2	π^* type natural anti-bonding orbital between Atom #1 and Atom #2
LP*(#) A1	Unoccupied/low occupancy lone pair(s)-type orbital on Atom #1 (e.g. d-orbitals on metal)

Threshold for energy printing: **5 kcal/mol**

No interactions stronger than 5 kcal/mol were found between valence and core orbitals.

No interactions between Rydberg type and other type orbitals are reported.

1E. For uncomplexed Cp^- ligand

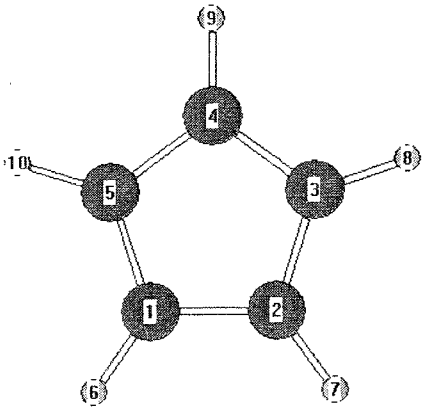

Atom No	Natural Charge
C 1	-0.37695
C 2	-0.37701
C 3	-0.37697
C 4	-0.37699
C 5	-0.37703
H 6	0.17699
H 7	0.17699
H 8	0.17698
H 9	0.17700
H 10	0.17700
Total	-1.00000

Molecular unit 1 (C5H5)
Charge unit 1 -1.00000

Second Order Perturbation Theory Analysis of Fock Matrix in NBO Basis

Donor NBO	Acceptor NBO	E kcal/mol
within unit 1		
BD (2) C 1 - C 2	LP (1) C 5	34.30
BD (2) C 1 - C 2	BD*(2) C 3 - C 4	17.54
BD (2) C 3 - C 4	LP (1) C 5	34.30
BD (2) C 3 - C 4	BD*(2) C 1 - C 2	17.54
LP (1) C 5	BD*(2) C 1 - C 2	76.23
LP (1) C 5	BD*(2) C 3 - C 4	76.23

2E. For uncomplexed Cp^{-}-^{t}Bu ligand (planar conformation)

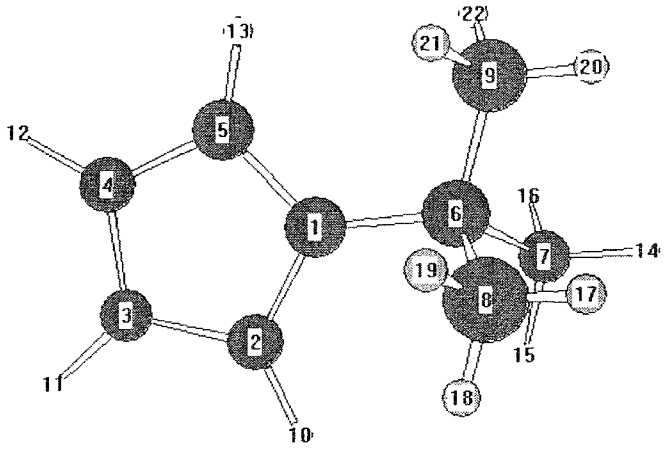

Atom No	Natural Charge
C 1	-0.17935
C 2	-0.36870
C 3	-0.35909
C 4	-0.36595
C 5	-0.36476
C 6	-0.04720
C 7	-0.66616
C 8	-0.66614
C 9	-0.66979
H 10	0.18283
H 11	0.18231
H 12	0.18241
H 13	0.18629
H 14	0.19291
H 15	0.22846
H 16	0.22653
H 17	0.19292
H 18	0.22852
H 19	0.22650
H 20	0.20264
H 21	0.22740
H 22	0.22742
Total	-1.00000

Molecular unit 1 (C9H13)
Charge unit 1 -1.00000

Second Order Perturbation Theory Analysis of Fock Matrix in NBO Basis

Donor NBO	Acceptor NBO	E kcal/mol
within unit 1		
BD (2) C 2 - C 3	LP (1) C 1	34.09
BD (2) C 2 - C 3	BD*(2) C 4 - C 5	17.84
BD (2) C 4 - C 5	LP (1) C 1	34.69
BD (2) C 4 - C 5	BD*(2) C 2 - C 3	18.48
LP (1) C 1	BD*(2) C 2 - C 3	78.95
LP (1) C 1	BD*(2) C 4 - C 5	82.53
LP (1) C 1	BD*(1) C 6 - C 7	6.55
LP (1) C 1	BD*(1) C 6 - C 8	6.56

3E. For uncomplexed Cp$^-$-^{t}Bu ligand (perpendicular conformation)

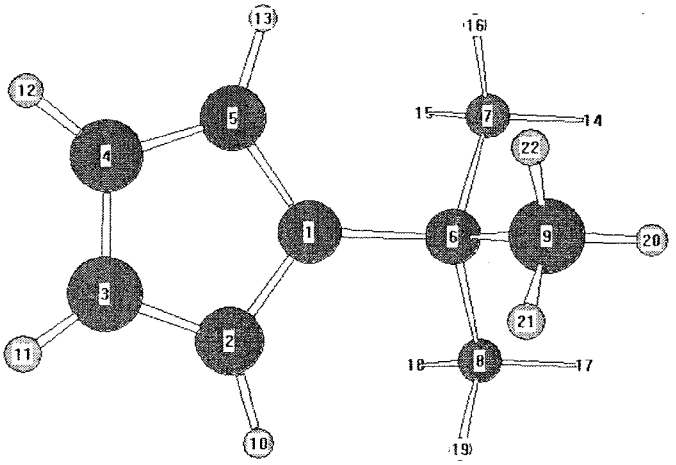

Atom No	Natural Charge
C 1	-0.18034
C 2	-0.36573
C 3	-0.36205
C 4	-0.36315
C 5	-0.36532
C 6	-0.04693
C 7	-0.66743
C 8	-0.66659
C 9	-0.66728
H 10	0.18370
H 11	0.18224
H 12	0.18225
H 13	0.18440
H 14	0.19955
H 15	0.22824
H 16	0.22571
H 17	0.19802
H 18	0.22781
H 19	0.22599
H 20	0.19122
H 21	0.22792
H 22	0.22777
Total	-1.00000

Molecular unit 1 (C9H13)
Charge unit 1 -1.00000

Second Order Perturbation Theory Analysis of Fock Matrix in NBO Basis

Donor NBO	Acceptor NBO	E kcal/mol
within unit 1		
BD (2) C 2 - C 3	LP (1) C 1	34.17
BD (2) C 2 - C 3	BD*(2) C 4 - C 5	18.10
BD (2) C 4 - C 5	LP (1) C 1	34.24
BD (2) C 4 - C 5	BD*(2) C 2 - C 3	18.20
LP (1) C 1	BD*(2) C 2 - C 3	80.02
LP (1) C 1	BD*(2) C 4 - C 5	80.49
LP (1) C 1	BD*(1) C 6 - C 9	8.84

4E. For uncomplexed Cp^- - $Si(CH_3)_3$ ligand

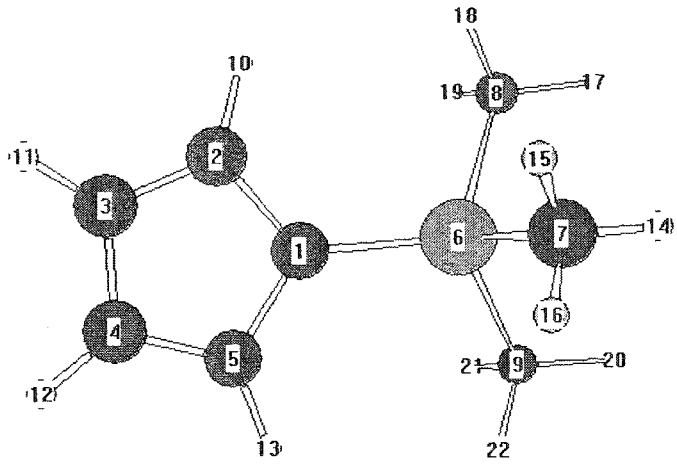

Atom	No	Natural Charge
C	1	-0.73222
C	2	-0.32327
C	3	-0.35606
C	4	-0.35625
C	5	-0.32319
Si	6	1.83578
C	7	-1.19800
C	8	-1.19310
C	9	-1.19300
H	10	0.19017
H	11	0.18716
H	12	0.18717
H	13	0.19024
H	14	0.21754
H	15	0.23610
H	16	0.23635
H	17	0.22062
H	18	0.23798
H	19	0.23858
H	20	0.22073
H	21	0.23857
H	22	0.23811
Total		-1.00000

Molecular unit 1 (C8H13Si)
Charge unit 1 -1.00000

Second Order Perturbation Theory Analysis of Fock Matrix in NBO Basis

Donor NBO					Acceptor NBO					E kcal/mol
within unit 1										
BD (	2) C	2	- C	3	LP (	1) C	1			29.30
BD (	2) C	2	- C	3	BD*(	2) C	4	- C	5	17.48
BD (	2) C	4	- C	5	LP (	1) C	1			29.30
BD (	2) C	4	- C	5	BD*(	2) C	2	- C	3	17.49
LP (	1) C	1			BD*(	2) C	2	- C	3	64.08
LP (	1) C	1			BD*(	2) C	4	- C	5	64.11
LP (	1) C	1			BD*(	1)Si	6	- C	7	13.17

5E. For uncomplexed Cp^- - CF_3 ligand

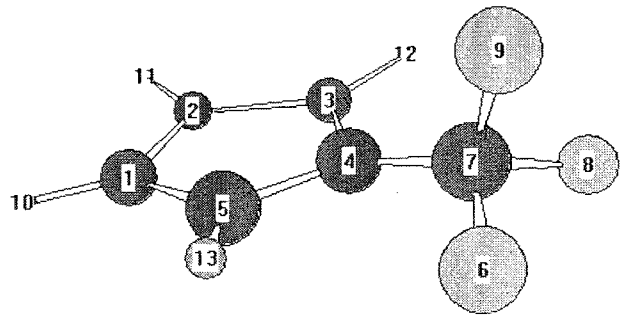

Atom	No	Natural Charge
C	1	-0.35201
C	2	-0.35199
C	3	-0.31263
C	4	-0.33262
C	5	-0.31263
F	6	-0.38843
C	7	1.02949
F	8	-0.38849
F	9	-0.40593
H	10	0.19756
H	11	0.19756
H	12	0.21005
H	13	0.21006
Total		-1.00000

Second Order Perturbation Theory Analysis of Fock Matrix in NBO Basis

Threshold for printing: 5 kcal/mol

Donor NBO	Acceptor NBO	kcal/mol
within unit 1		
BD (1) C 1- C 5	BD*(1) C 4- C 7	5.00
BD (2) C 1- C 5	LP (1) C 4	31.77
BD (2) C 1- C 5	BD*(2) C 2- C 3	18.29
BD (1) C 2- C 3	BD*(1) C 4- C 7	5.00
BD (2) C 2- C 3	LP (1) C 4	31.78
BD (2) C 2- C 3	BD*(2) C 1- C 5	18.29
LP (1) C 4	BD*(2) C 1- C 5	68.66
LP (1) C 4	BD*(2) C 2- C 3	68.66
LP (1) C 4	BD*(1) F 6- C 7	10.05
LP (1) C 4	BD*(1) C 7- F 8	10.13
LP (1) C 4	BD*(1) C 7- F 9	48.75
LP (3) F 6	BD*(1) C 7- F 8	12.77
LP (3) F 6	BD*(1) C 7- F 9	6.68
LP (1) F 8	RY*(1) C 7	6.36
LP (3) F 8	BD*(1) F 6- C 7	12.77
LP (3) F 8	BD*(1) C 7- F 9	6.67
LP (3) F 9	BD*(1) F 6- C 7	8.91
LP (3) F 9	BD*(1) C 7- F 8	8.90

6E. For uncomplexed Cp^- - SiF_3 ligand

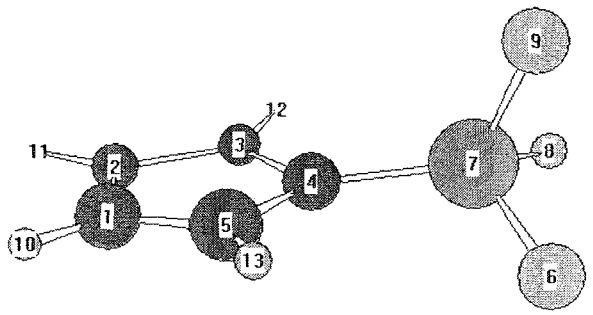

Atom No	Natural Charge
C 1	-0.34203
C 2	-0.34451
C 3	-0.30157
C 4	-0.81291
C 5	-0.30254
F 6	-0.62895
Si 7	2.15782
F 8	-0.62882
F 9	-0.63075
H 10	0.20315
H 11	0.20342
H 12	0.21544
H 13	0.21226
* Total *	-1.00000

Second Order Perturbation Theory Analysis of Fock Matrix in NBO Basis

Threshold for printing: 5 kcal/mol

Donor NBO	Acceptor NBO	E kcal/mol
BD (2) C 1- C 5	LP (1) C 4	31.75
BD (2) C 1- C 5	BD*(2) C 2- C 3	17.96
BD (2) C 2- C 3	LP (1) C 4	31.60
BD (2) C 2- C 3	BD*(2) C 1- C 5	18.14
BD (1) C 4-Si 7	BD*(1)Si 7- F 9	5.47
LP (1) C 4	BD*(2) C 1- C 5	53.12
LP (1) C 4	BD*(2) C 2- C 3	53.14
LP (1) C 4	BD*(1) F 6-Si 7	10.45
LP (1) C 4	BD*(1)Si 7- F 9	28.49
LP (2) F 6	BD*(1) C 4-Si 7	5.05
LP (2) F 6	BD*(1)Si 7- F 9	7.34
LP (3) F 6	BD*(1)Si 7- F 8	10.91
LP (2) F 8	BD*(1) C 4-Si 7	5.02
LP (2) F 8	BD*(1)Si 7- F 9	7.17
LP (3) F 8	BD*(1) F 6-Si 7	10.56
LP (2) F 9	BD*(1) C 4-Si 7	5.92
LP (2) F 9	BD*(1) F 6-Si 7	4.91
LP (3) F 9	BD*(1) F 6-Si 7	5.90
LP (3) F 9	BD*(1)Si 7- F 8	8.49

7E. For unsubstituted Cp complex.

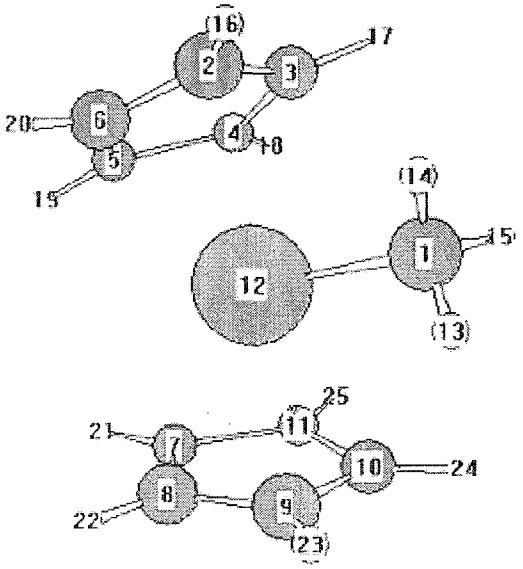

Atom No	Natural Charge
C 1	-0.43182
C 2	-0.30000
C 3	-0.27388
C 4	-0.32049
C 5	-0.29560
C 6	-0.31445
C 7	-0.28935
C 8	-0.31454
C 9	-0.30583
C 10	-0.27477
C 11	-0.31980
Zr12	1.74132
H 13	0.23987
H 14	0.23995
H 15	0.26314
H 16	0.26641
H 17	0.26822
H 18	0.26559
H 19	0.26292
H 20	0.26484
H 21	0.26271
H 22	0.26483
H 23	0.26644
H 24	0.26865
H 25	0.26563
Total	1.00000

Molecular unit 1 (CH3Zr)
Charge unit 1 1.35246

Molecular unit 2 (C5H5)
Charge unit 2 -0.17644

Molecular unit 3 (C5H5)
Charge unit 3 -0.17603

Second Order Perturbation Theory Analysis of Fock Matrix in NBO Basis

Donor NBO	Acceptor NBO	E kcal/mol
within unit 1		
LP*(1)Zr 12	LP*(2)Zr 12	5.41
LP*(3)Zr 12	LP*(4)Zr 12	11.59
LP*(3)Zr 12	LP*(5)Zr 12	22.29
BD*(1) C 1 -Zr 12	LP*(4)Zr 12	25.62
from unit 1 to unit 2		
LP*(1)Zr 12	BD*(2) C 2 - C 3	22.63

LP*(1)Zr 12	BD*(2) C 5 - C 6	10.66
LP*(3)Zr 12	BD*(2) C 5 - C 6	10.12
from unit 1 to unit 3		
LP*(1)Zr 12	BD*(2) C 7 - C 8	10.09
LP*(1)Zr 12	BD*(2) C 9 - C 10	25.74
LP*(3)Zr 12	BD*(2) C 7 - C 8	11.90
from unit 2 to unit 1		
BD (1) C 2 - C 3	LP*(3)Zr 12	8.53
BD (2) C 2 - C 3	LP*(2)Zr 12	10.11
BD (2) C 2 - C 3	LP*(3)Zr 12	29.93
BD (2) C 2 - C 3	LP*(4)Zr 12	11.85
BD (2) C 2 - C 3	BD*(1) C 1 -Zr 12	5.72
BD (1) C 2 - C 6	LP*(3)Zr 12	8.94
BD (1) C 3 - C 4	LP*(1)Zr 12	7.31
BD (1) C 4 - C 5	LP*(1)Zr 12	1.60
BD (1) C 4 - C 5	LP*(2)Zr 12	8.97
BD (2) C 5 - C 6	LP*(1)Zr 12	8.76
BD (2) C 5 - C 6	LP*(2)Zr 12	29.47
BD (2) C 5 - C 6	LP*(3)Zr 12	8.47
BD (2) C 5 - C 6	LP*(4)Zr 12	6.68
BD (2) C 5 - C 6	BD*(1) C 1 -Zr 12	5.17
LP (1) C 4	LP*(1)Zr 12	42.91
LP (1) C 4	LP*(2)Zr 12	20.62
LP (1) C 4	LP*(3)Zr 12	5.55
LP (1) C 4	LP*(4)Zr 12	8.08
BD*(2) C 5 - C 6	BD*(1) C 1 -Zr 12	8.15
within unit 2		
BD (2) C 2 - C 3	LP (1) C 4	59.63
BD (2) C 2 - C 3	BD*(2) C 5 - C 6	20.03
BD (2) C 5 - C 6	LP (1) C 4	53.10
BD (2) C 5 - C 6	BD*(2) C 2 - C 3	19.07
LP (1) C 4	BD*(2) C 2 - C 3	54.72
LP (1) C 4	BD*(2) C 5 - C 6	57.85
from unit 3 to unit 1		
BD (1) C 7 - C 8	LP*(2)Zr 12	9.04
BD (2) C 7 - C 8	LP*(1)Zr 12	6.76
BD (2) C 7 - C 8	LP*(2)Zr 12	31.04
BD (2) C 7 - C 8	LP*(3)Zr 12	6.15
BD (2) C 7 - C 8	LP*(4)Zr 12	6.85
BD (2) C 7 - C 8	BD*(1) C 1 -Zr 12	5.88
BD (1) C 7 - C 11	LP*(2)Zr 12	8.21
BD (1) C 8 - C 9	LP*(3)Zr 12	8.68
BD (2) C 9 - C 10	LP*(2)Zr 12	9.87
BD (2) C 9 - C 10	LP*(3)Zr 12	32.38
BD (2) C 9 - C 10	LP*(4)Zr 12	12.65
BD (2) C 9 - C 10	BD*(1) C 1 -Zr 12	5.96
BD (1) C 10 - C 11	LP*(1)Zr 12	7.31
LP (1) C 11	LP*(1)Zr 12	47.79
LP (1) C 11	LP*(4)Zr 12	7.11
BD*(2) C 7 - C 8	BD*(1) C 1 -Zr 12	5.05
within unit 3		
BD (2) C 7 - C 8	LP (1) C 11	53.00
BD (2) C 7 - C 8	BD*(2) C 9 - C 10	19.08
BD (2) C 9 - C 10	LP (1) C 11	58.68
BD (2) C 9 - C 10	BD*(2) C 7 - C 8	19.88
LP (1) C 11	BD*(2) C 7 - C 8	57.83
LP (1) C 11	BD*(2) C 9 - C 10	55.22

8E. For structure II b (Chapter 2).

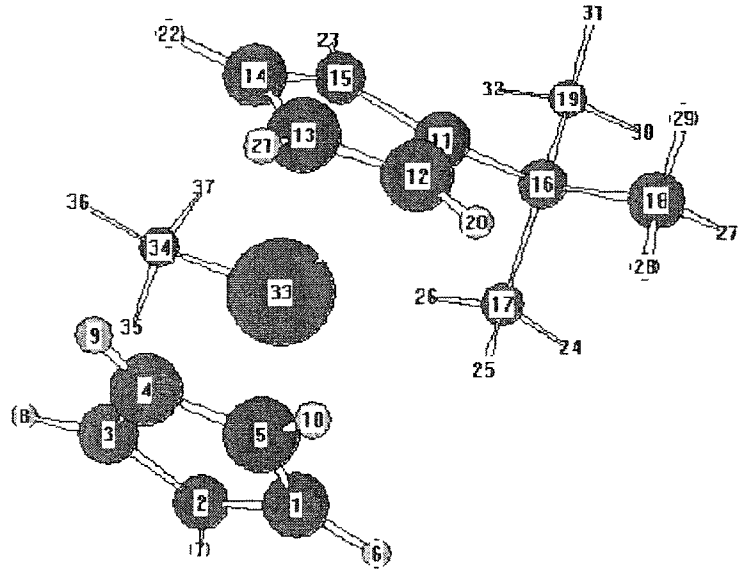

Atom	No	Natural Charge
C	1	-0.33959
C	2	-0.33543
C	3	-0.30419
C	4	-0.35421
C	5	-0.33164
H	6	0.28818
H	7	0.29173
H	8	0.29524
H	9	0.29381
H	10	0.28869
C	11	-0.11519
C	12	-0.36136
C	13	-0.32110
C	14	-0.30026
C	15	-0.31807
C	16	-0.06207
C	17	-0.70326
C	18	-0.68519
C	19	-0.68615
H	20	0.28738
H	21	0.29054
H	22	0.29310
H	23	0.28968
H	24	0.30725
H	25	0.23875
H	26	0.25297
H	27	0.25687
H	28	0.23495
H	29	0.26137
H	30	0.25722
H	31	0.26101
H	32	0.23810
Zr	33	1.68339
C	34	-1.19151
H	35	0.25234
H	36	0.27538
H	37	0.25129
Total		1.00000

Molecular unit	1	(C5H5)
Charge unit	1	-0.184741
Molecular unit	2	(C9H13)
Charge unit	2	-0.08347
Molecular unit	3	(CH3Zr)
Charge unit	3	1.26789

Second Order Perturbation Theory Analysis of Fock Matrix in NBO Basis

Donor NBO	Acceptor NBO	E kcal/mol
within unit 1		
BD (2) C 1 - C 5	LP (1) C 4	54.25
BD (2) C 1 - C 5	BD*(2) C 2 - C 3	17.74
BD (2) C 2 - C 3	LP (1) C 4	58.59
BD (2) C 2 - C 3	BD*(2) C 1 - C 5	19.81
LP (1) C 4	BD*(2) C 1 - C 5	58.11
LP (1) C 4	BD*(2) C 2 - C 3	55.26
from unit 1 to unit 3		
BD (1) C 1 - C 2	LP*(3)Zr 33	10.62
BD (1) C 1 - C 5	LP*(2)Zr 33	9.41
BD (2) C 1 - C 5	LP*(1)Zr 33	8.86
BD (2) C 1 - C 5	LP*(2)Zr 33	24.55
BD (2) C 1 - C 5	LP*(3)Zr 33	6.27
BD (2) C 1 - C 5	BD*(1)Zr 33 - C 34	6.12
BD (1) C 2 - C 3	LP*(3)Zr 33	10.01
BD (2) C 2 - C 3	LP*(2)Zr 33	12.56
BD (2) C 2 - C 3	LP*(3)Zr 33	21.82
BD (2) C 2 - C 3	LP*(5)Zr 33	10.62
BD (1) C 3 - C 4	LP*(1)Zr 33	7.97
BD (1) C 3 - C 4	LP*(5)Zr 33	5.82
BD (1) C 4 - C 5	LP*(2)Zr 33	10.44
BD (1) C 4 - C 5	LP*(4)Zr 33	6.26
LP (1) C 4	LP*(1)Zr 33	38.67
LP (1) C 4	LP*(2)Zr 33	22.13
LP (1) C 4	LP*(3)Zr 33	10.74
LP (1) C 4	LP*(5)Zr 33	11.35
BD*(2) C 1 - C 5	BD*(1)Zr 33 - C 34	6.89
within unit 2		
BD (2) C 11 - C 15	LP (1) C 12	58.46
BD (2) C 11 - C 15	BD*(2) C 13 - C 14	19.97
BD (2) C 13 - C 14	LP (1) C 12	58.97
BD (2) C 13 - C 14	BD*(2) C 11 - C 15	18.50
LP (1) C 12	BD*(2) C 11 - C 15	60.59
LP (1) C 12	BD*(2) C 13 - C 14	59.34
from unit 2 to unit 3		
BD (1) C 11 - C 12	LP*(2)Zr 33	9.40
BD (1) C 11 - C 12	LP*(3)Zr 33	6.11
BD (1) C 11 - C 15	LP*(3)Zr 33	11.27
BD (2) C 11 - C 15	LP*(3)Zr 33	33.14
BD (2) C 11 - C 15	LP*(4)Zr 33	5.02
BD (2) C 11 - C 15	LP*(5)Zr 33	9.71
BD (1) C 12 - C 13	LP*(2)Zr 33	12.20
BD (1) C 12 - C 13	LP*(4)Zr 33	6.90
BD (1) C 13 - C 14	LP*(1)Zr 33	7.23
BD (2) C 13 - C 14	LP*(1)Zr 33	24.20
BD (2) C 13 - C 14	LP*(5)Zr 33	8.08
BD (1) C 14 - C 15	LP*(1)Zr 33	5.91
BD (1) C 14 - C 15	LP*(3)Zr 33	7.67
BD (1) C 17 - H 25	LP*(4)Zr 33	10.63
BD (1) C 17 - H 25	LP*(5)Zr 33	9.87
BD (1) C 17 - H 26	LP*(3)Zr 33	6.75
BD (1) C 17 - H 26	LP*(5)Zr 33	6.57
LP (1) C 12	LP*(2)Zr 33	56.36
LP (1) C 12	BD*(1)Zr 33 - C 34	14.31
from unit 3 to unit 1		
LP*(1)Zr 33	BD*(2) C 1 - C 5	15.45
LP*(1)Zr 33	BD*(2) C 2 - C 3	27.52
LP*(4)Zr 33	BD*(2) C 1 - C 5	41.35
LP*(4)Zr 33	BD*(2) C 2 - C 3	22.63
from unit 3 to unit 2		
LP*(1)Zr 33	BD*(2) C 11 - C 15	18.25

LP*(1)Zr 33		BD*(2) C 13 - C 14	6.48
LP*(2)Zr 33		BD*(2) C 11 - C 15	17.52
LP*(3)Zr 33		BD*(2) C 13 - C 14	11.07
LP*(4)Zr 33		BD*(2) C 11 - C 15	13.06
LP*(4)Zr 33		BD*(2) C 13 - C 14	47.69
within unit 3			
LP*(1)Zr 33		LP*(2)Zr 33	10.31
BD*(1)Zr 33 - C 34		LP*(5)Zr 33	19.98

9E. For structure V (Chapter 2).

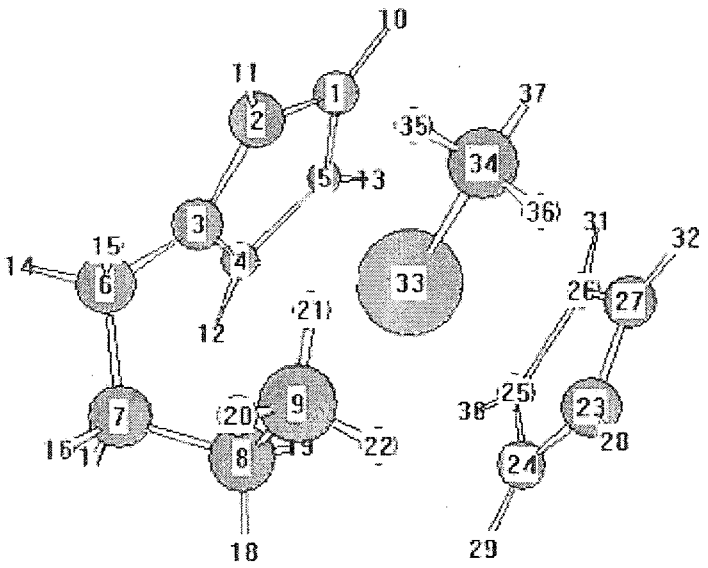

Atom No	Natural Charge
C 1	-0.31108
C 2	-0.29798
C 3	-0.12476
C 4	-0.35212
C 5	-0.30858
C 6	-0.48727
C 7	-0.46619
C 8	-0.44488
C 9	-0.71507
H 10	0.29345
H 11	0.28846
H 12	0.28521
H 13	0.28870
H 14	0.28964
H 15	0.25671
H 16	0.27091
H 17	0.25664
H 18	0.29489
H 19	0.19299
H 20	0.29567
H 21	0.23598
H 22	0.26974
C 23	-0.33754
C 24	-0.32363
C 25	-0.33433
C 26	-0.34352
C 27	-0.29171
H 28	0.28886
H 29	0.28611
H 30	0.28808
H 31	0.29210
H 32	0.29411
Zr 33	1.58962
C 34	-1.16063
H 35	0.24568
H 36	0.24779
H 37	0.26795
Total	1.00000

Molecular unit	1	(C9H13)	
Charge unit	1		0.01104
Molecular unit	2	(C5H5)	
Charge unit	2		-0.18145
Molecular unit	3	(CH3Zr)	
Charge unit	3		1.17041

Second Order Perturbation Theory Analysis of Fock Matrix in NBO Basis

Donor NBO	Acceptor NBO	E kcal/mol
within unit 1		
BD (2) C 1 - C 2	LP (1) C 3	61.44
BD (2) C 1 - C 2	BD*(2) C 4 - C 5	21.02
BD (2) C 4 - C 5	LP (1) C 3	54.16
BD (2) C 4 - C 5	BD*(2) C 1 - C 2	17.51
BD (1) C 6 - H 14	LP (1) C 3	7.04
BD (1) C 6 - H 15	BD*(1) C 3 - C 4	5.26
LP (1) C 3	BD*(2) C 1 - C 2	61.06
LP (1) C 3	BD*(2) C 4 - C 5	59.18
from unit 1 to unit 3		
BD (1) C 1 - C 2	LP*(1)Zr 33	7.53
BD (1) C 1 - C 2	LP*(3)Zr 33	6.66
BD (2) C 1 - C 2	LP*(1)Zr 33	23.64
BD (2) C 1 - C 2	LP*(3)Zr 33	13.61
BD (2) C 1 - C 2	LP*(5)Zr 33	7.80
BD (1) C 1 - C 5	LP*(1)Zr 33	8.76
BD (1) C 1 - C 5	LP*(5)Zr 33	5.02
BD (1) C 2 - C 3	LP*(3)Zr 33	12.65
BD (1) C 2 - C 3	LP*(5)Zr 33	5.03
BD (1) C 2 - H 11	LP*(3)Zr 33	5.13
BD (1) C 3 - C 4	LP*(2)Zr 33	12.00
BD (1) C 4 - C 5	LP*(2)Zr 33	12.42
BD (2) C 4 - C 5	LP*(2)Zr 33	26.65
BD (2) C 4 - C 5	LP*(4)Zr 33	7.92
BD (2) C 4 - C 5	LP*(5)Zr 33	6.32
BD (1) C 4 - H 12	LP*(2)Zr 33	5.07
BD (1) C 8 - H 19	LP*(4)Zr 33	26.73
BD (1) C 9 - H 21	LP*(3)Zr 33	9.21
BD (1) C 9 - H 21	LP*(5)Zr 33	5.83
LP (1) C 3	LP*(1)Zr 33	48.36
LP (1) C 3	LP*(2)Zr 33	7.74
LP (1) C 3	LP*(3)Zr 33	31.07
LP (1) C 3	LP*(5)Zr 33	6.94
BD*(2) C 4 - C 5	BD*(1)Zr 33 - C 34	17.56
within unit 2		
BD (2) C 23 - C 27	LP (1) C 26	60.73
BD (2) C 23 - C 27	BD*(2) C 24 - C 25	20.41
BD (2) C 24 - C 25	LP (1) C 26	55.42
BD (2) C 24 - C 25	BD*(2) C 23 - C 27	17.32
BD (1) C 25 - C 26	LP (1) C 26	5.47
BD (1) C 26 - C 27	LP (1) C 26	5.02
LP (1) C 26	BD*(2) C 23 - C 27	57.54
LP (1) C 26	BD*(2) C 24 - C 25	55.99
from unit 2 to unit 3		
BD (1) C 23 - C 24	LP*(3)Zr 33	13.75
BD (1) C 23 - C 27	LP*(3)Zr 33	10.04
BD (1) C 23 - C 27	LP*(5)Zr 33	5.06
BD (2) C 23 - C 27	LP*(2)Zr 33	18.28
BD (2) C 23 - C 27	LP*(3)Zr 33	17.82
BD (2) C 23 - C 27	LP*(5)Zr 33	9.99
BD (2) C 23 - C 27	BD*(1)Zr 33 - C 34	5.19
BD (1) C 24 - C 25	LP*(2)Zr 33	8.40
BD (1) C 24 - C 25	LP*(3)Zr 33	6.89
BD (2) C 24 - C 25	LP*(1)Zr 33	6.10
BD (2) C 24 - C 25	LP*(2)Zr 33	23.32
BD (2) C 24 - C 25	LP*(3)Zr 33	10.60
BD (1) C 25 - C 26	LP*(2)Zr 33	10.63
BD (1) C 26 - C 27	LP*(1)Zr 33	10.18
BD (1) C 26 - C 27	LP*(5)Zr 33	6.20

LP (1) C 26	LP*(1)Zr 33	42.13
LP (1) C 26	LP*(2)Zr 33	25.00
LP (1) C 26	LP*(3)Zr 33	10.38
LP (1) C 26	LP*(5)Zr 33	10.87
LP (1) C 26	BD*(1)Zr 33 - C 34	5.19
BD*(2) C 24 - C 25	BD*(1)Zr 33 - C 34	6.59
from unit 3 to unit 1		
LP*(1)Zr 33	BD*(2) C 1 - C 2	6.29
LP*(1)Zr 33	BD*(2) C 4 - C 5	7.18
LP*(2)Zr 33	BD*(2) C 1 - C 2	6.63
LP*(2)Zr 33	BD*(2) C 4 - C 5	7.75
LP*(3)Zr 33	BD*(2) C 1 - C 2	14.16
LP*(3)Zr 33	BD*(2) C 4 - C 5	15.31
LP*(4)Zr 33	BD*(2) C 1 - C 2	22.60
from unit 3 to unit 2		
LP*(1)Zr 33	BD*(2) C 23 - C 27	24.51
LP*(1)Zr 33	BD*(2) C 24 - C 25	14.77
LP*(4)Zr 33	BD*(2) C 23 - C 27	13.49
LP*(4)Zr 33	BD*(2) C 24 - C 25	24.56
within unit 3		
BD (1)C 34 - H 37	LP*(4)Zr 33	5.05
LP*(1)Zr 33	LP*(2)Zr 33	8.41
BD*(1)Zr 33 - C 34	LP*(5)Zr 33	16.87

10E. For structure I (Chapter 3).

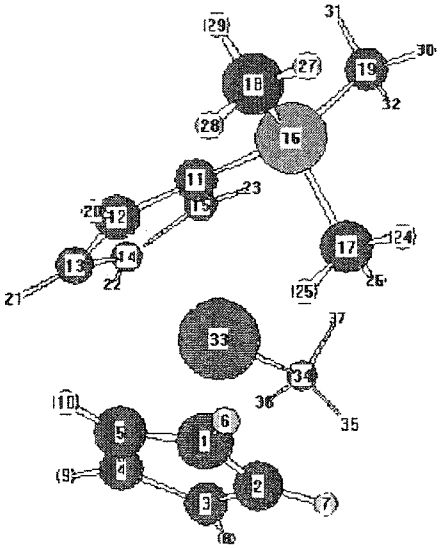

Atom No		Natural Charge
C	1	-0.33400
C	2	-0.33622
C	3	-0.30032
C	4	-0.35232
C	5	-0.33115
H	6	0.28700
H	7	0.29079
H	8	0.29445
H	9	0.29318
H	10	0.28850
C	11	-0.60432
C	12	-0.35042
C	13	-0.31365
C	14	-0.30127
C	15	-0.30186
Si	16	1.84732
C	17	-1.21093
C	18	-1.22563
C	19	-1.22634
H	20	0.28370
H	21	0.28804
H	22	0.29142
H	23	0.28548
H	24	0.32462
H	25	0.25651
H	26	0.27344
H	27	0.27834
H	28	0.26441
H	29	0.28183
H	30	0.27910
H	31	0.28149
H	32	0.26757
Zr	33	1.65893
C	34	-1.18082
H	35	0.25068
H	36	0.27475
H	37	0.24971
Total		1.00000

Molecular unit 1 (C5H5)
Charge unit 1 -0.20009

Molecular unit 2 (C8H13Si)
Charge unit 2 -0.05315

Molecular unit 3 (CH3Zr)
Charge unit 3 1.25324

Second Order Perturbation Theory Analysis of Fock Matrix in NBO Basis

Donor NBO	Acceptor NBO	E kcal/mol
within unit 1		
BD (2) C 1 - C 5	LP (1) C 4	54.56
BD (2) C 1 - C 5	BD*(2) C 2 - C 3	17.53
BD (2) C 2 - C 3	LP (1) C 4	59.36
BD (2) C 2 - C 3	BD*(2) C 1 - C 5	20.00
LP (1) C 4	BD*(2) C 1 - C 5	57.15
LP (1) C 4	BD*(2) C 2 - C 3	55.87
from unit 1 to unit 3		
BD (1) C 1 - C 2	LP*(3)Zr 33	11.34
BD (1) C 1 - C 5	LP*(2)Zr 33	8.99
BD (2) C 1 - C 5	LP*(1)Zr 33	8.67
BD (2) C 1 - C 5	LP*(2)Zr 33	23.61
BD (2) C 1 - C 5	LP*(3)Zr 33	6.33
BD (2) C 1 - C 5	LP*(5)Zr 33	5.12
BD (2) C 1 - C 5	BD*(1)Zr 33 - C 34	5.96
BD (1) C 2 - C 3	LP*(3)Zr 33	10.69
BD (1) C 2 - C 3	LP*(5)Zr 33	5.26
BD (2) C 2 - C 3	LP*(2)Zr 33	13.65
BD (2) C 2 - C 3	LP*(3)Zr 33	22.54
BD (2) C 2 - C 3	LP*(5)Zr 33	11.50
BD (1) C 3 - C 4	LP*(1)Zr 33	8.44
BD (1) C 3 - C 4	LP*(5)Zr 33	5.96
BD (1) C 4 - C 5	LP*(2)Zr 33	10.36
BD (1) C 4 - C 5	LP*(3)Zr 33	0.23
BD (1) C 4 - C 5	LP*(5)Zr 33	5.11
LP (1) C 4	LP*(1)Zr 33	38.67
LP (1) C 4	LP*(2)Zr 33	24.18
LP (1) C 4	LP*(3)Zr 33	9.21
LP (1) C 4	LP*(5)Zr 33	11.22
BD*(2) C 1 - C 5	BD*(1)Zr 33 - C 34	5.44
within unit 2		
BD (2) C 12 - C 13	LP (1) C 11	55.20
BD (2) C 12 - C 13	BD*(2) C 14 - C 15	17.31
BD (2) C 14 - C 15	LP (1) C 11	60.87
BD (2) C 14 - C 15	BD*(2) C 12 - C 13	20.25
LP (1) C 11	BD*(2) C 12 - C 13	57.53
LP (1) C 11	BD*(2) C 14 - C 15	53.53
LP (1) C 11	BD*(1)Si 16 - C 17	5.72
from unit 2 to unit 3		
BD (1) C 11 - C 12	LP*(2)Zr 33	11.50
BD (1) C 11 - C 12	LP*(3)Zr 33	6.13
BD (1) C 11 - C 15	LP*(3)Zr 33	13.29
BD (1) C 11 - C 15	LP*(5)Zr 33	5.91
BD (1) C 11 -Si 16	LP*(1)Zr 33	8.26
BD (1) C 11 -Si 16	LP*(5)Zr 33	5.78
BD (1) C 12 - C 13	LP*(2)Zr 33	12.23
BD (2) C 12 - C 13	LP*(2)Zr 33	29.63
BD (2) C 12 - C 13	LP*(5)Zr 33	7.53
BD (1) C 13 - C 14	LP*(1)Zr 33	7.27
BD (1) C 14 - C 15	LP*(1)Zr 33	6.58
BD (1) C 14 - C 15	LP*(3)Zr 33	5.91
BD (2) C 14 - C 15	LP*(1)Zr 33	23.86
BD (2) C 14 - C 15	LP*(3)Zr 33	11.76
BD (2) C 14 - C 15	LP*(5)Zr 33	8.59
BD (1)Si 16 - C 17	LP*(1)Zr 33	7.01
BD (1)Si 16 - C 17	LP*(4)Zr 33	6.89
BD (1) C 17 - H 25	LP*(4)Zr 33	18.47
BD (1) C 17 - H 26	LP*(3)Zr 33	10.51
BD (1) C 17 - H 26	LP*(5)Zr 33	5.24
LP (1) C 11	LP*(1)Zr 33	48.07
LP (1) C 11	LP*(2)Zr 33	5.89

LP (1) C 11	LP*(3)Zr 33	37.44
LP (1) C 11	LP*(5)Zr 33	7.53
BD*(2) C 12 - C 13	BD*(1)Zr 33 - C 34	20.75
from unit 3 to unit 1		
LP*(1)Zr 33	BD*(2) C 1 - C 5	14.84
LP*(1)Zr 33	BD*(2) C 2 - C 3	27.00
LP*(3)Zr 33	BD*(2) C 1 - C 5	5.98
LP*(4)Zr 33	BD*(2) C 1 - C 5	29.08
LP*(4)Zr 33	BD*(2) C 2 - C 3	8.71
from unit 3 to unit 2		
LP*(1)Zr 33	BD*(2) C 12 - C 13	5.65
LP*(2)Zr 33	BD*(2) C 14 - C 15	7.34
LP*(3)Zr 33	BD*(2) C 12 - C 13	16.82
LP*(3)Zr 33	BD*(2) C 14 - C 15	10.49
LP*(4)Zr 33	BD*(2) C 14 - C 15	19.52
within unit 3		
BD*(1)Zr 33 - C 34	LP*(5)Zr 33	16.98

11E. For structure IV (n=0) (Chapter 3).

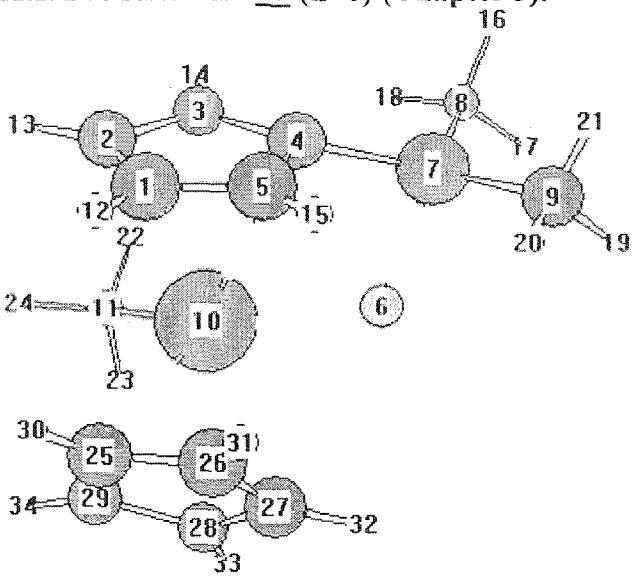

Atom No		Natural Charge			
C	1	-0.28545			
C	2	-0.26642			
C	3	-0.27178			
C	4	-0.64347			
C	5	-0.30721			
F	6	-0.64841			
Si	7	1.98141			
C	8	-1.17972			
C	9	-1.17995			
Zr	10	1.55969	Molecular unit	1	(C7H10Si)
C	11	-1.11444	Charge unit	1	0.52402
H	12	0.26143			
H	13	0.26412	Molecular unit	2	(F)
H	14	0.25901	Charge unit	2	-0.64841
H	15	0.25728			
H	16	0.27676	Molecular unit	3	(CH3Zr)
H	17	0.27686	Charge unit	3	1.24820
H	18	0.26513			
H	19	0.27614	Molecular unit	4	(C5H5)
H	20	0.26273	Charge unit	4	-0.18381
H	21	0.27714			
H	22	0.23083			
H	23	0.23777			
H	24	0.25434			
C	25	-0.31798			
C	26	-0.30818			
C	27	-0.28778			
C	28	-0.30038			
C	29	-0.27688			
H	30	0.26103			
H	31	0.25741			
H	32	0.26109			
H	33	0.26343			
H	34	0.26443			
Total		1.00000			

Second Order Perturbation Theory Analysis of Fock Matrix in NBO Basis

Donor NBO	Acceptor NBO	E kcal/mol

within unit 1

BD (	2)	C	1	- C	5	LP (	1)	C	4	63.44
BD (	2)	C	1	- C	5	BD*(	2)	C	2 - C 3	19.23
BD (	2)	C	2	- C	3	LP (	1)	C	4	70.72
BD (	2)	C	2	- C	3	BD*(	2)	C	1 - C 5	21.41
LP (	1)	C	4			LP*(	1)	Si	7	34.56
LP (	1)	C	4			BD*(	2)	C	1 - C 5	57.47
LP (	1)	C	4			BD*(	2)	C	2 - C 3	52.15

from unit 1 to unit 3

BD (	1)	C	1	- C	2	LP*(	1)	Zr	10	5.35
BD (	1)	C	1	- C	5	LP*(	2)	Zr	10	10.22
BD (	2)	C	1	- C	5	LP*(	2)	Zr	10	30.32
BD (	2)	C	2	- C	3	LP*(	1)	Zr	10	23.03
BD (	2)	C	2	- C	3	LP*(	3)	Zr	10	15.39
BD (	2)	C	2	- C	3	LP*(	5)	Zr	10	8.38
BD (	1)	C	3	- C	4	LP*(	3)	Zr	10	11.31
BD (	1)	C	4	- C	5	LP*(	2)	Zr	10	10.10
BD (	1)	C	4	-Si	7	LP*(	1)	Zr	10	7.35
LP (	1)	C	4			LP*(	1)	Zr	10	37.41
LP (	1)	C	4			LP*(	2)	Zr	10	9.03
LP (	1)	C	4			LP*(	3)	Zr	10	32.24
LP (	1)	C	4			LP*(	5)	Zr	10	5.10
BD*(	2)	C	1	- C	5	BD*(	1)	Zr	10 - C 11	16.03

from unit 2 to unit 1

LP (	1)	F	6			LP*(	1)	Si	7	10.61
LP (	4)	F	6			LP*(	1)	Si	7	100.94

from unit 2 to unit 3

LP (	1)	F	6			LP*(	4)	Zr	10	7.51
LP (	3)	F	6			LP*(	3)	Zr	10	10.12
LP (	3)	F	6			LP*(	4)	Zr	10	34.72
LP (	3)	F	6			LP*(	5)	Zr	10	13.64
LP (	4)	F	6			LP*(	1)	Zr	10	5.18
LP (	4)	F	6			LP*(	4)	Zr	10	19.82

from unit 3 to unit 1

LP*(	2)	Zr	10			BD*(	2)	C	2 - C 3	6.30
LP*(	3)	Zr	10			BD*(	2)	C	1 - C 5	13.16
LP*(	3)	Zr	10			BD*(	2)	C	2 - C 3	10.17
LP*(	4)	Zr	10			LP*(	1)	Si	7	38.35
LP*(	4)	Zr	10			BD*(	2)	C	2 - C 3	14.50

within unit 3

LP*(	2)	Zr	10			LP*(	1)	Zr	10	6.69
BD*(	1)	Zr	10	- C	11	LP*(	5)	Zr	10	16.53

from unit 3 to unit 4

LP*(	1)	Zr	10			BD*(	2)	C	26 - C 27	12.36
LP*(	1)	Zr	10			BD*(	2)	C	28 - C 29	28.47
LP*(	4)	Zr	10			BD*(	2)	C	26 - C 27	22.25
LP*(	4)	Zr	10			BD*(	2)	C	28 - C 29	8.51

from unit 4 to unit 3

BD (	1)	C	25	- C	26	LP*(	2)	Zr	10	10.96
BD (	1)	C	25	- C	29	LP*(	1)	Zr	10	6.41
BD (	1)	C	26	- C	27	LP*(	2)	Zr	10	6.24
BD (	1)	C	26	- C	27	LP*(	3)	Zr	10	5.06
BD (	2)	C	26	- C	27	LP*(	1)	Zr	10	16.89
BD (	2)	C	26	- C	27	LP*(	2)	Zr	10	20.08
BD (	2)	C	26	- C	27	LP*(	3)	Zr	10	9.60
BD (	2)	C	26	- C	27	LP*(	5)	Zr	10	5.76
BD (	2)	C	26	- C	27	BD*(	1)	Zr	10 - C 11	5.10
BD (	1)	C	27	- C	28	LP*(	3)	Zr	10	10.13
BD (	1)	C	28	- C	29	LP*(	3)	Zr	10	10.47
BD (	2)	C	28	- C	29	LP*(	2)	Zr	10	14.98
BD (	2)	C	28	- C	29	LP*(	3)	Zr	10	28.50
BD (	2)	C	28	- C	29	LP*(	5)	Zr	10	12.06
BD (	2)	C	28	- C	29	BD*(	1)	Zr	10 - C 11	5.80

LP (1) C 25	LP*(1)Zr 10	30.87
LP (1) C 25	LP*(2)Zr 10	43.27

within unit 4

BD (2) C 26 - C 27	LP (1) C 25	56.35
BD (2) C 26 - C 27	BD*(2) C 28 - C 29	18.53
BD (2) C 28 - C 29	LP (1) C 25	61.50
BD (2) C 28 - C 29	BD*(2) C 26 - C 27	21.12
LP (1) C 25	BD*(2) C 26 - C 27	57.82
LP (1) C 25	BD*(2) C 28 - C 29	55.85